

https://dspace.org/

# Excavating through the kalahari group rock masses: practical experience from a small-scale shaft sinking project

**Mateveke, Raymond; Mateveke, Raymond**

**2019**

https://hdl.handle.net/10539/29154

Mateveke, Raymond, (2019). Excavating through the Kalahari Group Rock masses :practical experience from a small scale shaft sinking project, University of the Witwatersrand, https://hdl.handle.net/10539/29154

Downloaded from a DSpace repository. https://dspace.org/

# EXCAVATING THROUGH THE KALAHARI GROUP ROCK MASSES: PRACTICAL EXPERIENCE FROM A SMALL-SCALE SHAFT SINKING PROJECT

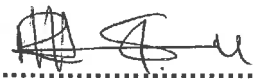
**RAYMOND MATEVEKE**

**A research report submitted to the Faculty of Engineering and the Built Environment, University of the Witwatersrand, Johannesburg, in fulfilment of the requirements for the degree of Master of Science in Engineering**

**Johannesburg, 2019**

## DECLARATION

I declare that this dissertation is my own, unaided work. It is being submitted for the degree of Master of Science in the University of the Witwatersrand, Johannesburg. It has not been submitted before for any degree or examination in any other university.



.....

**(Signature of Candidate)**

..... 27th ..... day of ..... AUGUST ..... (year) ..... 2019 .....

at ..... WITS UNIVERSITY .....

## ABSTRACT

Tunnelling projects in the weak Kalahari rock masses of the Northern Cape, South Africa present significant design challenges for both large and small-scale excavations. Most of the design of tunnelling and support carried out at present in the Kalahari is based on experience, analytical and empirical methods. The approach typically makes use of limited geotechnical information from the project site.

The Kalahari basin is a complex geotechnical environment. Tunnelling projects are sensitive to the variable ground and groundwater conditions. A detailed site investigation to establish the geological and geotechnical model is critical in the selection of the appropriate excavation method and tunnel design. A review of early tunnelling projects revealed that in situ stresses and water infiltration is a long-term stability concern for inadequately lined tunnels through the red clay and weathered rock masses.

This project explores the use of numerical modelling to predict the expected failure modes of the weak rock masses, with emphasis placed on concrete liner support for maintaining stability. The support models are analysed using 2D numerical models to determine the Factor of Safety of the liner. A support design criterion for reinforced and unreinforced concrete is introduced and applied to the models to evaluate the lining thickness. The effect of using 2D plane strain models instead of 3D analysis was also investigated. The total displacement of numerical models built in RS2 was compared to RS3 models.

## ACKNOWLEDGEMENTS

I acknowledge the guidance and assistance I got from my supervisor, Professor T.R. Stacey. His wide knowledge and experience on the subject, coupled with his patience and drive for excellence is much appreciated. Nicolaas C. Steenkamp for assistance with interpretation of the geology and hydrogeological assessments at the project site.

Worley Parsons, South Africa for allowing me to participate in the Kalahari project and in providing most of the resources used in this research.

I would like to thank the Management and staff at Black Rock Mines for their cooperation, and for affording me the opportunity to use their operations as a case study.

## TABLE OF CONTENTS


1 INTRODUCTION ..... 1
1.1 Background ..... 1
1.2 Definition of the Problem ..... 5
1.3 Objective and Scope of Research ..... 5
1.4 Research Methodology ..... 6
1.5 Content of Dissertation ..... 7
2 LITERATURE REVIEW ..... 8
2.1 Site Investigation ..... 8
2.2 Rock Mass Classification Systems ..... 11
2.3 Swelling Rock Masses ..... 27
2.4 Integration of Geotechnical and Structural Design Components ..... 31
2.5 Grouting (Cementation) ..... 32
2.6 Modelling Methods ..... 35
2.7 Challenges Associated with the Kalahari Rock Formation ..... 37
3 TUNNELLING THROUGH THE KALAHARI – A PRACTICAL EXAMPLE ..... 40
3.1 Site Investigation ..... 40
3.2 Geotechnical Inspection of Early Tunneling Projects ..... 41
3.3 Numerical Modelling ..... 43
3.4 Tunneling Works: Ventilation Shaft ..... 46
3.5 Delimitations ..... 50
4 RESULTS AND DISCUSSION ..... 51
4.1 Project Setting ..... 51
4.2 Geotechnical Characteristics ..... 56
4.3 Inspection of Early Tunneling Projects ..... 61
4.4 Numerical Analysis of a Small-Scale Shaft ..... 65
4.5 Recent Tunnelling Works: Ventilation Shaft ..... 76
4.6 Implication on Future Projects ..... 76
5 CONCLUSIONS AND RECOMMENDATIONS ..... 78
6 REFERENCES ..... 81


## LIST OF TABLES


Table 1: Rock Mass Rating System (Bieniawski, 1989) ..... 13
Table 2: Guidelines for excavation and Support of 10 m span rock tunnels in accordance with the RMR system (After Bieniawski, 1989). ..... 15
Table 3: RQD-values and volumetric jointing (NGI, 2015) ..... 16
Table 4: Jn – values (NGI, 2015) ..... 17
Table 5: Jr – values (NGI, 2015) ..... 17
Table 6: Ja – values (NGI, 2015) ..... 18
Table 7: Jw – values (NGI, 2015) ..... 19
Table 8: SRF-values (NGI, 2015) ..... 20

Table 9: ESR-values (NGI, 2015) ..... 21
Table 10: Ventilation shaft water inflow ..... 55
Table 11: Simplified Stratigraphy of GLV 01 ..... 56
Table 12: Summary of Geotechnical Properties of Sand and Clay ..... 57
Table 13: 'Kalahari' Laboratory results for the Grading Analysis, Atterberg Limits, Activity and material classification ..... 59
Table 14: 'Kalahari' Laboratory results for the Shear Box ..... 59
Table 15: Summary of Geotechnical Properties of Calcrete, Tillite and Manganese ..... 60
Table 16: Summary of findings of mapping exercise at the Decline ..... 61
Table 17: Rock mass properties of Kalahari units ..... 65

## LIST OF FIGURES

Figure 1: South African Mine Fatalities by Commodity (Minerals Council South Africa, 2019) ..... 1
Figure 2: Annual Production per Commodity, June 2004-June 2016 (Chamber of Mines, 2016) ..... 2
Figure 3: Distribution and Thickness of the Kalahari Group of Southern Africa (after Thomas and Shaw, 1990 and Thomas and Shaw, 1991). ..... 3
Figure 4: Simplified Stratigraphy (Council for Geoscience, 2012) ..... 4
Figure 5: Procedure for Measurement and Calculation of RQD (After Deere, 1989). ..... 10
Figure 6: Empirical data used in the development of the Rock Mass Rating system, I.-Rock types recorded, II.-Case history project types, III.- The range of case excavation spans, IV.- Range of case histories excavation depths and V.-Range of calculated RMR values (after Bieniawski, 1989) ..... 12
Figure 7: Guidelines for Excavation and Support of Rock Tunnels in accordance with the Q-System (NGI, 2015). ..... 22
Figure 8: General chart for GSI estimates from the geological observations (Hoek & Marinos, 2000) ..... 24
Figure 9: GSI estimates for heterogeneous rock masses such as Flysch (Marinos & Hoek, 2001) ..... 25
Figure 10: GSI chart for confined molasse; mainly applicable for tunnels (Hoek et al., 2005) ..... 26
Figure 11: GSI chart for fissile Molasse where bedding planes of siltstones-mudstones are frequent and well defined. (Surface excavations and slopes, Hoek et al., 2005) ..... 27
Figure 12: Effects of rock swelling in tunnelling (Kovári, Amstad & Anagnostou, 1988) ..... 30
Figure 13: Yielding support principle (Kovári, 2007) ..... 31
Figure 14: Overbreak Void filled by Grouting (after Houlsby, 1990) ..... 33
Figure 15: Suitability and comparison of grouts (after Houlsby, 1990) ..... 35
Figure 16: General Classification of Numerical Methods ..... 35
Figure 17: 2D Finite Element domain discretisation (Bobet, 2010) ..... 36
Figure 18: Simplified representation of the challenges with direct borehole correlation in heterogeneous ground (after Crockford, 2012) ..... 38
Figure 19: Geological cross section for Nchwaning I Decline (Steenkamp, 2013a) ..... 42
Figure 20: Old Vent shaft Stratigraphy (Steenkamp, 2013b) ..... 43
Figure 21: Elements for Finite Element Analysis ..... 44
Figure 22: Displacement boundary conditions used in all 2D numerical models ..... 45
Figure 23: Displacement boundary conditions used in all 3D numerical models ..... 45
Figure 24: Vent shaft pre-cementation and dewatering holes ..... 48
Figure 25: As-built layout of Oscillator piles ..... 48
Figure 26: Use of oscillator piles as temporary support in the sands ..... 49

Figure 27: Use of ARMCO back shutters as temporary support in the red clay ..... 49
Figure 28: The range of Kalahari sand colours, orange in the top row and darker red-orange in the second and third row. A calcrete lens is visible in the fourth row and gravels in the bottom row on the right-hand side of the photo. ..... 52
Figure 29: The Calcreted Conglomerate and Calcreted red clay contacts. ..... 53
Figure 30: Highly weathered and fresh tillite ..... 54
Figure 31: The sharp discontinuity (centre of photo) between tillite (left) and manganese seam 1 (right). 54
Figure 32: Hydrogeological log of the ventilation shaft (Chironga, 2012). ..... 55
Figure 33: Sample particle size distribution based on HRB material classification ..... 57
Figure 34: Potential Expansiveness graph of Red clay (After van der Merwe, 1964) ..... 58
Figure 35: View inside a void showing cribbing support along the red clay section of the decline. ..... 62
Figure 36: Damaged concrete lining in the clay section. ..... 62
Figure 37: Additional Lining Installed in Red Clay Horizon ..... 63
Figure 38: Shaft lining scaling off exposing the Red Clay ..... 64
Figure 39: Location where signs of instability were observed ..... 64
Figure 40: Total displacement in Calcrete zone ..... 67
Figure 41: Total displacement in Clay zone ..... 68
Figure 42: Support Capacity plot for a 300 mm liner in Clay ..... 70
Figure 43: FOS vs Swelling Pressure for the different liner thickness in Clay. ..... 71
Figure 44: Support Capacity plot for a 300 mm liner in Clay at a Swelling Pressure of 1.6. ..... 72
Figure 45: Support Capacity plot for a 400 mm liner in Clay at a Swelling Pressure of 2.2. ..... 73
Figure 46: Reinforced liner vs Unreinforced liner FOS ..... 74
Figure 47: Total displacement in Clay of the RS3 model ..... 75
Figure 48: Flow chart for tunnel support estimation in the Kalahari weak formations ..... 80

## LIST OF APPENDICES

Appendix A: Site Investigation
Appendix B: Laboratory Test Results
Appendix C: Early Tunnelling Projects Inspection
Appendix D: Derivation of Drucker Prager Constants

## LIST OF SYMBOLS AND ABBREVIATIONS

| Abbreviation | Description |
|---|---|
| Mt | Metric tonne |
| Ma | Mega-annum (Million years) |
| FOS | Factor of Safety |
| RQD | Rock Quality Designation |
| UCS | Uniaxial Compressive Strength |
| NGI | Norwegian Geotechnical Institute |
| mbgl | Metres below ground level |
| % | Percentage |
| ϕ | Frictional angle |
| MPa | Mega Pascal |
| kPa | Kilo Pascal |
| $MN/m^3$ | Mega Newtons per cubic metre |
| m | metre |
| mm | millimetre |
| $m^3/day$ | Cubic metre per day |
| Mn | Manganese |

# 1 INTRODUCTION

## 1.1 Background

The mining industry represents a significant component of the South African economy and this has been the case for over 100 years. In 2017, statistics indicated that the industry made up 6.8% of the economy (Chamber of Mines South Africa, 2017). However, South Africa is host to some of the world's deepest and most challenging mining conditions. There is a demand to progressively improve the industry's safety performance to equal that of international standards (zero harm). A study of fatal accidents by commodity between 2004 and 2018 is shown in Figure 1. The gold mining sector has the greatest number of fatalities. There has been a substantial progressive improvement in safety performance except for the relapse in 2017, which culminated in 90 fatalities. The statistics stated in Figure 1 (Minerals Council South Africa, 2019) show that South Africa still has a long way to go in attaining world safety performance targets of zero fatalities.

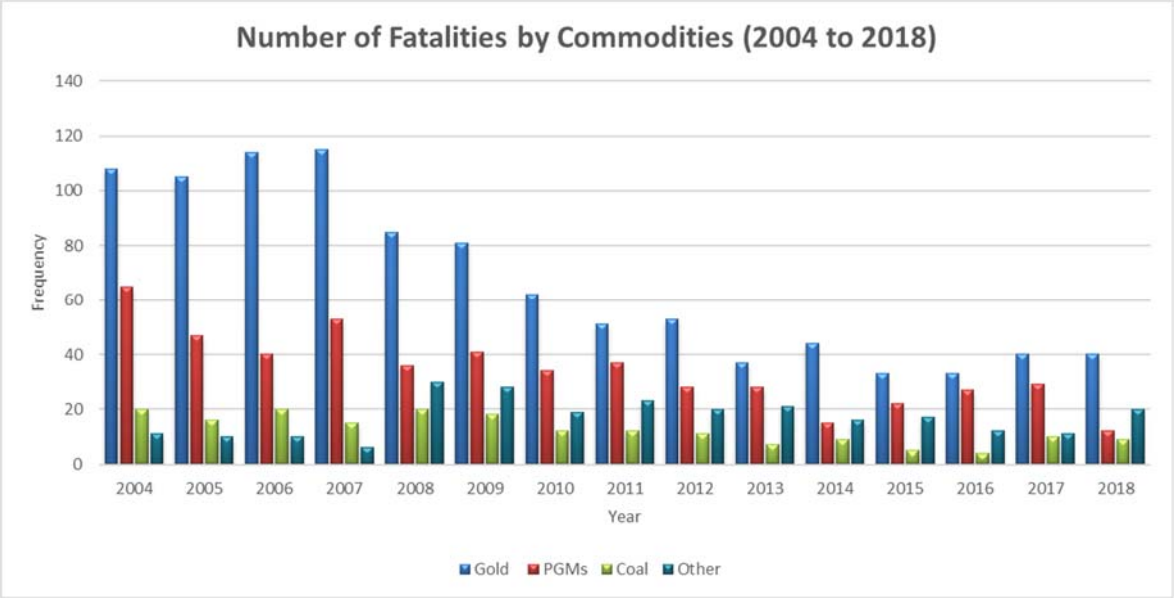



**Figure 1: South African Mine Fatalities by Commodity (Minerals Council South Africa, 2019)**

Manganese ore is used in the manufacture of steel. It gives the steel strength and hardness. South Africa accounts for about 78% of the world's identified manganese reserves, with Ukraine in second place accounting for approximately 10% (Chamber of Mines, 2016). The Transvaal Supergroup rocks host some of the largest deposits of iron and manganese in the world. A large iron ore mine near the town of Kathu in the Northern Cape (Sishen Iron Ore) possesses a potential of 1000 Mt of ore in its high grade (65% iron) haematite deposit (Van Schalkwyk and Beukes 1986). The Kalahari Manganese Field, the northwest of Kuruman, is one of the biggest occurrences, with the Hotazel formation (Voelwater subgroup) containing over 13,600 Mt of ore with a manganese content of over 20% (Beukes and Dreyer, 1986).

The Kalahari Basin is rich in mineral deposits and has great potential for further mineral exploration and exploitation. In the manganese field, the Mamatwan low-grade deposit is viable for open pit operations, whilst the high-grade Wessels type of deposit is viable for underground operations. South Africa plays a leading role in the mining and supply of manganese. An analysis of the production statistics revealed that the production of manganese and iron ore increased substantially over the past 10 years (Figure 2). Timely mine infrastructure development is required for the production growth to enjoy the increasing commodity prices. However, tunnelling in the Kalahari rock masses has challenges that are to be addressed and risks mitigated for future growth. There is no satisfactory replacement for manganese and new projects are envisaged to benefit from the high cyclic prices.

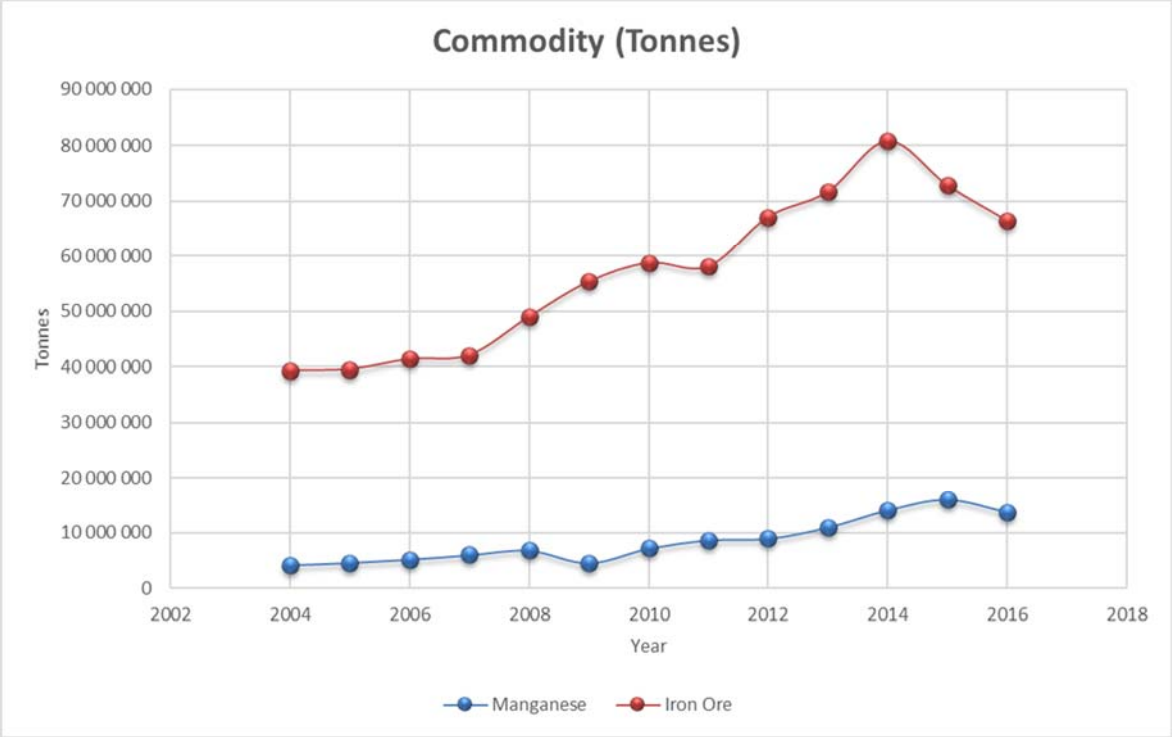



**Figure 2: Annual Production per Commodity, June 2004-June 2016 (Chamber of Mines, 2016)**

Figure 3 shows the distribution and thickness of the Kalahari Group across southern Africa. The entire Early Proterozoic (2300 to 2100 Ma) Kalahari manganese field (Gutzmer et al., 1997) in the Kuruman area is covered by calcretized sediments of the Cenozoic Kalahari Group (Key et al., 1998; Gutzmer et al., 1997; Thomas & Shaw, 1990; Jennings, 1986; Nel et al., 1986).

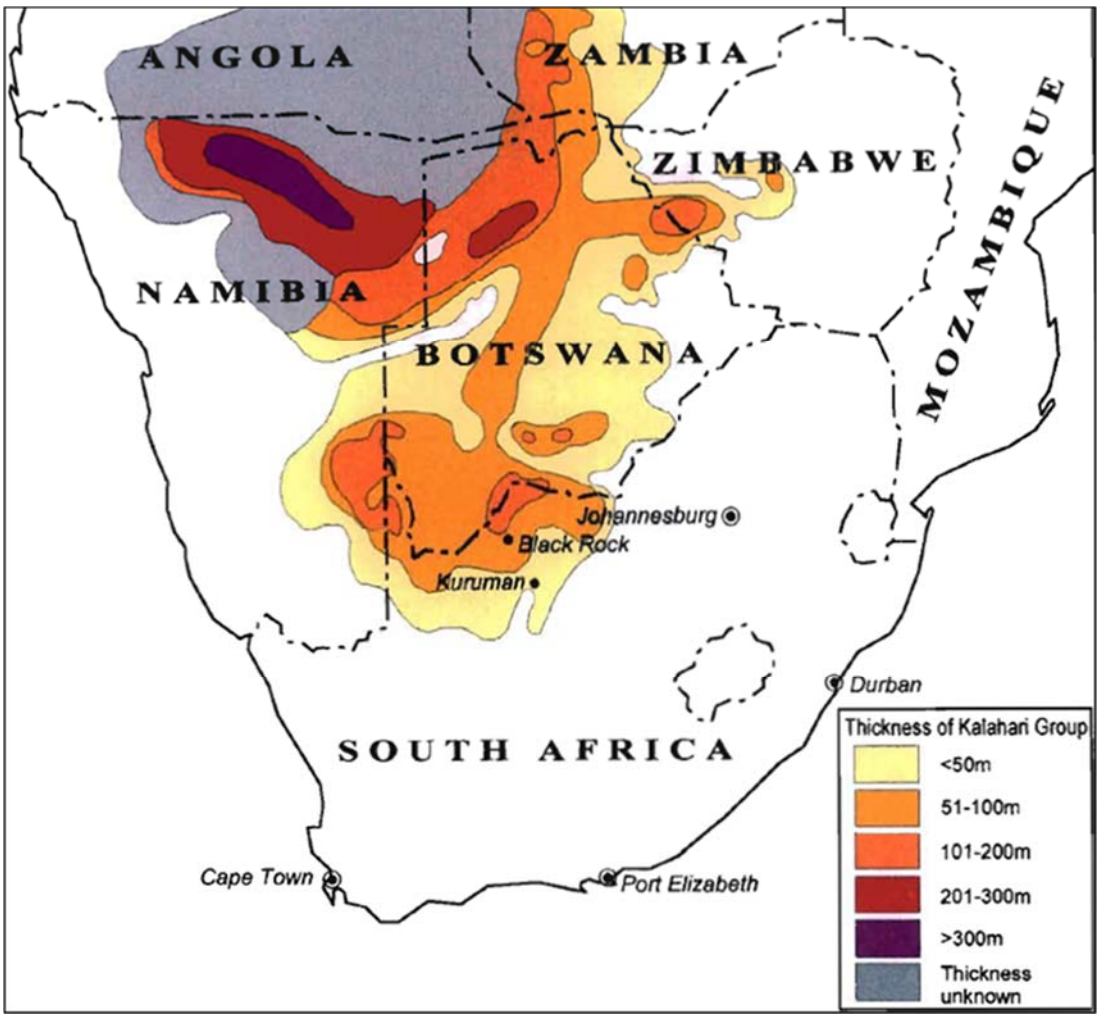



**Figure 3: Distribution and Thickness of the Kalahari Group of Southern Africa (after Thomas and Shaw, 1990 and Thomas and Shaw, 1991).**

The Kalahari Group has a basal soft, clay gravel of fluvial origin (Wessels Formation), followed by calcareous claystone with interlayered gravel (Budin Formation), overlain by clay-containing calcareous sandstone (Eden Formation) and calcrete of the Mokalanen Formation with the surface Aeolian sand of the Gordonia Formation (Haddon and McCarthy, 2005). The red clay layer in turn unconformably blankets the Olifantshoek Supergroup.

The northern part of the Dwyka Group is characterised by a highly variable lithology, low massive diamictite (± 20 %) and high mudstone/sandstone (± 40 %) content (Visser et al., 1990). The Dwyka consist of diamictite with subordinate vorved shale and mudstone bearing scraped and facetted pebbles, fluvio-gracial gravels, and conglomerate (Johnson et al., 2006). The Ecca Group consists of dark-grey shale and carbon-rich shales with interlayered sandstone (Johnson et al., 2006).

The Voelwater Formation and the underlying Ongeluk Andesite Formation form part of the Cox Subgroup, which in turn form part of the Griqualand West Supergroup. The Ongeluk lavas, which form the basal lithology of the area, formed as a thick shallow-marine volcanic sequence of pillow lavas, massive flows and hyaloclastite (Cornell et al., 1996). The volcanics attain a thickness of approximately 900 m (Jennings, 1986). Both the Griqualand West Supergroup, and the Lucknow and Mapedi Formations of the Olifantshoek Supergroup, are Vaalian in age (Visser, 1984).

Figure 4 provides a simplified stratigraphic column of the geology present at Black Rock, Gloria mine.

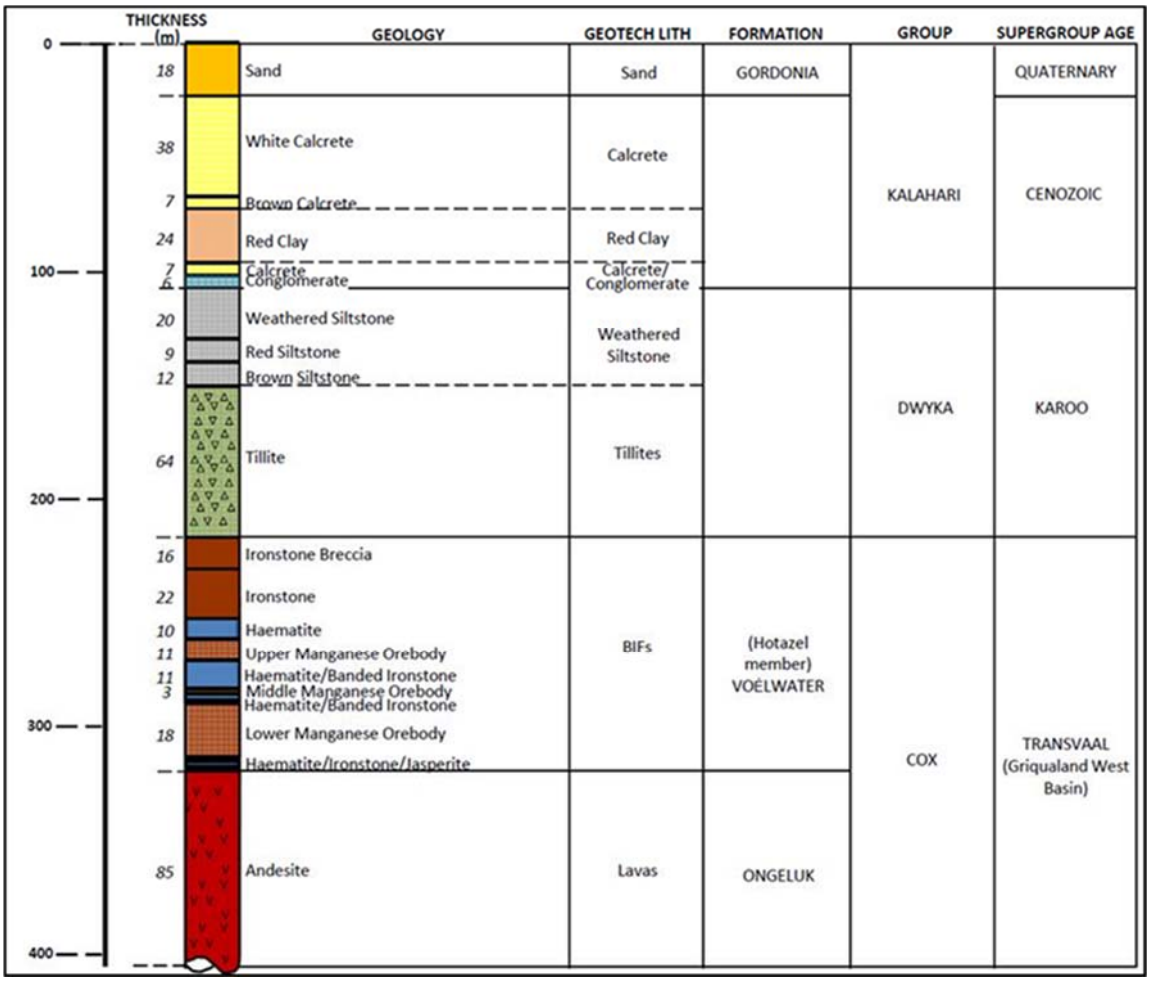



**Figure 4: Simplified Stratigraphy (Council for Geoscience, 2012)**

Operational manganese mines in the Northern Cape have been dealing with some geotechnical challenges in and around underground accesses in the past few years. This can somewhat be related to the age of the underground infrastructure and also the complex nature of the geology and geotechnical environment. The Kalahari group sediments cover the entire Kalahari manganese field. The group comprises unconsolidated sands of the Gordonia Formation, calcretes, calc-arenites, conglomerates and a thick unit of Clay (Tankard et al., 1982). Major weakness zones of Red Clay or weathered rock formation with water inflow present one of the most complex conditions in Kalahari tunnelling. This is significant when the clay is expansive and extremely hygroscopic.

Hygroscopic clay may cause excavation problems, and in severe cases, has caused tunnel collapses resulting in added costs and delays in project delivery. Lengthy delays have been experienced when excavating through the Kalahari formation, especially in the water-bearing gravels, conglomerates and expansive clay horizons. In one operation, flooding of the shaft bottom in Red clay resulted in the failure of the shaft walls (cave-in) creating an enormous void. The void required a tedious and costly corrective process. On another operation, the concrete lining failed in the Red clay section.

In many cases, the assessment of rock support requirements is based mainly on experience, since there are no clearly defined guidelines for the design of tunnels in the Kalahari. Rock mass classification may be applied for empirical estimation of support requirements. In most tunnelling projects it is applied as the practical basis for tunnel support design. Weakness zones containing swelling clay are however not fully covered in any of the most commonly used classification systems e.g. Q system, Rock Mass Rating system and the new Austrian tunnelling method (NATM) (Palmstrom and Broch, 2006). It is recommended that in such ground, special investigations and measurements should be performed and special analyses conducted to evaluate the results with respect to excavation and ground support (Palmstrom and Broch, 2006).

## 1.2 Definition of the Problem

Tunnelling through the challenging Kalahari rock formation is becoming increasingly common, with new mines such as Tshipi, Kalagadi, and Kudumane being developed to access the rich manganese orebodies. The importance of delivery of tunnelling projects on schedule and on cost cannot be overemphasised in this challenging economic environment. Recent instances of cave-in illustrate that tunnelling instabilities are not incidents that belong to the past alone.

The problem identified is that there is insufficient knowledge on support design in weak Kalahari formations containing swelling clay. Therefore, there is a need to effectively discuss swelling and squeezing rock mass failure in the design process for reliable tunnel design. The way experience and empirical support design methods are applied to tunnelling in the Kalahari is largely misunderstood and, in most cases, inappropriate. This is because of the lack of agreed support design concepts for the Kalahari formation and a resulting inadequacy of acceptable design criteria, which are critical in evaluating support performance. The absence of recognized pre-cementation methods for the Kalahari has resulted in the lack of defined evaluation parameters. These parameters are relevant for determining the quality and performance capabilities of grouting materials for the Kalahari.

The research described in this dissertation is aimed at investigating support design criteria that can be implemented. This is done by integrating geotechnical and structural design concepts to optimise the support design and excavability of tunnelling projects. The assessment of geotechnical and hydrogeological parameters upon shaft sinking performance after pre-cementation is aimed at facilitating the determination of the appropriate pre-cementation process and materials to produce satisfactory results. This could enable an informed, unbiased selection of pre-cementation method and grout material that can be used.

## 1.3 Objective and Scope of Research

The objective of this research is to enhance the knowledge of the effect of Red Clay and weathered Kalahari rock formations on ground support using numerical modelling. The main goal was to establish easy to follow practical procedures for estimating ground support in the Kalahari by integrating geotechnical and structural design components into a single package.

The research seeks to meet the following objectives:

- To assess and discuss the relevance of pre-cementation of the unconsolidated Kalahari formation on tunnelling projects.
- To study the applicability/reliability of Two-dimensional (2D) numerical modelling for tunnel support design in a weak and weathered Kalahari rock mass.
- To assess the impact on stability / risk of using 2D plane strain models instead of Three-dimensional (3D) models.
- To outline a support design criterion that integrates geotechnical and structural design components into a single package in the design of shaft lining support.
- To outline a detailed geotechnical risk assessment method for tunnelling in the Kalahari formation.
- To analyse the combined effects of swelling and squeezing of rock mass on tunnel stability in weakness zones containing swelling clay and weathered rock.

## 1.4 Research Methodology

An investigation of pertinent parameters required to understand the geotechnical environment of the Kalahari was carried out. This included a geotechnical site investigation and review of literature on available geological and geotechnical properties. Further, to build a better understanding of tunnel support design in the weak Kalahari formation, numerical modelling was carried out to determine the support requirements. The methodology adopted can be summarized as follows:

- Past research on available geotechnical and geological published literature was reviewed.
- Past research on previous tunnelling projects and experience in the area was reviewed.
- Geotechnical site investigation, borehole drilling and core logging for rock mass characterisation and rock/soil sample laboratory testing to determine parameters for design.
- Study of groundwater conditions was done to quantify the risk of mud rush or cave-in during tunnelling.
- The execution of pre-cementation of the unconsolidated Kalahari rock mass to fill voids and increase the strength of the rock mass.
- Small scale tunnelling project stability and support design evaluation (Case study).
- Comparison of the assessed Factor of Safety (FOS) and deformation, using 2D vs. 3D models.

## 1.5 Content of Dissertation

Chapter 1, the present chapter, provides an overview of the problem, and the work carried out. Chapter 2 details the concepts and literature about the geotechnical design of small scale tunnels through the Kalahari rock masses. Covered in this Chapter is a discussion on site investigation, rock mass classification, swelling rock mass, and pre-cementation.

The design criteria, based on integrating geotechnical and structural design components, are also covered in this chapter. Chapter 3 presents the methodology used to define the geotechnical setting and numerical models analysed in the study. Chapter 4 discusses the numerical analysis of small scale tunnelling through the weak Kalahari formation with a focus on the selection of appropriate lining thickness. It also includes a discussion of the results in the chapter. A discussion of the principal findings of this research is presented in Chapter 5, as well as conclusions and recommendations for future work. Finally, the appendices include detailed information on various items covered in the research.

# 2 LITERATURE REVIEW

Chapter 1 summed up the problem, the objectives of the research and the research methodology. It was established in Chapter 1 that the geotechnical risks and support design criteria of tunnelling in the Kalahari formation cannot be overlooked. This prompted a review of the literature to better predict the behaviour of the rock mass during and post excavation. Various design tools have been developed for geotechnical engineering, these include the construction of a geological and rock mass model from site investigation and the application of rock mass classification systems. The geotechnical theories relevant to site investigation, rock mass classification, rock mass behaviour, rock mass strengthening, and tunnel support design are outlined in Chapter 2. A summary of the literature survey is given at the end of the chapter.

## 2.1 Site Investigation

Unforeseen geological conditions and the associated geotechnical problems are a major contributor to cost and schedule overruns on large civil engineering projects (Hoek & Palmeiri, 1998). The best solution is to define the geological and geotechnical conditions early and as accurately as possible through a detailed site investigation. A site investigation provides means through which geological, geohydrological and geotechnical information is acquired to develop a model of the rock mass. A geological or geotechnical model provides a 3D view of the subsurface for a project site or area of study. The basis for any tunnel or underground work design hinges on an accurate geological and geotechnical model (Fookes, 1997; Hoek & Palmeiri, 1998; Knill, 2003; Baynes, 2010).

The fact that an investigation has been carried out and reported can offer a false sense of confidence. Unless the information collected is of high quality, uncertainty within the rock mass model will, therefore, arise both from inadequacy and error (Clayton et al., 1995). Site investigation should be an integral part of the construction process. Unfortunately, it is often seen as a necessary evil — a process which must be passed through by a designer if he or she is to avoid being thought incompetent, but one which shows little of value and takes precious time and money (Clayton et al., 1995). This is an unfortunate way in which site investigation is viewed and, if it is not targeted to precise geotechnical issues, then it is of little value.

### 2.1.1 Phase I Study- Preliminary Site Review

A desktop study and walkover survey are two essential components of a site investigation. They are performed at the onset of a site investigation to provide as much information on the expected ground conditions and the possible challenges they will pose to the project. This information is also necessary for the development of a strategic site investigation plan. A desktop study provides invaluable information pertaining to site conditions, previous experiences and land use, at a minimum cost (Hoek & Palmeiri, 1988; Hoek, 1999). A thorough desktop study will also allow for a more focused field investigation which lowers overall site investigation costs (Clayton et al., 1995). The walkover survey is carried out after a desktop study has been completed, and once preliminary plans have been made for any ground investigation site work. This is done to gain valuable information on the geology, likely construction problems and to assess access for the investigation team and equipment (Clayton et al., 1995).

A Phase 1 review should incorporate the study of all published data for the region. It should be used not only to look at the project site (which will usually be in the control of the client) but also at its surrounding areas. Phase I results should be properly presented in a report which brings together the details of:

- Site topography
- Geology
- Hydrogeology
- Geotechnical problems and parameters
- Existing works and services
- Previous land use
- Expected project risk and
- Proposed ground investigation methods

Review of previous works in the region as well as existing laboratory and field testing data provides local insight into the geotechnical behaviour of the subsurface. Local experience may also provide insight into the predictability of conditions, the ability for subsurface data correlation and the minimum amount of additional ground investigation required to develop the complete model (Fookes, 1997).

### 2.1.2 Phase II Study- Subsurface Investigation

The Phase II subsurface investigation is used to substantiate the initial rock mass model developed from the desktop study and walkover review. Subsurface investigations involve direct (drilling, probing and trial pitting) and/ or indirect methods (geophysical methods) (Clayton et al., 1995). In most cases, a direct method of investigation which involves subsurface drilling coupled with in situ or laboratory tests is primarily used. Direct ground investigations, in conjunction with field testing and subsequent laboratory testing constitute most of the subsurface investigation scheme (Clayton et al., 1995).

The primary functions of any ground investigation process are:

- Locating specific ‘targets’, such as voids and geological features.
- Determining the lateral variability of the rock mass.
- Profiling, including the determination of groundwater conditions.
- Rock mass classification and parameters determination.

Rock coring provides a one-dimensional profile of the subsurface, which under appropriate circumstances, may be correlated with additional nearby boreholes to develop a two or three-dimensional section or model (Knill, 2003). Borehole core is logged for geological and geotechnical details including rock type; discontinuity spacing and condition; qualitative strength; core recovery and Rock Quality Designation index (RQD). Sampling is carried out on the rock types for laboratory testing.

RQD was developed by Deere to provide a quantitative estimate of rock mass quality from drill core logs (Deere et al.,1967). In geotechnical core logging, the RQD value for each unit of the core (run) is recorded together with core recovery values. RQD is defined as the percentage of intact core pieces greater than 10 cm in length over the total length of the core run (Figure 5) (Deere, 1989). RQD provides a way of correlating natural fracturing intensity with engineering performance of a rock mass. It is required for the application of classification systems, as discussed in Section 2.2.

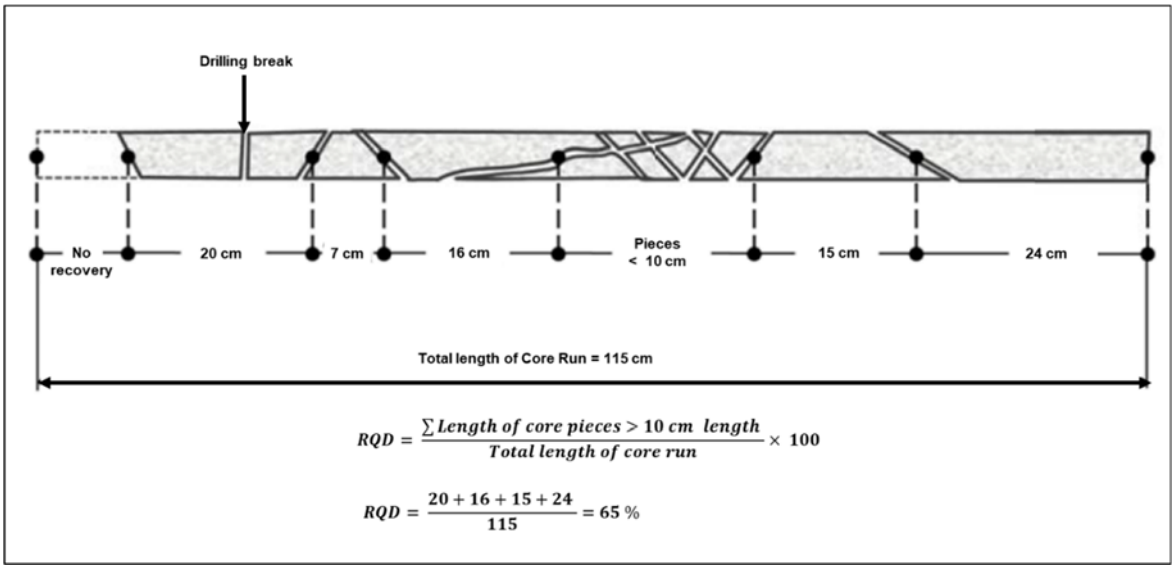



**Figure 5: Procedure for Measurement and Calculation of RQD (After Deere, 1989).**

For tunnelling projects in the Kalahari formation, geophysical methods may be used to delineate the upper layer topography of Red clay unit (vertical profiling), identify potential cavities and areas where groundwater may accumulate causing favourable conditions for potential influx during construction or development. Commonly applied geophysical techniques include seismic refraction and ground penetration radar surveys (Hoek, 2007). The success of a geophysical survey will depend upon the choice of the best geophysical method, and the best geophysical method is likely to be the one which is most sensitive to the variation in the ground properties associated with the target (Clayton et al., 1995). Geophysical methods are often used together with a drilling scheme, to allow far more precise interpolation between boreholes (Knill, 2003).

The design of excavations in rock involves, among other things, the evaluation of the mechanical properties of rock materials. For reasons of economics, it is never feasible to measure fully the characteristics of a complex rock mass (Bieniawski, 1974). Different laboratory testing methods exist depending on the rock type and quality of core obtained. The most common laboratory strength tests are intact compressive strength, deformability, and degradability. Unconfined Compressive Strength (UCS) tests and point load index tests are regularly used for the determination of intact material strength, while abrasive tests are used to assess the material “hardness” for the determination of appropriate mechanical excavation tools. Deformation constants are the most important parameters in design as they are used in numerical evaluation. In the case of swelling rock units, swelling and slaking tests may be performed to quantify the behaviour of the rock when exposed to water and/or air.

## 2.2 Rock Mass Classification Systems

Site investigation provides an insight into the properties of the rock mass present at the site. The behaviour of the rock mass during excavation is not certain and will not be until completion of the project. Uncertainty in ground conditions, whatever the origin, contributes to the jeopardy that the project will not meet cost or programme targets, or proving on completion to be inadequate or could fail (Knill 2003). To minimize this uncertainty of rock mass behaviour, it is common practice in engineering design to use various classification systems to predict the rock mass behaviour.

Classification systems are empirical correlations between various quantifiable rock mass properties and the observed mechanical behaviour during excavations (Crockford, 2012). The three most widely used classification systems are Rock Mass Rating (Bieniawski, 1989); Rock Tunnelling Quality Index (Barton et al., 1974); and Geological Strength Index (Hoek et al., 1992). When applying empirical systems to a given project, it is imperative that the systems are being applied in conditions for which they were developed (Bieniawski, 1989). A classification system loses relevance and reliability when applied in a field for which it is not designed, or when it is applied to a site with conditions which were not analysed in the empirical development of the system (Hoek, 2007). By reviewing the development and source of the classification system's empirical data, the relevance of a given system can be determined for a given project.

### 2.2.1 Rock Mass Rating System

The Rock Mass Rating (RMR) system, or the Geomechanics Classification system, was developed by Bieniawski during 1972 to 1973 in South Africa to assess the stability and support requirements of tunnels (Bieniawski, 1973a). Since then, it has been successfully refined and improved by Bieniawski and other authors to apply the RMR system in other geotechnical fields such as mining, slopes, and dam foundations. In the process of developing alternative applications, the RMR system benefitted from the inclusion of numerous additional case studies which enabled Bieniawski to refine the system further, to RMR89 commonly used today. Initially 49 case histories were used for the formulation of the system, adding 62 coal mining cases in 1984, and 78 tunnelling and mining cases in 1987. For the revised RMR in 1989, the system had been applied to 351 cases. The distribution of applications, rock types, span ranges, depth ranges, and RMR ratings are shown in Figure 6 (Bieniawski, 1989).

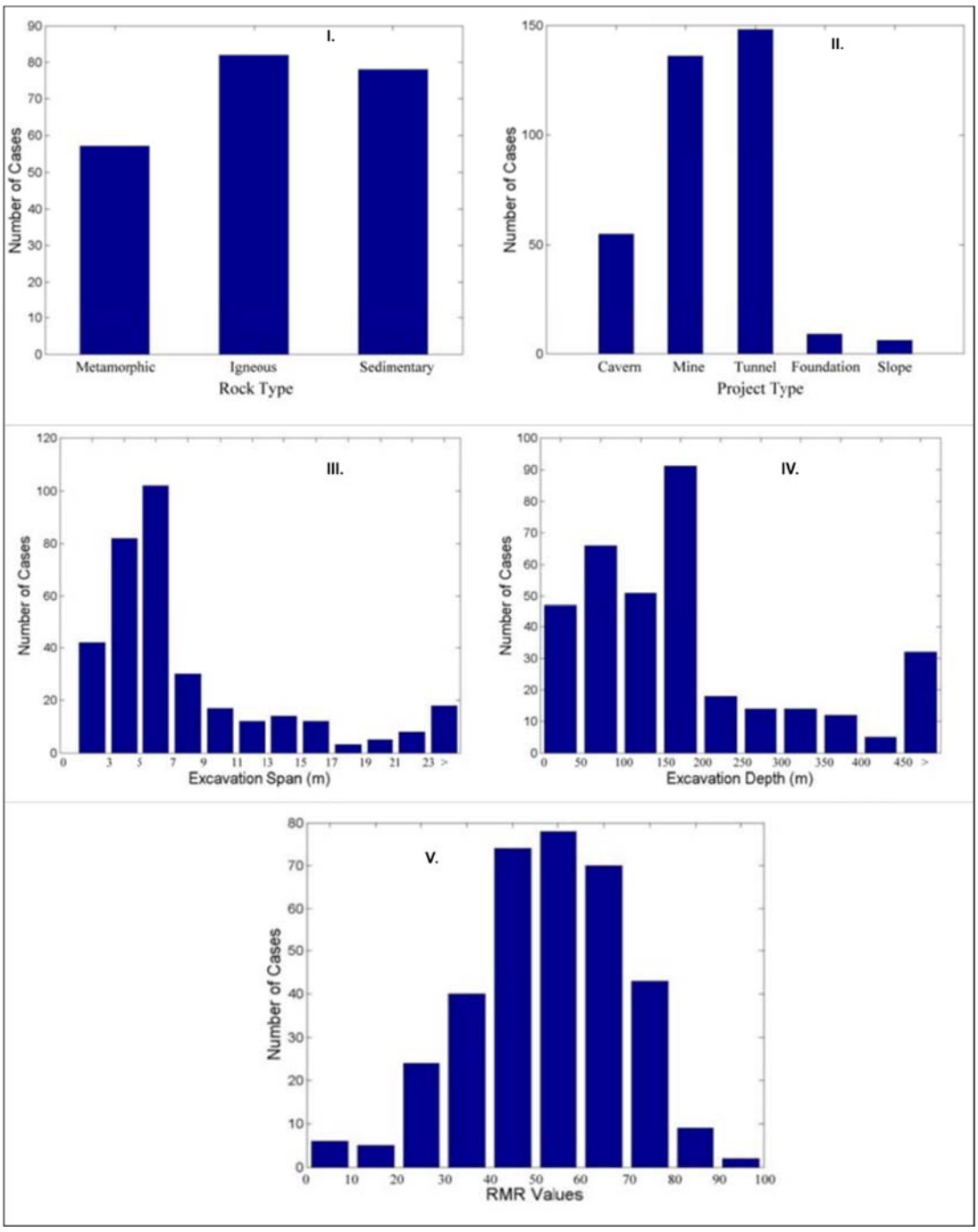



**Figure 6: Empirical data used in the development of the Rock Mass Rating system, I.-Rock types recorded, II.-Case history project types, III.- The range of case excavation spans, IV.- Range of case histories excavation depths and V.-Range of calculated RMR values (after Bieniawski, 1989)**

The RMR system uses a few basic parameters relating to the geometry and mechanical conditions of the rock mass. Six parameters are used to classify the rock mass, and these are characterized during site investigation. These six parameters are the UCS of the rock, RQD, the spacing of discontinuities, the condition of discontinuities, the groundwater conditions, and the orientation of discontinuities.

The parameters are assigned values using Bieniawski's RMR chart shown in Table 1, and appropriate RMR values for each parameter (Section A and D of the chart) are selected and summed. The summed values are then assigned a rock mass class (Section E of the chart), which then may be used to determine the average standup time, the cohesion of the rock mass, and the friction angle of the rock mass (Section F). From the classification of the rock mass, Bieniawski provides suggested support options for a 10.0 m span drill and blast tunnel, as shown in Table 2 (Bieniawski, 1989).

In applying this classification system, the rock mass is divided into a number of structural units, and each unit is classified separately. The boundaries of the structural units usually coincide with a major structural feature such as a fault or with a change in rock type. In some cases, significant changes in discontinuity spacing or characteristics, within the same rock type, may necessitate the division of the rock mass into a number of small structural units (Bieniawski, 1989).

**Table 1: Rock Mass Rating System (Bieniawski, 1989)**

**(a) Five basic rock mass classification parameters and their ratings**

| | Parameter | | Range of Vaules | | | | | | |
|---|---|---|---|---|---|---|---|---|---|
| 1 | Strength of intact rock material | Point load strength index (MPa) | >10 | 4–10 | 2–4 | 1–2 | for this low range uniaxial compressive strength is preferred | | |
| | | Uniaxial Compressive Strength (MPa) | >250 | 100–250 | 50–100 | 25–50 | 5–25 | 1–5 | <1 |
| | | Rating | 15 | 12 | 7 | 4 | 2 | 1 | 0 |
| 2 | Drill Core Quality RQD (%) | | 90–100 | 75–90 | 50–75 | 25–50 | <25 | | |
| | Rating | | 20 | 17 | 13 | 8 | 3 | | |
| 3 | Joint Spacing (m) | | >2 | 0.6-2 | 0.2–0.6 | 0.06–0.2 | <0.06 | | |
| | Rating | | 20 | 15 | 10 | 8 | 5 | | |
| 4 | Condition of Joints | | Not continuous, very rough surfaces, unweathered, no separation | Slightly weathered surfaces, slightly weathered, separation < 1 mm | Slightly rough surfaces, highly weathered, separation < 1 mm | Continuous, slickensided surfaces, or gouge < 5mm thick, or separation 1–5 mm | Continuous joints, soft gouge > 5mm thick, or separation > 5 mm | | |
| | Rating | | 30 | 25 | 20 | 10 | 0 | | |
| 5 | Groundwater | Inflow per 10 m tunnel length (1/min) | none | <10 | 10–25 | 25–125 | >125 | | |
| | | Joint water pressure / major in situ stress | 0 | 0–0.1 | 0.1–0.2 | 0.2–0.5 | >0.5 | | |
| | | General conditions | dry | damp | wet | dripping | flowing | | |
| | Rating | | 15 | 10 | 7 | 4 | 0 | | |

**(b) Guidelines for classification of discontinuity conditions**

| Parameter | Ratings | | | | |
|---|---|---|---|---|---|
| Discontinuity length (persistence) | <1 m | 1–3 m | 3–10 m | 10–20 m | >20 m |
| | 6 | 4 | 2 | 1 | 0 |
| Separation (aperture) | None | <0.1 mm | 0.1–1.0 mm | 1–5 mm | >5 mm |
| | 6 | 5 | 4 | 1 | 0 |
| Roughness | Very rough | Rough | Slightly rough | Smooth | Slickensided |
| | 6 | 5 | 3 | 1 | 0 |
| Infilling (gouge) | Hard filling | | | Soft filling | |
| | None | <5 mm | >5 mm | <5 mm | >5 mm |
| | 6 | 4 | 2 | 2 | 0 |
| Weathering | Unweathered | Slightly weathered | Moderately weathered | Highly weathered | Decomposed |
| | 6 | 5 | 3 | 1 | 0 |

**(c) Effects of joint orientation in tunneling**

| Strike perpendicular to tunnel axis | | | | Strike parallel to tunnel axis | | Dip 0° – 20° |
|---|---|---|---|---|---|---|
| Drive with dip | | Drive against dip | | | | |
| Dip 45° – 90° | Dip 20° – 45° | Dip 45° – 90° | Dip 20° – 45° | Dip 45° – 90° | Dip 20° – 45° | Irrespective of strike |
| Very favorable | favorable | fair | unfavorable | Very unfavorable | fair | fair |

**(d) Rating adjustment for joint orientations**

| Strike and dip orientation of joints | | Very favorable | favorable | fair | unfavorable | Very unfavorable |
|---|---|---|---|---|---|---|
| Ratings | Tunnels | 0 | -2 | -5 | -10 | -12 |
| | Foundations | 0 | -2 | -7 | -15 | -25 |
| | Slopes | 0 | -5 | -25 | -50 | -60 |

**(e) Rock mass classes determined from total ratings**

| Rating | 100-81 | 80-61 | 60-41 | 40-21 | <20 |
|---|---|---|---|---|---|
| Class no. | I | II | III | IV | V |
| Description | Very good rock | Good rock | Fair rock | Poor rock | Very poor rock |

**(f) Meaning of rock mass classes**

| Class no. | I | II | III | IV | V |
|---|---|---|---|---|---|
| Average stand-up time | 20 years for 15 m span | 1 year for 10 m span | 1 week for 5 m span | 10 hours for 2.5 m span | 30 minutes for 1 m span |
| Cohesion of rock mass (kPa) | >400 | 300–400 | 200–300 | 100–200 | <100 |
| Friction angle of rock mass (degrees) | >45 | 35–45 | 25–35 | 15–25 | <15 |

RMR = Σ (classification parameters) + discontinuity orientation adjustment

**Table 2: Guidelines for excavation and Support of 10 m span rock tunnels in accordance with the RMR system (After Bieniawski, 1989).**

| Rock mass class | Excavation | Rock bolts (20 mm diameter, fully grouted) | Shotcrete | Steel sets |
|---|---|---|---|---|
| I - Very good rock *RMR*: 81-100 | Full face, 3 m advance. | Generally no support required except spot bolting. | | |
| II - Good rock *RMR*: 61-80 | Full face , 1-1.5 m advance. Complete support 20 m from face. | Locally, bolts in crown 3 m long, spaced 2.5 m with occasional wire mesh. | 50 mm in crown where required. | None. |
| III - Fair rock *RMR*: 41-60 | Top heading and bench 1.5-3 m advance in top heading. Commence support after each blast. Complete support 10 m from face. | Systematic bolts 4 m long, spaced 1.5 - 2 m in crown and walls with wire mesh in crown. | 50-100 mm in crown and 30 mm in sides. | None. |
| IV - Poor rock *RMR*: 21-40 | Top heading and bench 1.0-1.5 m advance in top heading. Install support concurrently with excavation, 10 m from face. | Systematic bolts 4-5 m long, spaced 1-1.5 m in crown and walls with wire mesh. | 100-150 mm in crown and 100 mm in sides. | Light to medium ribs spaced 1.5 m where required. |
| V – Very poor rock *RMR*: < 20 | Multiple drifts 0.5-1.5 m advance in top heading. Install support concurrently with excavation. Shotcrete as soon as possible after blasting. | Systematic bolts 5-6 m long, spaced 1-1.5 m in crown and walls with wire mesh. Bolt invert. | 150-200 mm in crown, 150 mm in sides, and 50 mm on face. | Medium to heavy ribs spaced 0.75 m with steel lagging and forepoling if required. Close invert. |

### 2.2.2 Rock Tunneling Quality Index

The Rock Tunnelling Quality Index, commonly known as the Q-System, was developed to quantitatively classify a rock mass to facilitate the design of a tunnel support system. The system was developed in 1974 by Barton, Lien, and Lunde at the Norwegian Geotechnical Institute (NGI), Norway, using 212 case records (Barton et al, 1974). These case histories were predominantly sourced from Scandinavian projects in hard rock conditions using 13 types of igneous rock, 26 types of metamorphic rock and 11 types of sedimentary rock. Of the 212 cases, 21 of the cases were within gneiss, and 48 of the cases were within granite (Barton, 1988). Among these, 180 were supported excavations and the rest permanently unsupported. The Q-system has since been adapted from a drill and blast tunnelling tool for use in TBM tunnels (Barton & Abrahao, 2003).

Similar to the RMR system, the Q-System uses six parameters characterized during the site investigation process in order to classify the rock mass. The six parameters are the RQD, the joint set number (Jn), unfavourable joint conditions (roughness and alteration), water inflow and the stress condition. The six parameters are assigned numerical values based on field observations, whether outcrop or core log, using Table 3 to Table 8. (Barton et al., 1974; NGI, 2015). NGI has continuously improved and updated the system and produced the Q-system handbook in 2012 and 2015 as a summary of NGI's Best Practice.

The numerical value of the rock mass quality Q is defined by the six parameters grouped into three quotients:

$$Q = \frac{RQD}{J_n} \cdot \frac{J_r}{J_a} \cdot \frac{J_w}{SRF} \qquad \text{Equation 1}$$

Where:

- RQD is Deere's Rock Quality Designation
- Joint Set Number (Jn)
- Joint roughness (Jr)
- Joint Alteration (Ja)
- Joint Water Factor (Jw)
- Stress Reduction Factor (SRF)

The first quotient (***RQD/$J_n$***) represents the structure of the rock mass, a crude measure of the block or particle size. The second quotient (***$J_r$/$J_a$***) represents the inter-block shear strength. The third quotient (***$J_w$/SRF***) is a complicated empirical factor describing the 'active stress'. SRF can be regarded as a total stress parameter. The parameter ***$J_w$*** is a measure of water pressure, which has an adverse effect on the shear strength of joints due to a reduction in effective normal stress. Each of the six parameters is determined according to a description found in Table 3 to Table 8.

**Table 3: RQD-values and volumetric jointing (NGI, 2015)**

| 1 RQD (Rock Quality Designation) | | | RQD |
|---|---|---|---|
| A | Very poor | (> 27 joints per $m^3$ ) | 0-25 |
| B | Poor | (20-27 joints per $m^3$) | 25-50 |
| C | Fair | (13-19 joints per $m^3$ ) | 50-75 |
| D | Good | (8-12 joints per $m^3$ ) | 75-90 |
| E | Excellent | (0-7 joints per $m^3$ ) | 90-100 |
| Note: i) Where RQD is reported or measured as ≤ 10 (including 0) the value 10 is used to evaluate the Q-value<br>ii) RQD-intervals of 5, i.e. 100, 95, 90, etc., are sufficiently accurate | | | |

**Table 4: Jn – values (NGI, 2015)**

| 2 Joint set number | | $J_n$ |
|---|---|---|
| A | Massive, no or few joints | 0.5-1.0 |
| B | One joint set | 2 |
| C | One joint set plus random joints | 3 |
| D | Two joint sets | 4 |
| E | Two joint sets plus random joints | 6 |
| F | Three joint sets | 9 |
| G | Three joint sets plus random joints | 12 |
| H | Four or more joint sets, random heavily jointed "sugar cube", etc | 15 |
| J | Crushed rock, earth like | 20 |
| Note: i) For tunnel intersections, use 3 x $J_n$<br>ii) For portals, use 2 x $J_n$ | | |

**Table 5: Jr – values (NGI, 2015)**

| 3 Joint Roughness Number | | $J_r$ |
|---|---|---|
| ***a)*** *Rock-wall contact, and*<br>***b)*** *Rock-wall contact before 10 cm of shear movement* | | |
| A | Discontinuous joints | 4 |
| B | Rough or irregular, undulating | 3 |
| C | Smooth, undulating | 2 |
| D | Slickensided, undulating | 1.5 |
| E | Rough, irregular, planar | 1.5 |
| F | Smooth, planar | 1 |
| G | Slickensided, planar | 0.5 |
| Note: i) Description refers to small scale features and intermediate scale features, in that order | | |
| ***c)*** *No rock-wall contact when sheared* | | |
| H | Zone containing clay minerals thick enough to prevent rock-wall contact when sheared | 1 |
| Note: ii) Add 1 if the mean spacing of the relevant joint set is greater than 3 m (dependent on the size of the underground opening)<br>iii) $J_r$ = 0.5 can be used for planar slickensided joints having lineations, provided the lineations are oriented in the estimated sliding direction | | |

**Table 6: Ja – values (NGI, 2015)**

| 4 | Joint Alteration Number | $\Phi_r$ approx. | $J_a$ |
|---|---|---|---|
| ***a)*** *Rock-wall contact (no mineral fillings, only coatings)* | | | |
| A | Tightly healed, hard, non-softening, impermeable filling, i.e., quartz or epidote. | | 0.75 |
| B | Unaltered joint walls, surface staining only. | 25-35° | 1 |
| C | Slightly altered joint walls. Non-softening mineral coatings; sandy particles, clay-free disintegrated rock, etc. | 25-30° | 2 |
| D | Silty or sandy clay coatings, small clay fraction (non-softening). | 20-25° | 3 |
| E | Softening or low friction clay mineral coatings, i.e., kaolinite or mica. Also chlorite, talc gypsum, graphite, etc., and small quantities of swelling clays. | 8-16° | 4 |
| ***b)*** *Rock-wall contact before 10 cm shear (thin mineral fillings)* | | | |
| F | Sandy particles, clay-free disintegrated rock, etc. | 25-30° | 4 |
| G | Strongly over-consolidated, non-softening, clay mineral fillings (continuous, but <5 mm thickness). | 16-24° | 6 |
| H | Medium or low over-consolidation, softening, clay mineral fillings (continuous, but <5 mm thickness). | 12-16° | 8 |
| J | Swelling-clay fillings, i.e., montmorillonite (continuous, but <5 mm thickness). Value of $J_a$ depends on percent of swelling clay-size particles. | 6-12° | 8-12 |
| ***c)*** *No rock-wall contact when sheared (thick mineral fillings)* | | | |
| K | Zones or bands of disintegrated or crushed rock. Strongly over-consolidated. | 16-24° | 6 |
| L | Zones or bands of clay, disintegrated or crushed rock. Medium or low over-consolidation or softening fillings. | 12-16° | 8 |
| M | Zones or bands of clay, disintegrated or crushed rock. Swelling clay. $J_a$ depends on percent of swelling clay-size particles. | 6-12° | 8-12 |
| N | Thick continuous zones or bands of clay. Strongly over-consolidated. | 12-16° | 10 |
| O | Thick, continuous zones or bands of clay. Medium to low over-consolidation. | 12-16° | 13 |
| P | Thick, continuous zones or bands with clay. Swelling clay. $J_a$ depends on percent of swelling clay-size particles. | 6-12° | 13-20 |

**Table 7: Jw – values (NGI, 2015)**

| 5 | Joint Water Reduction Factor | $J_w$ |
|---|---|---|
| A | Dry excavations or minor inflow ( humid or a few drips) | 1.0 |
| B | Medium inflow, occasional outwash of joint fillings (many drips/"rain") | 0.66 |
| C | Jet inflow or high pressure in competent rock with unfilled joints | 0.5 |
| D | Large inflow or high pressure, considerable outwash of joint fillings | 0.33 |
| E | Exceptionally high inflow or water pressure decaying with time. Causes outwash of material and perhaps cave in | 0.2-0.1 |
| F | Exceptionally high inflow or water pressure continuing without noticeable decay. Causes outwash of material and perhaps cave in | 0.1-0.05 |

Note: i) Factors C to F are crude estimates. Increase $J_w$ if the rock is drained or grouting is carried out

ii) Special problems caused by ice formation are not considered

**Table 8: SRF-values (NGI, 2015)**

| 6 Stress Reduction Factor | | | | SRF |
|---|---|---|---|---|
| ***a)*** *Weak zones intersecting the underground opening, which may cause loosening of rock mass* | | | | |
| A | Multiple occurrences of weak zones within a short section containing clay or chemically disintegrated, very loose surrounding rock (any depth), or long sections with incompetent (weak) rock (any depth). For squeezing, see 6L and 6M | | | 10 |
| B | Multiple shear zones within a short section in competent clay-free rock with loose surrounding rock (any depth) | | | 7.5 |
| C | Single weak zones with or without clay or chemical disintegrated rock (depth ≤ 50m) | | | 5 |
| D | Loose, open joints, heavily jointed or "sugar cube", etc. (any depth) | | | 5 |
| E | Single weak zones with or without clay or chemical disintegrated rock (depth > 50m) | | | 2.5 |
| Note: i) Reduce these values of SRF by 25-50% if the weak zones only influence but do not intersect the underground opening | | | | |
| ***b)*** *Competent, mainly massive rock, stress problems* | | $\sigma_c / \sigma_1$ | $\sigma_\theta / \sigma_c$ | **SRF** |
| F | Low stress, near surface, open joints | >200 | <0.01 | 2.5 |
| G | Medium stress, favourable stress condition | 200-10 | 0.01-0.3 | 1 |
| H | High stress, very tight structure. Usually favourable to stability. May also be unfavourable to stability dependent on the orientation of stresses compared to jointing/weakness planes* | 10-5 | 0.3-0.4 | 0.5-2<br>2-5* |
| J | Moderate spalling and/or slabbing after > 1 hour in massive rock | 5-3 | 0.5-0.65 | 5-50 |
| K | Spalling or rock burst after a few minutes in massive rock | 3-2 | 0.65-1 | 50-200 |
| L | Heavy rock burst and immediate dynamic deformation in massive rock | <2 | >1 | 200-400 |
| Note: ii) For strongly anisotropic virgin stress field (if measured): when $5 \le \sigma_1 / \sigma_3 \le 10$, reduce $\sigma_c$ to $0.75\ \sigma_c$. When $\sigma_1 / \sigma_3 > 10$, reduce $\sigma_c$ to $0.5\ \sigma_c$, where $\sigma_c$ = unconfined compression strength, $\sigma_1$ and $\sigma_3$ are the major and minor principal stresses, and $\sigma_\theta$ = maximum tangential stress (estimated from elastic theory)<br>iii) When the depth of the crown below the surface is less than the span; suggest SRF increase from 2.5 to 5 for such cases (see F) | | | | |
| ***c)*** *Squeezing rock: plastic deformation in incompetent rock under the influence of high pressure* | | | $\sigma_\theta / \sigma_c$ | **SRF** |
| M | Mild squeezing rock pressure | | 1-5 | 5-10 |
| N | Heavy squeezing rock pressure | | >5 | 10-20 |
| Note: iv) Determination of squeezing rock conditions must be made according to relevant literature (i.e. Singh et al., 1992 and Bhasin and Grimstad, 1996) | | | | |
| ***d)*** *Swelling rock: chemical swelling activity depending on the presence of water* | | | | **SRF** |
| O | Mild swelling rock pressure | | | 5-10 |
| P | Heavy swelling rock pressure | | | 10-15 |

Using the Q-system, the rock mass quality is rated on a logarithmic scale where each order of magnitude represents a class of rock quality. High Q-values indicate good stability and low values mean poor stability. To relate the Q value to the stability and support requirements of underground excavations, Barton et al. (1974) defined an additional parameter called the Equivalent Dimension, $D_e$, of the excavation. This dimension is defined as:

$$De = \frac{Span}{ESR} \qquad \text{Equation 2}$$

Where;

ESR = Excavation Support Ratio

The value of ESR is a quantity, related to the use of the excavation and to the degree of safety which is demanded of the support system installed to maintain the stability of the excavation. Barton et al. (1974) and NGI (2015) suggested the following values in Table 9. A low ESR value indicates the need for a high level of safety while higher ESR values indicate that a lower level of safety will be acceptable. It is recommended to use ESR = 1.0 when Q ≤ 0.1 for the types of excavation B, C and D. The reason for that, is that the stability problems may be severe with such low Q-values, perhaps with risk for cave-in (NGI, 2015).

**Table 9: ESR-values (NGI, 2015)**

| 7 | Type of excavation | ESR |
|---|---|---|
| A | Temporary mine openings, etc. | *ca.* 3-5 |
| B | Vertical shafts*: i) circular sections<br>ii) rectangular/square section<br>* Dependant of purpose. May be lower than given values. | *ca.* 2.5<br>*ca.* 2.0 |
| C | Permanent mine openings, water tunnels for hydro power (exclude high pressure penstocks), water supply tunnels, pilot tunnels, drifts and headings for large openings. | 1.6 |
| D | Minor road and railway tunnels, surge chambers, access tunnels, sewage tunnels, etc. | 1.3 |
| E | Power houses, storage rooms, water treatment plants, major road and railway tunnels, civil defence chambers, portals, intersections, etc. | 1.0 |
| F | Underground nuclear power stations, railways stations, sports and public facilitates, factories, etc. | 0.8 |
| G | Very important caverns and underground openings with a long lifetime, ≈ 100 years, or without access for maintenance. | 0.5 |

* The degree of confidence in these figures will be roughly in proportion to the number of relevant case records, hence the ***ca.*** (approximately) for few or no records (Barton et al., 1974)

The chart, where equivalent dimension, $D_e$ is plotted against the value Q, is used to define several support categories. Grimstad and Barton (1993) updated the support chart based on 1050 examples mainly from Norwegian underground excavations. In 2002, an update was made based on more than 900 new examples from underground excavations in Norway, Switzerland, and India. This update also included analytical research with respect to the thickness, spacing, and reinforcement of reinforced ribs of sprayed concrete (RRS) as a function of the load and the rock mass quality (Grimstad et al., 2002).

The updated chart for rock support design reflects the increased use of fibre reinforced shotcrete and the wide application of the reinforced ribs of sprayed concrete. The updated Q support chart based on numerical analysis and deformation measurements of RRS from recent case histories in Norway is shown in Figure 7 (NGI, 2015).

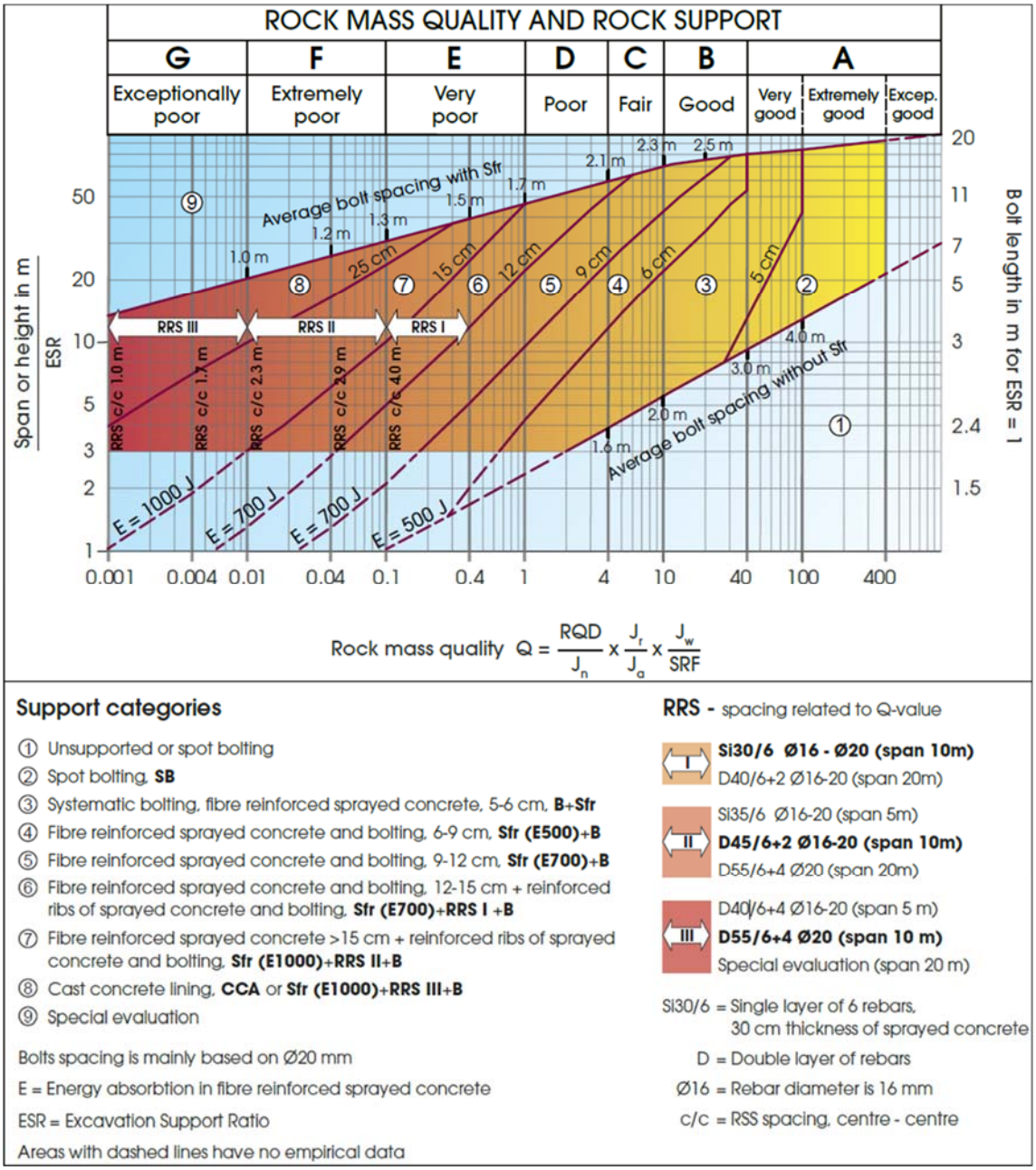



**Figure 7: Guidelines for Excavation and Support of Rock Tunnels in accordance with the Q-System (NGI, 2015).**

### 2.2.3 Geological Strength Index (GSI)

Geological strength index (GSI) varies significantly from the RMR and Q systems, where the rock mass is classified for the estimation of underground excavation and support design. Hoek introduced the GSI to facilitate the determination of rock mass properties of both hard and weak rock masses for use in rock engineering (Hoek, 1994). It was developed for the estimation of rock mass properties, to capture the influence of structures within a rock mass on the strength of the material.

The GSI index was developed out of a need for a quantifiable characterisation of the rock mass for use in the Hoek-Brown failure criterion (Hoek and Brown, 1988). GSI was developed on the recognition that a rock mass failure criterion would have no practical value unless it could be related to geological observations that could be made quickly and easily in the field.

In the early days, the use of modified RMR classification worked well because most of the problems were in reasonable quality rock masses (30<RMR<70) and under moderate stress conditions (Marinos et al., 2005). However, it became obvious that the RMR system was not appropriate for weak rock masses due to its dependence on RQD, wherein such rocks RQD approaches zero (Marinos et al., 2005). The relationship between RMR and the constants of the Hoek-Brown failure criterion begins to breakdown for severely fractured and weak rock masses. GSI does not include RQD, but places emphasis on the rock mass characteristics such as lithology, structure, geological history and discontinuity surface conditions. GSI was developed for use in the Hoek-Brown failure criterion for hard rock cases in Canada (Hoek et al., 1992); work which was further refined in the late nineties (Hoek, 1994; Hoek et al., 1995; Hoek & Brown, 1997). In 1998 the system was expanded to apply to weak rock masses from extensive tunnelling work through incredibly difficult ground in Greece (Hoek et al., 1998; Marinos & Hoek, 2000; 2001).

The GSI of a rock mass is determined using one of several GSI charts, with the general chart for jointed rocks shown in Figure 8. Charts associate the rock mass structure and the discontinuity conditions for a rock mass to determine the influence of the structure on the rock mass by assigning an index value. A high GSI implies that the structure degrades the rock mass to a lesser extent from measured intact properties; whereas a small GSI value indicates the structure largely influences the rock mass strength and intact values are not representative. It is highly recommended by the authors that a range of values be selected to represent a rock mass, and not one individual value (Marinos et al., 2005).

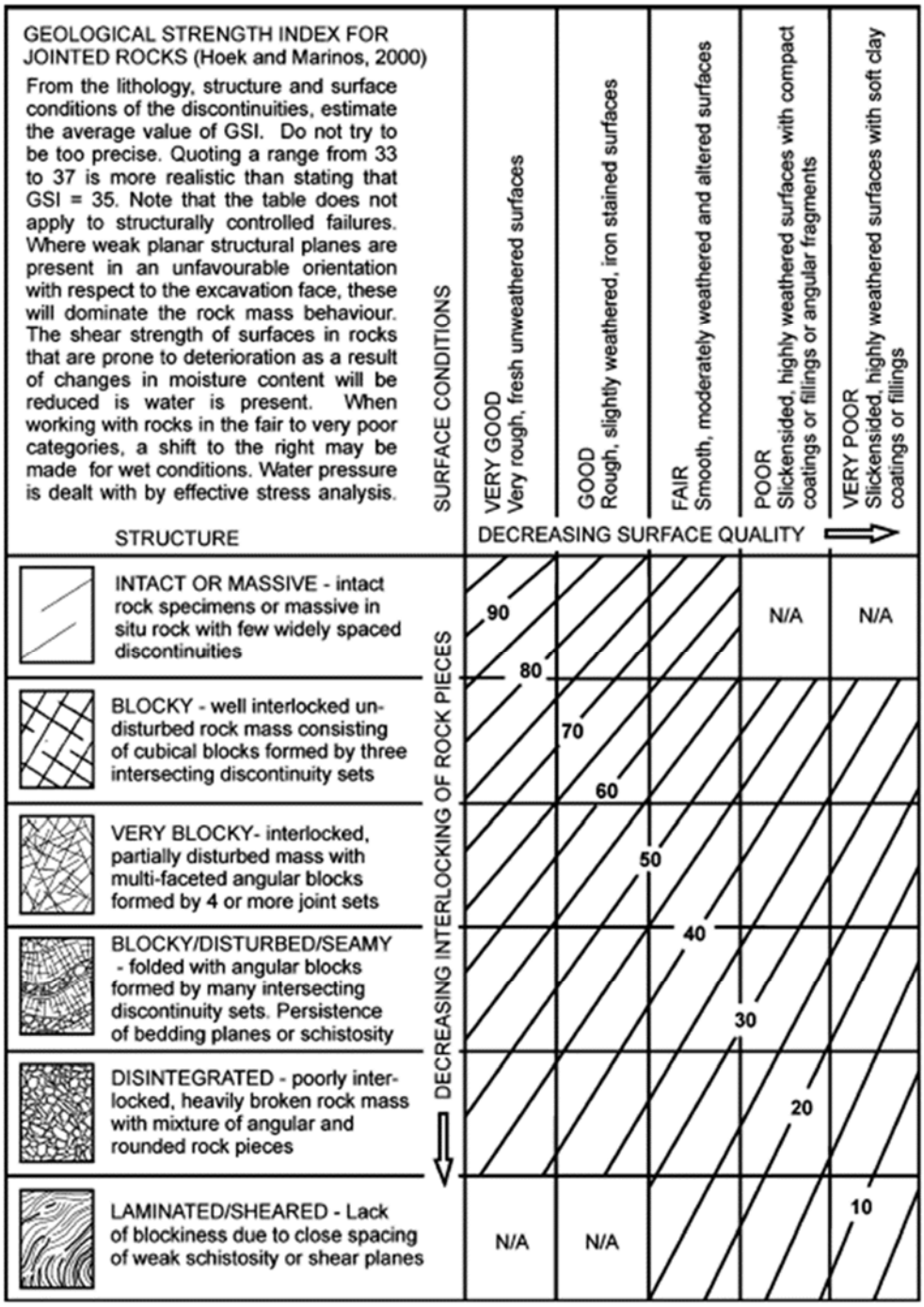



**Figure 8: General chart for GSI estimates from the geological observations (Hoek & Marinos, 2000)**

As mentioned earlier, GSI was adapted to apply to weaker rock masses using case histories from Greece. The modifications are illustrated by the development of the flysch and molasse GSI charts (Marinos & Hoek, 2001; Hoek et al, 2005). The flysch chart, Figure 9, is designed for weak heterogeneous rock masses which have evidence of tectonic fatigue or shear loading; whereas molasse charts are designed for similarly weak heterogeneous rock masses with no tectonic disturbance.

GSI charts for molasse are subdivided into confined or unconfined applications, Figure 10 and Figure 11 respectively. The flysch and molasse charts were designed for specific units and behaviour and should not be broadly applied.

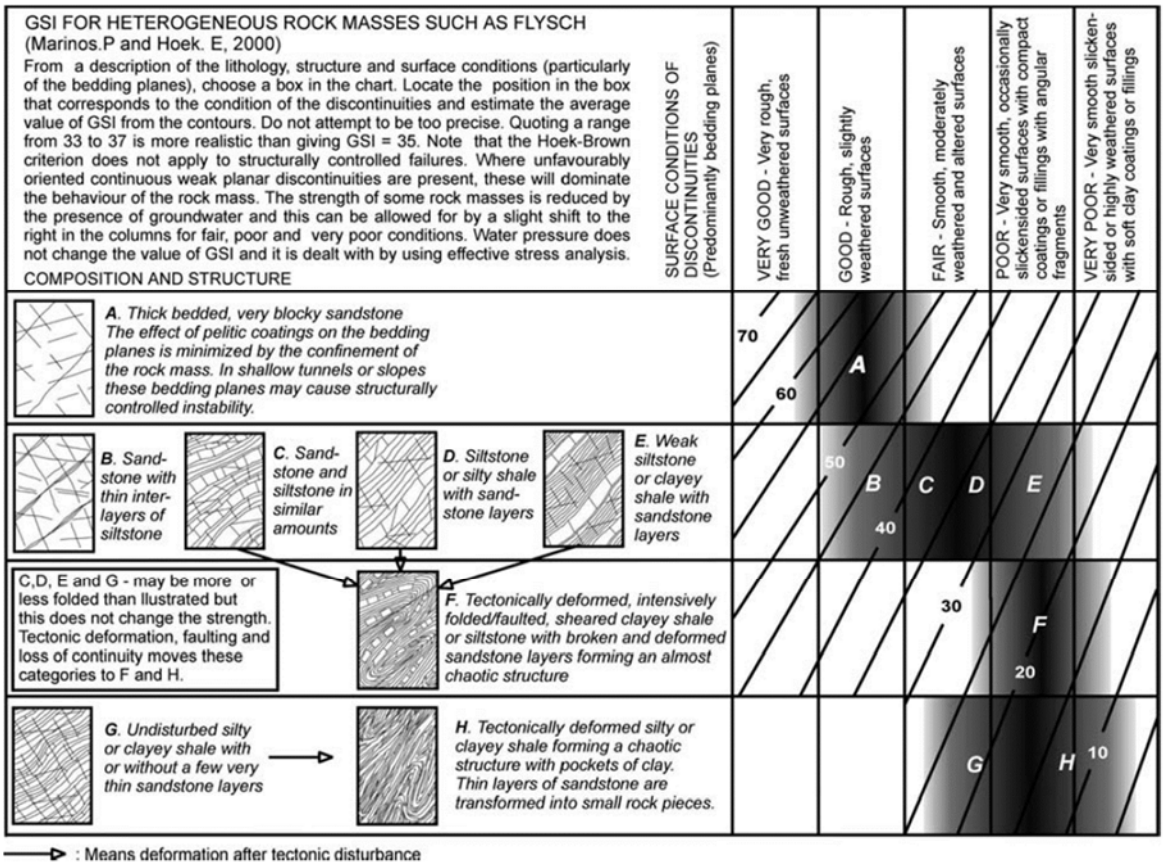
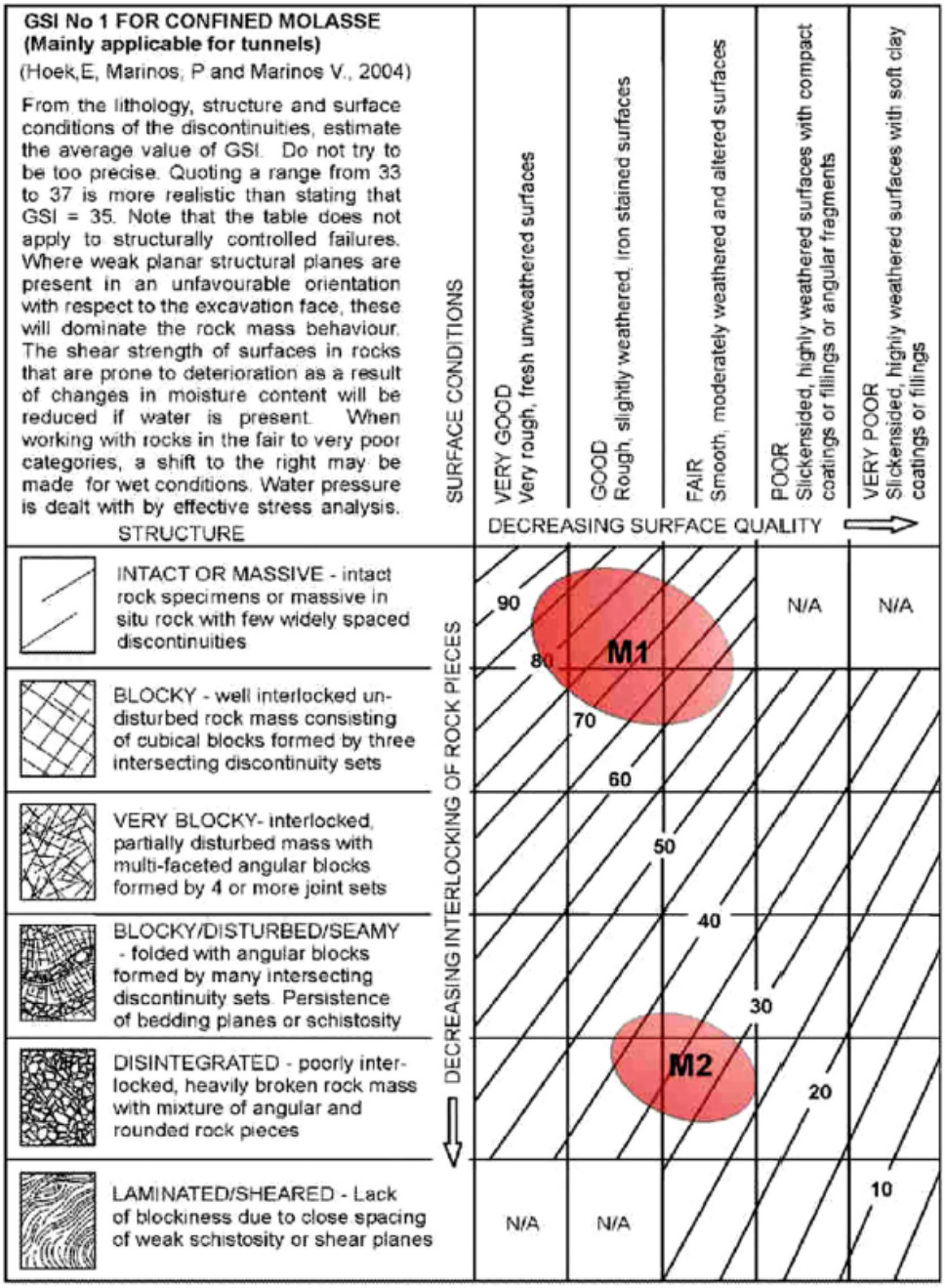



**Figure 9: GSI estimates for heterogeneous rock masses such as Flysch (Marinos & Hoek, 2001)**




Notes: When there are no discontinuities, use laboratory test results directly
M1 - Confined molasse, either homogeneous or with sandstone and siltstone alterations
M2 - Heavily broken or brecciated molasse in fault zones
The GSI chart should not be used for loose conglomerates - treat as weakly cemented river gravel

**Figure 10: GSI chart for confined molasse; mainly applicable for tunnels (Hoek et al., 2005)**

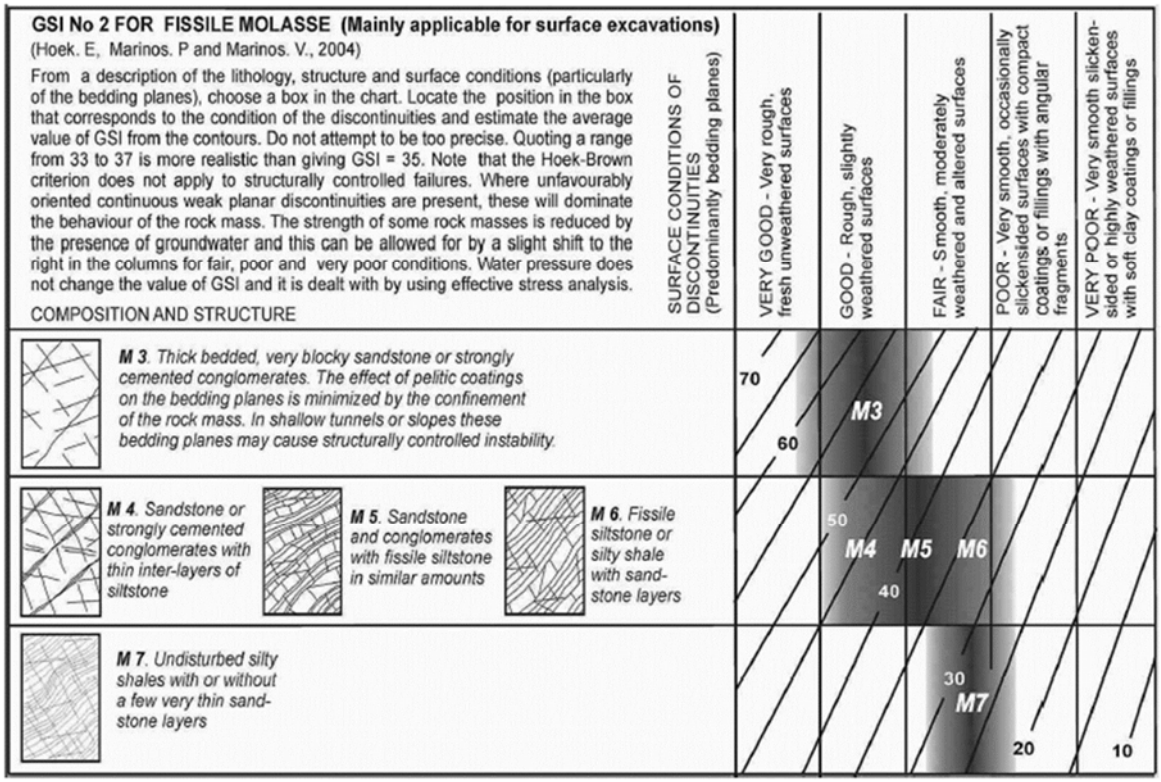



**Figure 11: GSI chart for fissile Molasse where bedding planes of siltstones-mudstones are frequent and well defined. (Surface excavations and slopes, Hoek et al., 2005)**

## 2.3 Swelling Rock Masses

Based on the results of literature review of swelling rock masses, it has been revealed that there is often a misconception in definitions of swelling and squeezing time-dependent deformations as a result of tunnelling (Gioda, 1982). It is, therefore, crucial to realise their differences before considering background information on swelling. Both squeezing (as a result of shearing of the ground) and swelling (as a result of volume increase in the ground) cause inward movement of the tunnel perimeter with time (Gioda, 1982). In principle, both processes, and the corresponding deformations, may occur simultaneously. The deformation and its magnitude may vary depending on the geological conditions, state of stress, tunnel shape and geometry, etc. (Barla, 1999).

Rocks composed of particular minerals such as clay minerals exhibit swelling behaviour while squeezing may occur in any type of mineral. Squeezing occurrences depend on the rock strength and stress, and this may occur anywhere, even simultaneously with swelling in weak rocks (Anagnostou, 1993), especially in the presence of rich clay minerals (Whittaker & Frith, 1990). Moreover, time-dependent deformation as a result of squeezing starts during excavation and can be controlled by the support system installed, whereas swelling deformation may require a significant time to occur (Whittaker & Frith, 1990). In the Kalahari formation, the weathered rock is expected to behave in a squeezing manner and the red clay is susceptible to swelling behaviour.

### 2.3.1 Swelling Process

According to International Society for Rock Mechanics (ISRM Commission, 1983) the swelling process is generally defined as a combination of physicochemical reactions involving water and stress relief, where stress changes usually have a significant effect. Swelling results in volume increase and takes place only in the presence of water and of particular mineral composition (Anagnostou, 1993). This composition includes the minerals that are capable of a physicochemical reaction with water such as the clay minerals of the Kalahari Red clay.

For clay minerals to expand and further cause instability problems in tunnels, certain factors must be fulfilled. There must be a potential for swelling and the potential need to be activated. The chemical composition of the clay minerals, the structure, conditions and processes forming them, and the existence of water, will influence the degree of expansion and swelling characteristics. The clay minerals' capacity to swell (Brekke & Selmer-Olsen, 1965) and the cause of swelling are thus of great importance regarding the extent of the stability issues and problems. The swelling potential presupposes, in most cases, wet conditions and the material undergoes both shrinkage and swelling because of drying and wetting cycles from water content changes (Pusch, 2012). Various clay minerals behave differently to the water content changes and will thus be a source of different volume changes which in turn might affect stability.

When the conditions for a swelling potential are present, a mobilisation of this potential will initiate the swelling process. For most expandable clay minerals, the swelling process first takes place as hydration, where water minerals are attached to the negatively charged clay surfaces. A transition of highly bonded water molecules on the clay surface to free pore water is gradually taking place and eventually major swelling might occur (Nilsen & Broch, 2009). The hydration field is followed by an osmotic swelling where water will flow in the direction of the highest ion concentration due to differences in the ion concentration between the unit layer and in the pore water (Nilsen & Broch, 2009). A significant factor limiting the volume increase when clays are subjected to swelling is the cementation of clay minerals caused by attractive forces between the clay particles and organic/ inorganic adhesives, such as carbonates and hydroxides (Nilsen & Broch, 2009; Pusch, 2012). The cementation of the particles entails the formation of molecular bindings making interlayers in the clay minerals impenetrable for cations and water molecules which impair the clay's ability to expand.

### 2.3.2 Laboratory Testing of Swelling

Historically, an oedometer test has been one of the most important swelling tests and is in use in tunnelling projects (Barla, 1999; Einstein & Bischoff, 1975). This is because the test simulates the tunnel invert in small scale conditions. However, there has been research into the use of triaxial tests, as this allows for a better understanding of swelling mechanisms which occur around an excavation (Steiner, 1993). Through the triaxial tests, it is possible to study the effect of pore pressure, lateral stressing, changes in stiffness and strength of the specimen under drained and undrained conditions (Barla, 1999). Triaxial tests can map the entire three-dimensional stress path, allowing simulation of an excavation life cycle. Despite these advantages, triaxial tests are costly, time-consuming and are not easy to conduct in comparison to one-dimensional oedometer test.

According to the suggested methods given by ISRM, three different tests which are used to measure swelling parameters are briefly explained (ISRM Commission, 1999). All the following laboratory techniques can be used for swelling rock as well as clay (ISRM Commission, 1999):

1. In the first test, a conventional oedometer test is used to determine the axial swelling stress, when the sample is literally confined and immersed in water. The test continues until the axial force reaches its maximum value or no further displacement occurs. Then, the axial stress is calculated using the measured axial force divided by the cross-section area of the sample.
2. The second test is used to determine the axial and radial free swelling strain. The test is carried out in a simple free swell cell where lateral deformation is allowed, and water can be added to the cell. The axial strain is measured and recorded as a function of elapsed time and therefore an axial swelling strain versus time curve can be obtained through this (Barla, 1999). The radial swelling strain is calculated using the measured radial displacement divided by the initial specimen diameter.
3. The third test which is an improved version of the oedometer test originally proposed by Huder and Amberg (1970) is employed to determine the axial swelling strain necessary to reduce axial swelling stress. First, the sample is loaded in a conventional oedometer while it is restricted laterally and is not immersed in water. The load is increased up to a certain level (desired level for the relevant application) and then water is added to the cell. The load is reduced in a stepwise manner until there would be no displacement for any load increment (Barla, 1999).

### 2.3.3 Stability and Lining Principles in Swelling Rock

Swelling of clay minerals may cause stability problems in tunnels, and further, resulting in time delays and cost overruns. The stability problems might occur during construction of the works, after completion and throughout the entire operational life (Selmer-Olsen & Palmstrom, 1989).

Essential factors influencing the stability of tunnels include factors such as rock mass quality, rock stresses, the influence of groundwater and the orientation, location, size, and shape of the construction work (Panthi, 2008).

These factors may vary from project to project, making it difficult to provide real correlations between them (Panthi, 2008). Clay formation is causing the greatest concern with regards to stability threats on tunnelling projects. The swelling character of clay minerals, highly disturbed rock mass of low quality and the interaction with high water pressure represent the most difficult conditions (Selmer-Olsen & Palmstrom, 1989). The combination of these conditions and an underestimation of swelling pressure may result in inadequate rock support and problems with lateral movement, collapse, and sliding of the rock mass. Some tunneling projects had to go through some form of repair work. This is because of either significant floor heave or failure of the lining as a result of swelling deformation (Figure 12).

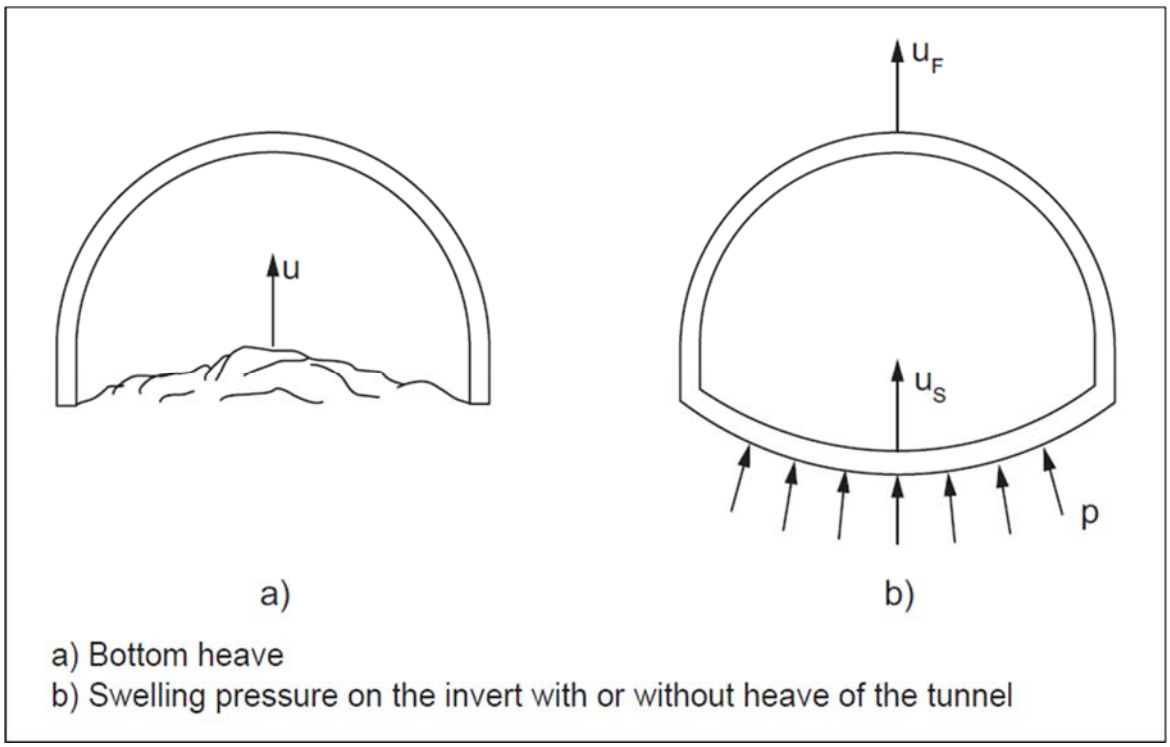



**Figure 12: Effects of rock swelling in tunnelling (Kovári, Amstad & Anagnostou, 1988)**

It should be noted that the swelling pressure is linked to support pressure, hence the tunnel lining design. In principle, the tunnel lining design is governed by long term deformations and is based on the ground in which the tunnel is driven. Consequently, the swelling process should be fully understood before designing the tunnel lining (Anagnostou, 2007). This requires a good understanding of rock/support interaction, i.e relationship between swelling and support pressure and the support pressure and different lining principles. However, there are still a lot of uncertainties regarding different lining principles within such rocks (Anagnostou, 2007).

When designing for tunnels excavated in potentially swelling rocks, the resisting (stiff) and yielding (flexible) support principles are applied (Wittke-Gattermann and Wittke, 2004). In the case of stiff support, the internal concrete lining of high bearing capacity is used to resist against swelling, and this will limit internal movement significantly. In the case of yielding support, construction of a yield zone can effectively reduce the swelling pressure. The yield zone (Figure 13) consists of a gap/ space between the lining and the rock mass so that the tunnel floor can heave without affecting the tunnel operation (Wittke-Gattermann and Wittke, 2004). A modern technique to allow floor heave to occur is to have a deformable layer which is installed between the invert arc and excavation boundary (Anagnostou, 1993). The concept of the flexible lining was seriously debated in the beginning; but it is becoming more accepted at least for shallow tunnels within weak rock (Wittke-Gattermann, 1998; Anagnostou et al., 2010). Based on the experiences from investigating tunneling within anhydrite rock formations in Spain, resisting support pressure stabilises the phenomenon while yielding support allows deformation to continue (Berdugo, 2007).

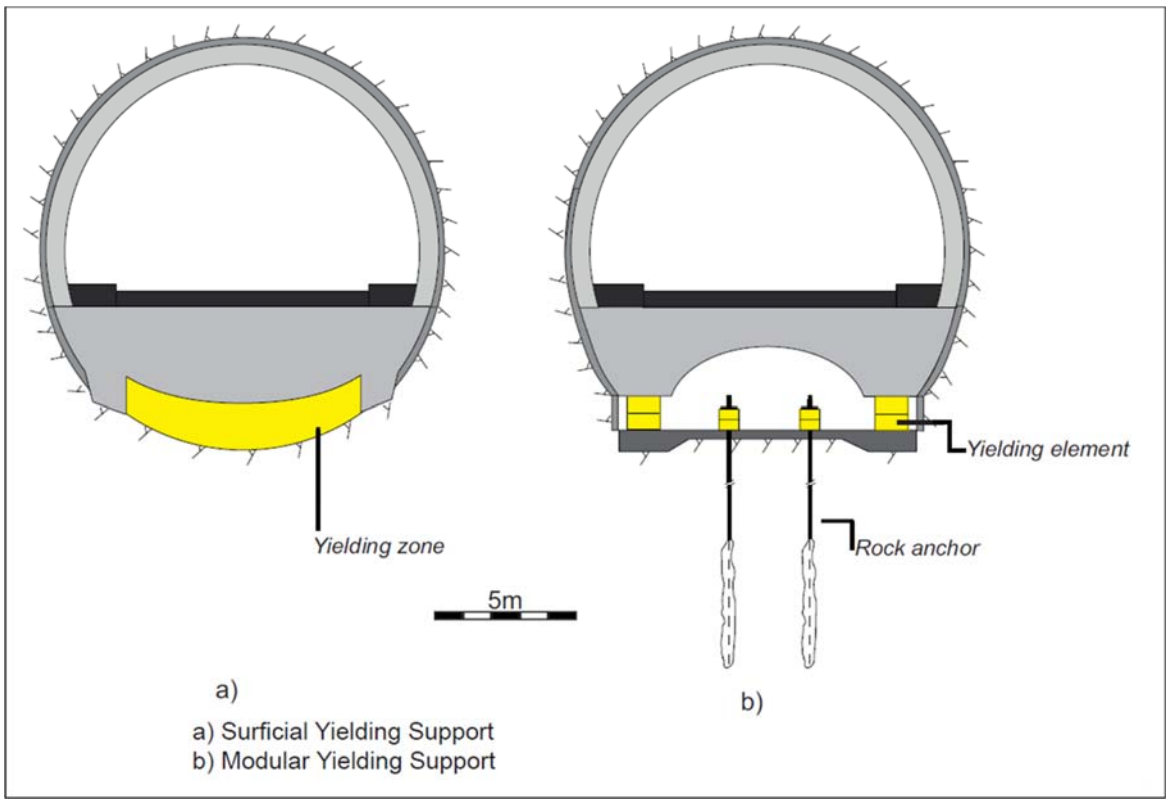



**Figure 13: Yielding support principle (Kovári, 2007)**

## 2.4 Integration of Geotechnical and Structural Design Components

Traditionally, the design of civil engineering tunnels in weak rock was divided into two separate activities. The site investigation, determination of rock mass characteristics, calculation of tunnel stability and the determination of “rock loads” were carried out by a geotechnical engineer (Hoek, 2003). The design of the final concrete lining was then carried out by a structural engineer using the information provided by the geotechnical engineer. In present day weak rock tunnelling the distinction between these two activities has become blurred because of the need for structural design at various stages in the construction process and because this construction process has a direct impact on the final lining design. Hence, there is an increasing tendency to integrate the geotechnical and structural design components into a single package (Hoek, 2003).

There are no universally accepted guidelines on how to assess the safety of a tunnel or the acceptability of design and this means that engineering judgment and experience play a very large role in the design of tunnel reinforcement and lining (Hoek et al., 2008). There is a general desire to define a Factor of Safety (FOS) for tunnel design but this has proved to be an extremely difficult task and there are very few methods that are considered acceptable (Hoek et al., 2008). One of these methods, described by Kaiser (1985) and Sauer et. al (1994), involve the use of support capacity diagrams and there are indeed a few tunnel design companies that use this methodology. However, there is no mention of this method in design guidelines such as the Tunnel Lining Design Guide published by the British Tunnelling Society (2004). As a result, the average tunnel designer is left with few options other than the use of tunnel classification systems (Barton et al., 1974; Bieniawski, 1973b), general empirical guidelines, and the advice of experienced tunnel consultants. The main difficulty of this approach is to decide when the design is acceptable (Hoek, 1992).

To remedy some of these problems, Hoek et al. (2008) presented two relatively complex case histories in sufficient detail from which tunnel designers can follow the use of support capacity diagrams as a tunnel design tool. The support capacity diagrams are based on elastic analysis of the support elements, and this implies that no tensile cracking or compressive crushing of the shotcrete and concrete is acceptable. A family of factor of safety plots in the support capacity diagrams is adapted to present a clear picture of the performance of the lining being designed in the support capacity calculations. It is recommended to adopt a policy of using the ultimate uniaxial compressive and tensile strengths of shotcrete or concrete and calculating a range of FOS (Hoek et al., 2008).

The final concrete lining is installed in a stable tunnel and carries no initial load except self-weight hence only 28-day properties are relevant in the support capacity diagrams. Loads are imposed on the final lining as a result of stress changes, changes in the groundwater conditions, changes in the characteristics of the initial support system and deterioration of the rock mass surrounding the tunnel (Hoek et al., 2008). The participation of temporary lining has been a matter of contention for many years. Tunnel designers in some countries are required to ignore the contribution of all initial reinforcement and shotcrete lining in calculating the support capacity of the final lining (Hoek et al., 2008).

However, this very conservative approach has changed and the International Tunnelling Association (1988) guidelines for the design of tunnels gives the following recommendations “An initial lining of shotcrete may be considered to participate in providing stability to the tunnel only when the long-term durability of shotcrete is preserved”. The long-term loads are induced by the reduction of the residual strength of the failed rock surrounding the tunnel, the elimination of temporary support and changes in groundwater conditions. In designing the final lining these changes have to be accommodated and a FOS in excess of 2.0 has to be provided by the lining for these “normal” loading conditions (Hoek et al., 2008).

Temporary lining may tolerate cracking or crushing and a factor of safety of 1.0, can be applied (Hoek, 2003). Where tensile cracking becomes an important consideration, more sophisticated non-linear structural design approaches, which allow for crack development should be used. All the loads that can occur during the operational life of the tunnel have to be taken into account and an appropriate factor of safety has to be used for the design (Hoek, 2003). According to German standard DIN 1045 (1988), the factor of safety that should be applied to unreinforced concrete is 2.1 while more ductile reinforced concrete can be designed with a factor of safety of 1.75 (Sauer et al., 1994).

## 2.5 Grouting (Cementation)

Costs for shaft sinking or tunnelling operations are extremely high. Therefore, precautions must be taken to avoid unproductive standing time of the working crews. Water inrushes and unconsolidated ground often cause stoppages to tunnelling operations because the walls are unsafe and must be stabilised. Pre-grouting can to a large extent be employed to avoid such delays. Grouting is one of the efficient ways to seal and strengthen the ground in geotechnical projects. It is used in both soil (Karol, 1990) and rock (Houlsby, 1990) environments with the same main purposes but with different methods.

### 2.5.1 Types and Purpose of Grouting

The primary purpose of any grouting project is to alter to the desired degree, the properties of an existing medium by the most economical means (Guyer, 2009). Some purposes of grouting are (Houlsby, 1990):

1. To reduce the flow of seepage through dam wall foundations. Under concrete dam walls, most of the foundation seepage is stopped by a grout curtain. Water decreases the stability of the dam wall foundation and blocking pore and fracture space to inhibit water flow is an important aspect of grouting.
2. To assist tunnelling or mining by reducing water inflow or strengthening the formation ahead of a tunnel or shaft. This is usually done by grouting a ring of holes ahead of the face.
3. To fill voids behind a concrete lining. Concrete pumped in a tunnel and used to line the tunnel will frequently slump away from the roof of the tunnel and will not fill high spots of the excavation. Grouting can be used to fill the resulting overbreak voids using existing holes formed in the concrete or drilled after. This type of grouting is known as backpack or contact grouting (Figure 14).
4. Grouting can be used to increase the strength of joint surfaces in several ways. This can be achieved by increasing normal stress across joint planes and thereby increasing joint shear strength. Increasing cohesion of joint planes, through the removal of infill material and then cementation or binding of the joint surfaces. The identified joint planes are connected by hydrofracturing followed by grouting of the joints for strengthening.

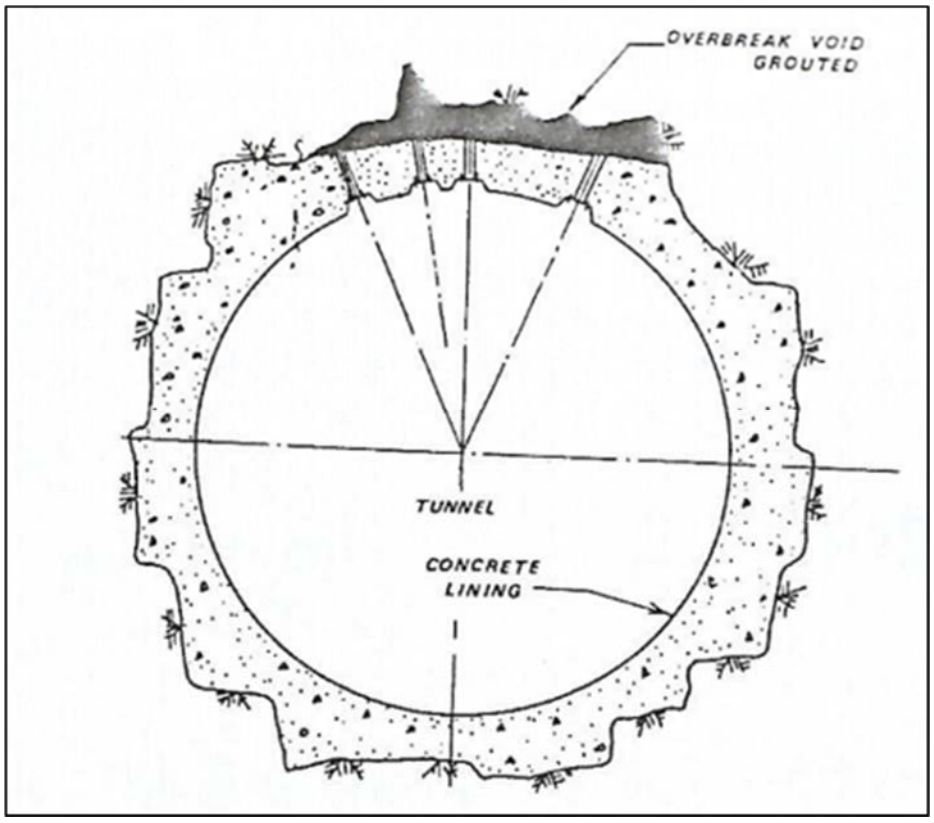



**Figure 14: Overbreak Void filled by Grouting (after Houlsby, 1990)**

There is a difference between grouting of cracks in rock formations and the grouting of voids in gravel or sands (Houlsby, 1990). Permeation grouting of gravel or sands can be done using cement based or chemical grouts. Cement grouting can be used in coarse gravel free of finer material, where it can penetrate reasonably well. Cement grout can only travel well in the larger voids, and in finer sized materials voids are too small to accept cement grout (Houlsby, 1990). In rock formations, cement grout is used as it gives a more economical and durable result. The decision about the type of grout depends on many factors, including the type of soil, the purpose of grouting, or even financial matters (Houlsby, 1990).

In cementitious grouting, the main ingredients are cement, bentonite, and water (Gustin et al., 2007). Cement is the main ingredient of cement-based grouts and its type should be determined according to the grain size distribution in the site-specific project. This means that in coarse soils, Portland cement may be considered efficient, but as the soil grains become fine, other types of cement such as ultrafine, microfine, and superfine cement may be applicable. Portland cement is hydraulic cement mainly composed of hydraulic calcium silicate (Warner, 2004). This kind of cement is hardened by the chemical reaction known as hydration in contact with water (Warner, 2004). Bentonite is colloidal clay from montmorillonite group with high water absorption. Some bentonites absorb water up to five times their own volume. They are used to increase the viscosity and cohesion of the grout and cause the bleeding of the grout to be lessened (Brady and Clauser, 1986).

Chemical grouting can also be used when the target soil is cohesionless and its stability is the main aim of the grouting. The primary advantages of chemical grouts are their low viscosity and good control of setting time (Guyer, 2009). These grouts do not have any particles to restrict flow through fine voids. Only two types of the more widely known types of chemical grouts are discussed briefly. With regard to precipitated grouts, precipitation is a process where the chemicals are mixed in liquid form for injection into a soil. After injection, a reaction between the chemicals result in precipitation of an insoluble material. Filling of the soil voids with an insoluble material results in a decrease in permeability of the soil mass and may, for some processes, bind the particles together with resulting strength increase. The most common type precipitation grouts utilize silicates, usually sodium silicate, being the primary chemical (Guyer, 2009).

Polymerized grouts: polymerization is a chemical reaction in which single organic molecules (monomers) combine to form new complex molecules which are cross linked, resulting in rigidity of the product (Guyer, 2009). In this process, the soluble monomers, mixed with suitable catalysts to produce and control polymerization, are injected into the voids to be filled. The mixture generally has a viscosity near that of water which it retains it for a fixed period, after which polymerization occurs rapidly. Because of the low viscosity, polymer grouts can be used in soils having permeability as low as $10^{-5}$ cm/sec, which would include sandy silt and silty sand. The resulting product is very stable with time (Guyer, 2009). The monomers may be toxic until polymerization occurs after which there is no danger. Some of the more common polymer type grouts utilize the following chemicals as the basic material: Acrylamide, Resorcinol-formaldehyde, Calcium Acrylate, and Epoxy Resin.

Figure 15 compares the suitability of various grouts in different formations. Figure 15 is only to give an indication of the uses of the various grouts. It is deliberately vague because anything more precise would be deceptive (Houlsby, 1990). Clay grouts are usually used with both chemical and cement grouts.

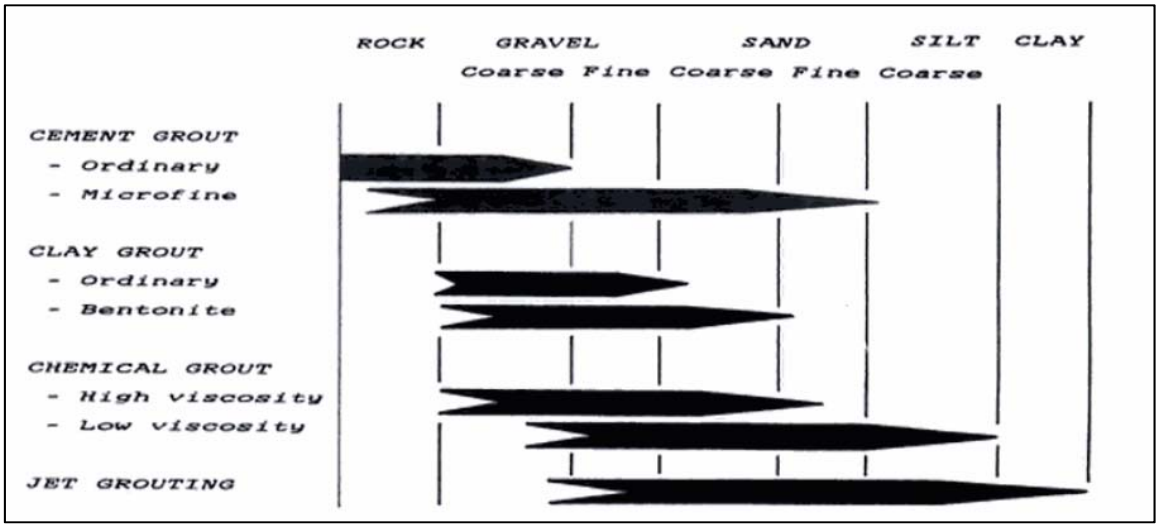



**Figure 15: Suitability and comparison of grouts (after Houlsby, 1990)**

## 2.6 Modelling Methods

Numerical simulation is a powerful tool for geotechnical engineering design, especially when complications and uncertainties are expected in excavations. Numerical methods can be used to predict the response of rock masses to disturbances or changes in ground conditions. Various numerical tools exist, and these differ in complexity and application. Generally, the numerical methods in the fields of civil and rock engineering can be categorized as below (Figure 16):

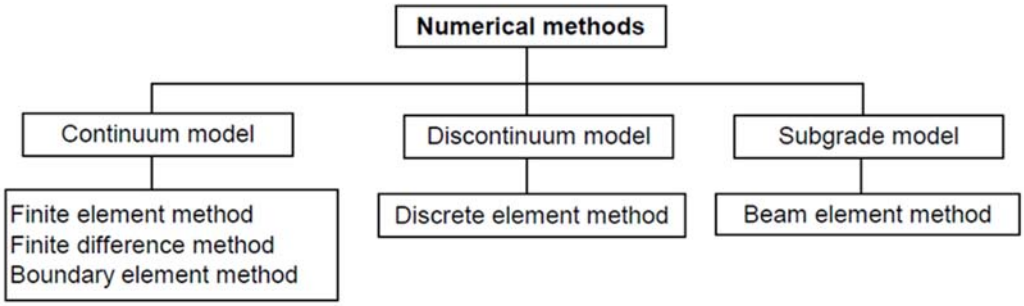



**Figure 16: General Classification of Numerical Methods**

These numerical methods are based on different theories and assumptions, and this makes each of them suitable for particular types of problems. Details of the strengths and weaknesses of each method are discussed by Pande et al. (1990) and Jing and Hudson (2002).

The numerical methods can be primarily divided into continuum and discontinuum methods. This review will focus on the continuum, Finite Element Methods (FEM), as this is the most widely used numerical method in science and engineering. The method uses constitutive models which govern the stress-strain behaviour of the material to determine the response of a medium to field stress changes.

In FEM, the model sphere is discretised into small scale elements which intersect at their nodes (Bobet, 2010) as shown in Figure 17. The method assumes that displacements at any point within an element can be approximated using interpolation functions by the displacements of nodes (Bobet, 2010; Jing, 2003). A Global Stiffness Matrix is used to define material behaviour at each node and the interaction of individual nodes with neighbouring nodes. By defining boundary conditions, the model will attempt to re-equilibrate by allowing nodal displacements, the magnitude, direction and dispersion of which are controlled by the Global Stiffness Matrix. In the case of inelastic material, this process is iterative (Jing, 2003).

Advantages of FEM analysis methods include: flexible mesh development/discretization which enables the representation of complex structures and boundaries with variable resolution, ability to handle material heterogeneity, and highly sophisticated codes using the method have been developed for the field of geomechanics (Jing & Hudson, 2002). Disadvantages of FEM analysis methods include; sensitivity to discretization, large memory requirements, long computation times in the case of iterative non-linear behaviour, and the progression of deformation is not captured (Jing & Hudson, 2002).

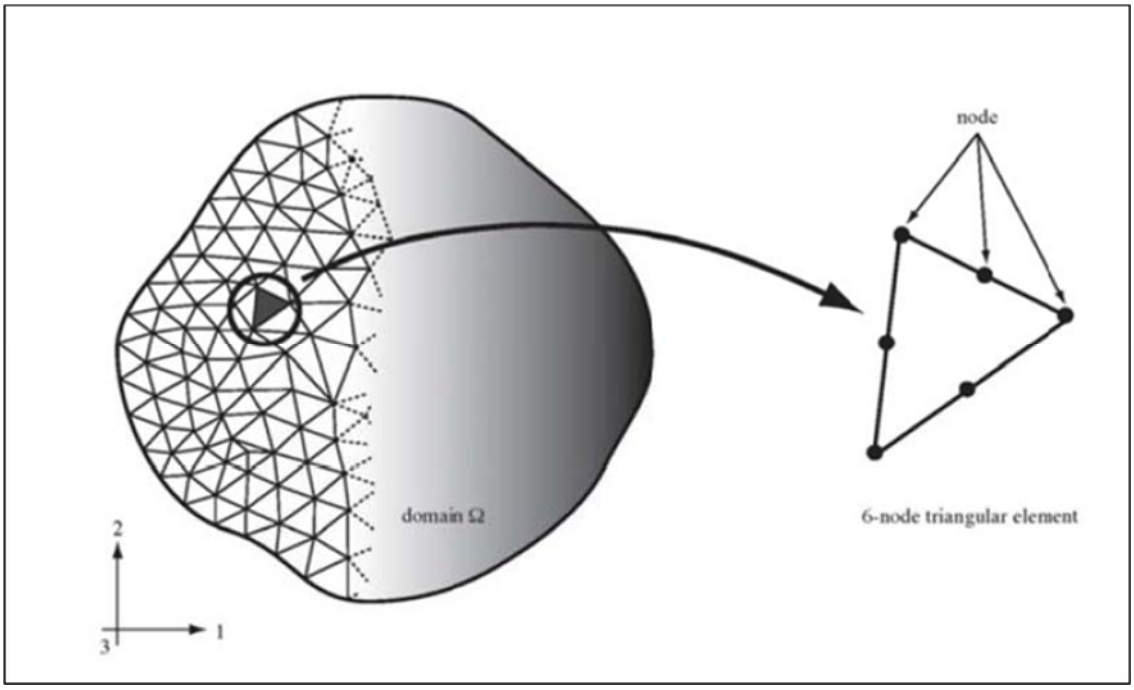



**Figure 17: 2D Finite Element domain discretisation (Bobet, 2010)**

3D geotechnical problems are often simplified and evaluated using 2D models, where plane strain conditions are assumed. In tunnelling, the third dimension is not uniform as it changes with the advance of the tunnel face. Several methods have been developed to simulate tunnel advance in two-dimensional models with the two most common being the Stress-Vector method and the Core-Softening method. The Core softening or replacement method is used in the 2D models (Rocscience, 2018).

## 2.7 Challenges Associated with the Kalahari Rock Formation

### 2.7.1 Geological Model Development

Site investigation involves gathering all relevant information concerning the site of a proposed development and its surrounding areas (Simons et al., 2002). The investigation process also includes analysing and assessing data that has been gathered, to be presented in the form of a report. The purpose of the geotechnical investigation is amongst others to determine the sequence, thickness, and extent of soil and rock types and groundwater conditions (Simons et al., 2002). In situ field testing to assess soil or rock characteristics and obtain representative samples for laboratory testing is also done during the investigation. Even with the most detailed site investigations, knowledge and understanding of the rock mass formation in the subsurface is spatially incomplete (Simons et al., 2002).

The material along the tunnel alignment will only be completely understood upon completion of the tunnel excavation (Hoek, 1998). The amalgamation of regional geology, structural data, surface mapping, and drilling profiles can often lead to the development of a reasonably accurate geological model, if not completely exact (Fookes, 1997). However, the ability to correlate between borehole profiles and regional data depends on matching the geological conditions to an appropriate scale for the borehole spacing.

In the Kalahari formation, if the geological setting is not adequately defined in the data interpretation stage, or borehole correlation is assumed to be direct, inaccurate geological sections may result as shown in Figure 18. In the Kalahari, a balance between increased site investigation and increased flexibility in the design must be met to develop an appropriate geological model. An increased borehole density at the area of study often reaches a threshold, after which the value added by each borehole is minimal in comparison with the associated drilling costs.

The Kalahari formation is prominently heterogeneous at a small scale and it is often not possible to correlate regularly spaced drill core profiles, as shown in Figure 18. In this case, the construction of geological sections is not reasonable. However, site conditions encountered based on other investigations such as geophysical surveys and local experience may be used to develop a rough model for rock mass conditions and the expected variability.

### 2.7.2 Laboratory Testing

The heterogeneity of the Kalahari sedimentary sequences means that an accurate estimate of the rock types and material behavior is often difficult to obtain. As a result of gradational lithology change, strength and behaviour of the rock material can vary significantly as a function of grain size, type and degree of cementation and the alteration of the material from weathering processes. Consequently, the same lithology is not guaranteed to behave similarly, and the geotechnical properties can be widespread.

The Kalahari weak formations such as weathered calcrete and clay present further challenges as geotechnical testing is typically intended for competent rock or non-fractured soil units. The weathered units are often found to be extremely fractured in situ, in part due to coring methods and/or due to time-dependent behaviour of the rock. The standard rock testing procedure requires a core sample of intact rock with a sample length to diameter ratio between 2.5 and 3.0 (International Society for Rock Mechanics (ISRM), 1979). Due to the high fracture density within weathered units, it is often difficult to find a completely intact piece of core adequate for UCS testing. When laboratory tests are not possible, especially in weaker units, Point Load index tests (PLT) are commonly used by geotechnical engineers. However, the uncertainty of the correlation between PLT results and UCS increases the challenge of adequately determining appropriate rock properties for the weaker and weathered sedimentary formations (Hoek & Brown, 1977).

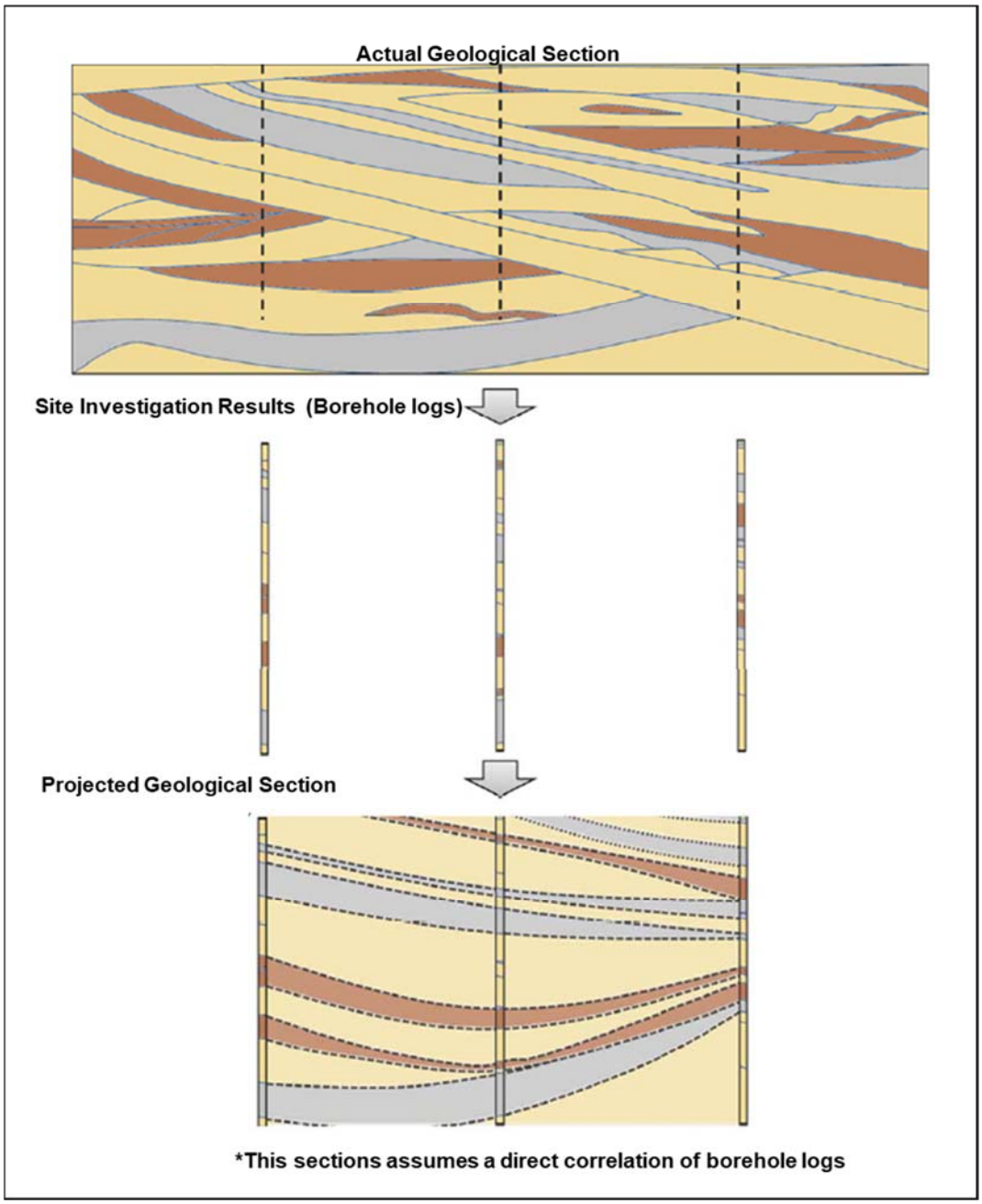



**Figure 18: Simplified representation of the challenges with direct borehole correlation in heterogeneous ground (after Crockford, 2012)**

### 2.7.3 Rock Mass Classification Systems

The use of classification systems in tunnel design is one of the most used empirical design methods. It is crucial to review the ground conditions and project details to determine the applicability of each system to a given project site. The most commonly used classification systems are more relevant for ground conditions within the bounds of dominant case histories.

Using the Q-system, though there are options of rating the joint alteration number and the stress reduction factor SRF with consideration of swelling, the effects of swelling clay in weakness zones have not been satisfactorily included in the system (Barton, 2002; Palmstrom and Broch, 2006). Furthermore, a very important factor of the size (thickness) of zones is not considered, although several features of weakness zones have been included in the Q-system when rating the SRF parameter for zones in competent rocks (Barton, 2002; Palmstrom and Broch, 2006). It should also be noted that the strength reduction of the rock mass with water absorption cannot be accounted for by any parameter in the Q-system. This is of significance for the weathered and weak rock masses containing clay and the clay section of the Kalahari formation.

The support pressure caused by swelling in weakness zones containing swelling clay can be substantial and this type of ground can be complicated to define. The swelling pressure in such cases cannot be considered with the original empirical diagram published by Barton et al. (1974), nor in later revisions of Q-system (i.e. Grimstad & Barton, 1993; Barton, 2002) nor in research on support pressure (Sheorey, 1985; Singh et al., 1992; Goel, 1994; Goel et al., 1996; Singh et al., 1997). It should also be noted that empirically very few cases of registered support pressure are within the area corresponding to the Q value range of 0.002 – 0.2, which represents rated rock mass quality of most of the weakness zones in the Kalahari formation.

In the case of GSI, throughout the development of the system, sedimentary sequences were often excluded from application due to prevalent controlling structures (Marinos et al., 2005). However, a further extension of the system for the case of tectonically undisturbed lithologically varied sedimentary rock, molasse, was developed (Hoek et al. 2005). The molasse rock type refers to a rock composed of Alp origin sediments which were deposited in a basin behind the mountain chain and are undisturbed. Molasse is also associated with material that behaves similarly, whether in Switzerland or Greece and the world over. The challenge becomes the adoption of the system for cases of variable sedimentary rocks outside of the two highlighted zones, M1 and M2 in Figure 10 for tunnels, yet that appears in the M3-M7 descriptions in Figure 11 which is not designed for use in tunnels. An approximate GSI value may be applied, using the descriptors of structure and surface conditions in Figure 8, though descriptions may not completely capture the material conditions. As the structure is often unique for each lithology present in the Kalahari sequence, an “average” GSI is not recommended, instead, rock type specific GSI is suggested.

# 3 TUNNELLING THROUGH THE KALAHARI – A PRACTICAL EXAMPLE

A review of the rock engineering characterisation for excavations in the Kalahari was covered in Chapter 2. Also covered was the review of the design principles and ground strengthening measures that can be applied to the rock masses. The reviews provide invaluable information in identifying objectives for appropriate site investigation procedures for a better understanding of the rock mass. An ideal excavation design is one where minimal disturbance is made to the surrounding rock mass and as little external material is added to the system; using the rock itself as the principal structural medium (Bieniawski, 1984).

The Kalahari formation has a history of tunnelling projects which provide access to the deep rich manganese resource. There have been challenges associated with the tunnelling projects, and competitive design options are progressively being implemented with each project. However, due to the highly variable and complicated geology, advance rates and execution of some of the recent projects have suffered major setbacks.

This chapter contains a description of the methodology used to define the geotechnical setting and numerical models analysed for this project. The assessment of existing excavations to understand the long-term stability issues of tunnels in the Kalahari is also covered. The model geometries, material properties, loading conditions, and modelling assumptions are all included. Also covered in this chapter is a brief description of the Gloria ventilation shaft project. The results that were obtained from these assessments will be discussed in Chapter 4.

## 3.1 Site Investigation

To better understand the conditions expected during excavation and underground construction a good knowledge of the geological and geotechnical setting is required. A detailed site investigation was carried out at the Gloria ventilation shaft.

### 3.1.1 Geotechnical Logging

The geotechnical data collection involved drilling and geotechnical logging of the Gloria ventilation shaft (GLV-01) centre line borehole. The geotechnical logging used the geotechnical sheet (Appendix A) and procedures acceptable for a Feasibility Study.

The collection of data entailed logging per drill run for each geotechnical domain identified. Supplementary to the logs and for record purposes, core photographs were taken by the geologist onsite. The geotechnical logs were processed for rock mass classification.

### 3.1.2 Laboratory Sample Collection

Sample collection for laboratory testing was carried out on-site. A total of 55 samples were collected, 13 of these were soil samples, and 42 were rock samples.

#### *3.1.2.1 Soil Sample Testing*

A total of 13 soil samples were taken and sent for laboratory tests. The following tests were conducted on the samples:

- ***Grading Analysis***: This test determines the soil particle size distribution and the classification of the soil mass for engineering purposes.
- ***Moisture Content****:* This test determines the amount of water in a mass of material. The water content assists in the interpretation of the effects of pore water pressure that may exist within the soil.
- ***Atterberg Limits***: This test determines linear shrinkage, plasticity and the liquid limit of the soil mass. The results are used to classify the soil mass for engineering use.
- ***Dispersive Grading***: This test determines the amount and degree to which a soil mass can be dispersed. This is useful in the calculation of differential settlement when the soil mass is subjected to loading. The results are used to classify the soil mass for engineering use.
- ***Falling Head Test****:* This test determines the rate at which water may flow within a soil mass, which ultimately defines soil mass permeability.
- ***Direct Shear Test****:* This test determines the soil or rock mass shear strength parameters, namely cohesion and friction angle.
- ***Free Swell Test****:* This test determines the amount and degree at which a particular soil mass can swell. This is particularly useful in the calculation of heave when the soil mass is subjected to loading.

#### *3.1.2.2 Rock Sample Testing*

A total sum of 41 hard rock samples were sent for laboratory testing. 24 samples were tested for Uniaxial Compressive Strength (UCS) and 17 samples were tested for Uniaxial Compressive Strength with Elastic Modulus and Poisson's ratio (UCM).

### 3.1.3 Hydrogeology

A hydrogeological study was carried out for conceptualisation and estimating inflows during shaft sinking. Air percussion and core drilling activities of boreholes within the vicinity of the ventilation shaft were monitored. Boreholes GL130-VVS, GL129 VMS and four exploration boreholes were assessed, and hydrogeologically logged.

## 3.2 Geotechnical Inspection of Early Tunneling Projects

For the complete understanding of the long-term behaviour of a rock mass, it is important to review previous tunnelling projects within the Kalahari Formation. Most of the early tunnelling projects through the Kalahari used conventional tunnelling methods in the weak rock masses, albeit with immense difficulty. However, two tunnelling projects do exist and provide insight into the long-term behaviour of the rock masses.

Two early projects, a decline and vertical shaft, through the Kalahari formation, which are used to access the mine and provide ventilation at Black Rock Mines were developed during the late 1970s. The decline tunnel has a quasi-rectangular cross section of 4.5 m wide by 2.5 m high, with a steep dip of 15°. The tunnel is approximately 600 m long, intersecting hard rock at approximately 160 m below surface. The vertical shaft is 120 m deep, circular with a radius of 5.0 m. Limited information is available with respect to excavation methods of either tunnel.

However, due to the dimensions and shape of the tunnels along with the support systems used, it can be inferred that the excavation and temporary support methods used for the tunnels were similar to the methods used in hard rock mining, which are well known. The final support used in the decline is a reinforced concrete lining (concrete with steel sets), which was cast in place using timber forms. In the shaft, an unreinforced concrete lining and shotcrete were used.

The decline was inspected in 2015 to determine its condition and to note any visible damage. The rock types intersected along the decline were inspected and recorded. The geological cross-section of the decline is shown in Figure 19.

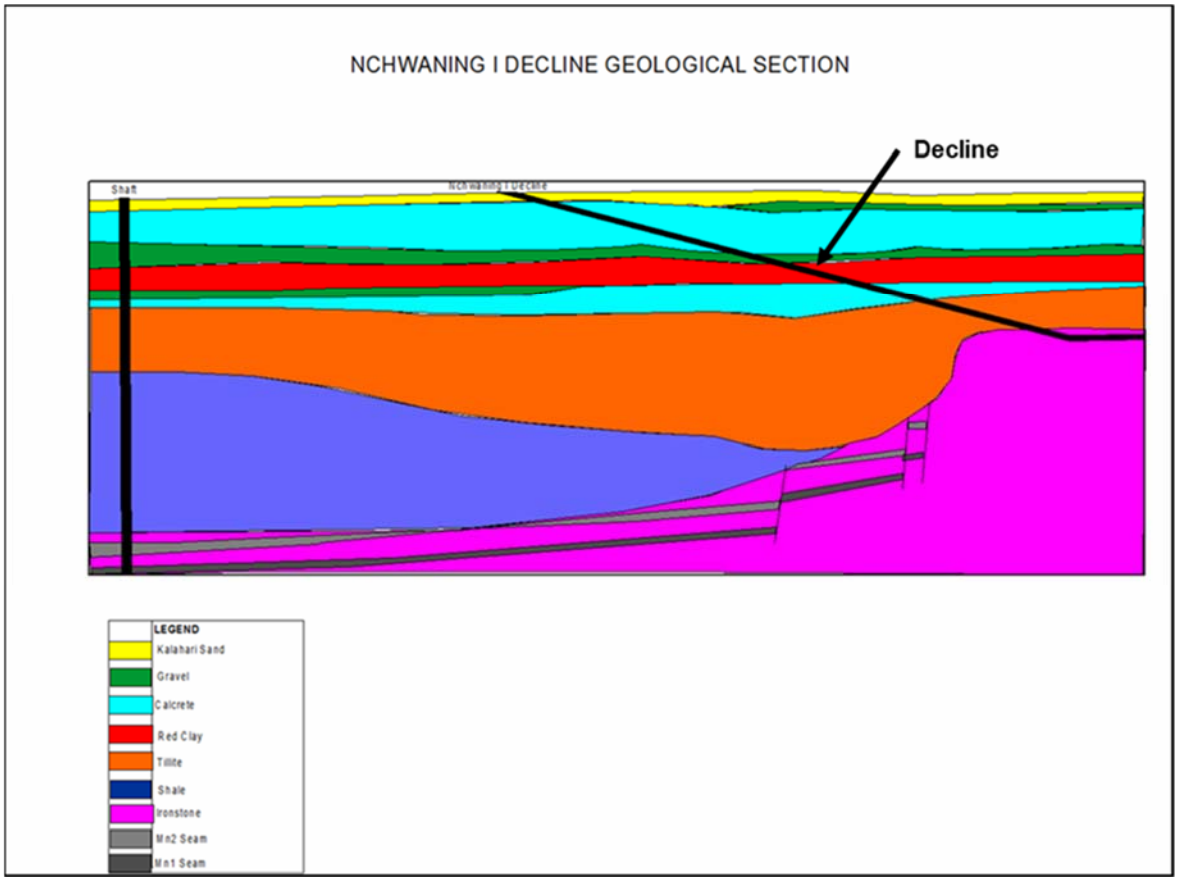



**Figure 19: Geological cross section for Nchwaning I Decline (Steenkamp, 2013a)**

The old ventilation shaft was inspected in 2016 to determine the condition of the shaft and to note any visible deterioration. The geological cross section of the shaft is shown in Figure 20.

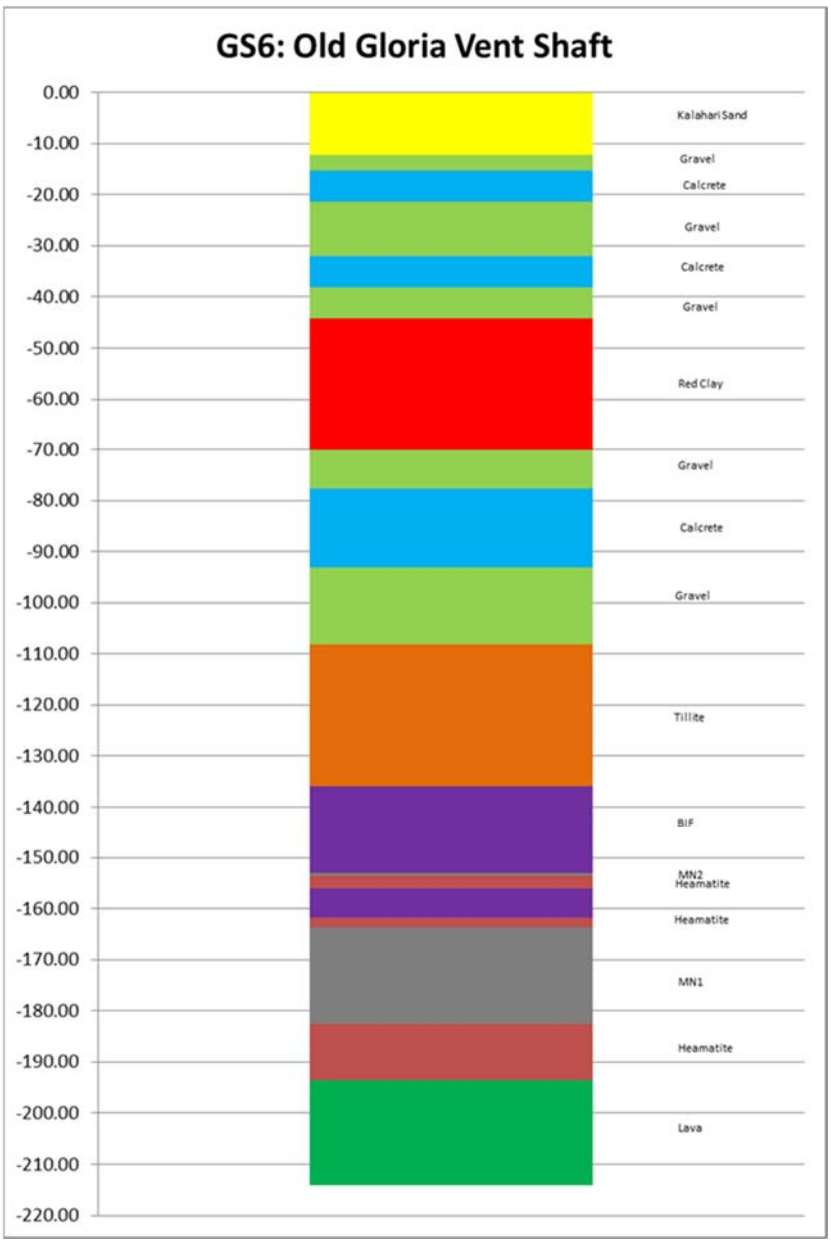



**Figure 20: Old Vent shaft Stratigraphy (Steenkamp, 2013b)**

## 3.3 Numerical Modelling

Empirical and numerical methods are often used to analyse excavation stability and to determine appropriate support systems for a given excavation. The common numerical methods in use include two-dimensional (2D) and three-dimensional (3D) FEM. Complex geotechnical conditions can be numerically assessed for potential instabilities using these powerful computational tools. The suggested support system designs for the excavations can also be tested using the numerical codes.

Numerical investigations were conducted using the 2D FEM software RS2 v. 9.0 and 3D FEM software RS3 v. 2.018 by RocScience. Linear isotropic material was assumed in all analyses, with the deformation properties of the materials being defined by the Young's modulus and Poisson's ratio.

### 3.3.1 Rocscience RS2

RS2 is a two-dimensional elasto-plastic finite element stress analysis program for underground and surface excavations in rock or soil. It is used to calculate stresses and displacements around underground openings and can be used to solve a wide range of mining, geotechnical and civil engineering problems. RS2 incorporates a 2-dimensional automatic finite element mesh generator, which can generate meshes based on either triangular or quadrilateral finite elements. For all the analyses that were carried out, 6 noded triangular elements were used. Figure 21 shows typical elements that can be used in RS2.

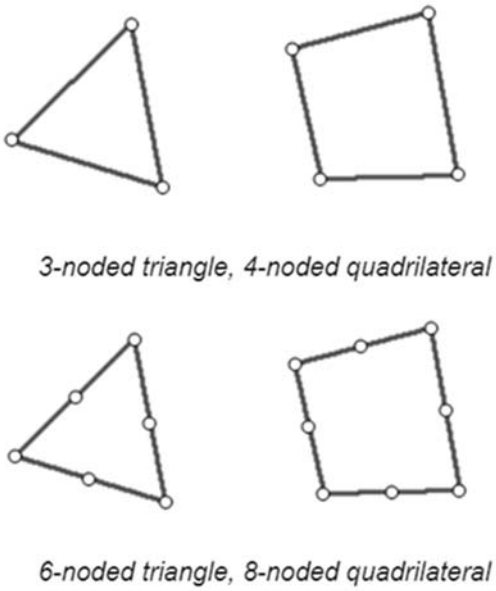



**Figure 21: Elements for Finite Element Analysis**

In general, elements with mid-side nodes (6-noded triangles or 8-noded quadrilaterals) will improve the accuracy of the results; however, computation time and file size will also increase. A uniform mesh was used throughout the model avoiding high aspect ratio (long "thin") elements since they can have adverse effects on the analysis results.

Often three-dimensional geotechnical problems are simplified and modelled using two-dimensional numerical models. In such problems, plane strain conditions are assumed (i.e. no deformation out of plane). In the case of tunnelling, the third dimension is not uniform and changes significantly with the advance of the tunnel, and this invalidates the plane strain condition. Several methods have been developed over the years to simulate tunnel advance in two-dimensional models. The two most common are the Stress-Vector and the Core-Softening method. The Core softening method was used in RS2 and this is detailed in RS2 tutorials (Rocscience, 2018). A Gaussian Elimination solver was used in solving the matrices produced in the finite element analysis.

The following sentences briefly describes the settings used in all RS2 models, unless specified otherwise. In all the RS2 models, the field stress represents the only loading imposed on the model except where swelling pressure was investigated. A constant field stress was applied to the models. The locked in stresses were kept at zero in all models, both in-plane and out-of-plane directions. The initial element loading was set as “field stress only”. All boundaries had their displacements set at zero. Figure 22 shows the displacement boundary conditions imposed on all the RS2 models.

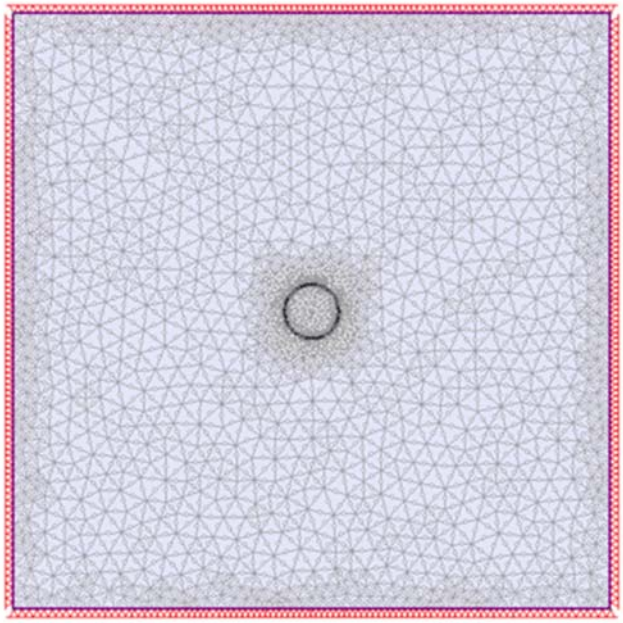


**Figure 22: Displacement boundary conditions used in all 2D numerical models**

### 3.3.2 Rocscience RS3

The basis for RS3 is the numerical formulation used by the two-dimensional program, RS2. The Finite Element scheme is the same in both programs, with RS3 extending the logic into 3-dimensional space. RS3 allows users to generate a 3D tetrahedral mesh with a single click or customize it to user specifications based on 4 or 10 noded tetrahedral finite elements. RS3 was used to evaluate the maximum displacement of the excavation. Figure 23 shows the displacement boundary conditions imposed on all the RS3 models.

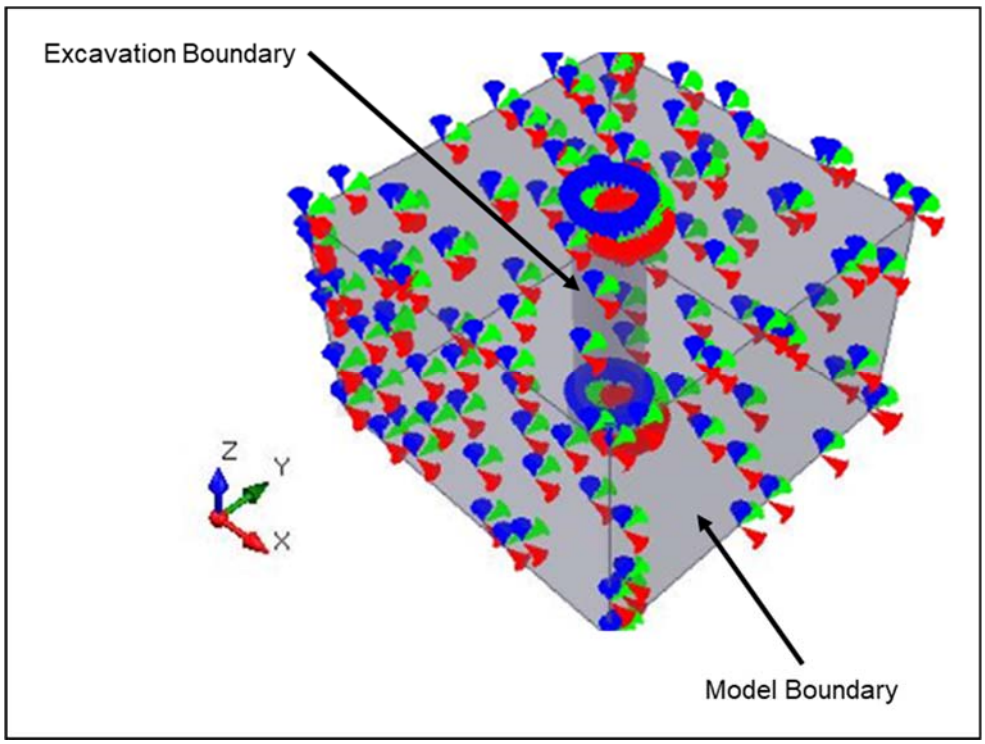



**Figure 23: Displacement boundary conditions used in all 3D numerical models**

### 3.3.3 Analysis Conducted

#### *3.3.3.1 Material Representation*

A 5.5 m diameter vertical excavation from the surface to a depth of 170 m was used for the analysis, applying the core softening method to simulate the advancing face in RS2. The excavation passes through the Kalahari sands, calcrete, red clay, weathered and fresh tillite and manganese of variable thickness. For simplicity, each rock unit was represented by a model.

#### *3.3.3.2 Stress Regime*

Weak formations such as calcrete and clay are encountered in the shaft, and the risk of failure (or squeezing) as a result of the local stress regime is an important consideration. An unconformity exists between the clays and underlying tillite, and a second unconformity exists at 105 m depth between the Karoo-age tillite and much older manganese and Banded Iron Formation rocks. It is likely that different in-situ stress regimes occur above and below the unconformities, primarily influencing the horizontal stress components. Detailed stress measurements are not available, and it is assumed that the vertical component of stress is equal to the weight of overlying strata. The horizontal component of field stress is equal to the vertical stress, multiplied by a factor, the k ratio. In the deeper rock units, tillites and manganese, it is assumed that the worst case would be, k =1.5. Above, in the clays, it is assumed that stress is at worst hydrostatic, and k = 1. It is considered unlikely that the weak formations are strong enough to retain any locked-in tectonic stresses.

#### *3.3.3.3 Swelling Pressure*

In the RS2 and RS3 models, the effect of swelling pressure on the concrete lining is simplified from an engineering perspective as uniformly distributed loads. Swelling pressure measured in the laboratory is not comparable with the in-situ swelling pressure. To quantify the swelling pressure on the concrete lining, numerical simulations have been carried out for the clay section with different swelling pressures ranging from zero to 2.2 MPa at an interval of 0.2 MPa.

#### *3.3.3.4 Support Design*

The concrete lining evaluation was carried out in RS2 using support capacity diagrams. Support capacity diagrams give the geotechnical engineer an easy method for determining the FOS of the concrete liner. In RS2 and RS3 the support capacity plots can only be used for elastic support material. Support capacity envelopes of 1.0, 1.2, 1.6, 1.75 and 2.1 were used in the RS2 analyses. Design FOS values of 2.1 and 1.75 were used to evaluate unreinforced and reinforced concrete lining thickness (Sauer et al.,1994).

## 3.4 Tunneling Works: Ventilation Shaft

This section is relevant to the stability of the ground during sinking of the ventilation shaft. Stable and competent ground conditions in the shaft are essential, not only for a higher advance rate but also to ensure a safe working environment. Groundwater management is critical in shaft or tunnelling projects, especially sinking while handling water in excess of 1000l/hr. The methodology implemented during shaft sinking is briefly outlined:

### 3.4.1 Groundwater Management

The groundwater management interventions applied to the ventilation sinking shaft process are:

- Pre-cementation of the area around the shaft perimeter using grout prior to sinking. The grout provided a thick impermeable sheet thus preventing water inflow into the shaft perimeter. Pre-cementation holes were established down to 79 m below surface. Figure 24 shows the position of the pre-cementation holes relative to the shaft perimeter.
- Dewatering boreholes which were depressurised during the sinking phase. Figure 24 shows the layout of the dewatering holes used. The boreholes can also be used to depressurise the aquifers as a long-term dewatering strategy to minimise water inflow into the shaft.
- Cover drilling was implemented during sinking. Where the cover holes are dry the holes are plugged with cement and sinking continues. Where the holes are wet, the holes are pre-treated with microfine cement or chemical grouts.

### 3.4.2 Temporary Support

As means of temporary support for sinking through the Kalahari sands, 1180 mm diameter reinforced oscillator piles were installed up to 29 m below surface. The as-built layout of the piles is shown in Figure 25. The piles provide a robust means of holding back the sands while maintaining the required outer shaft diameter during sinking. There is no risk of the sands caving during sinking as shown in Figure 26.

In the Red Clays, ARMCO ring barriers with mass concrete backfilling were used (Figure 27). This method was selected as it provides areal coverage and maintains structural integrity of the excavation in the clays. The rings will be installed in 1.2 m lifts up to a depth of 6.0 m below lining.

### 3.4.3 Geotechnical Shaft Inspection

The shaft was monitored for deviations and conditions. These daily inspections were logged and recorded the following:

- Advance of shaft bottom.
- Discontinuity properties.
- Water inflow.
- Position of lining above shaft bottom.
- Temporary support installed.
- Condition of the installed lining and deviations.

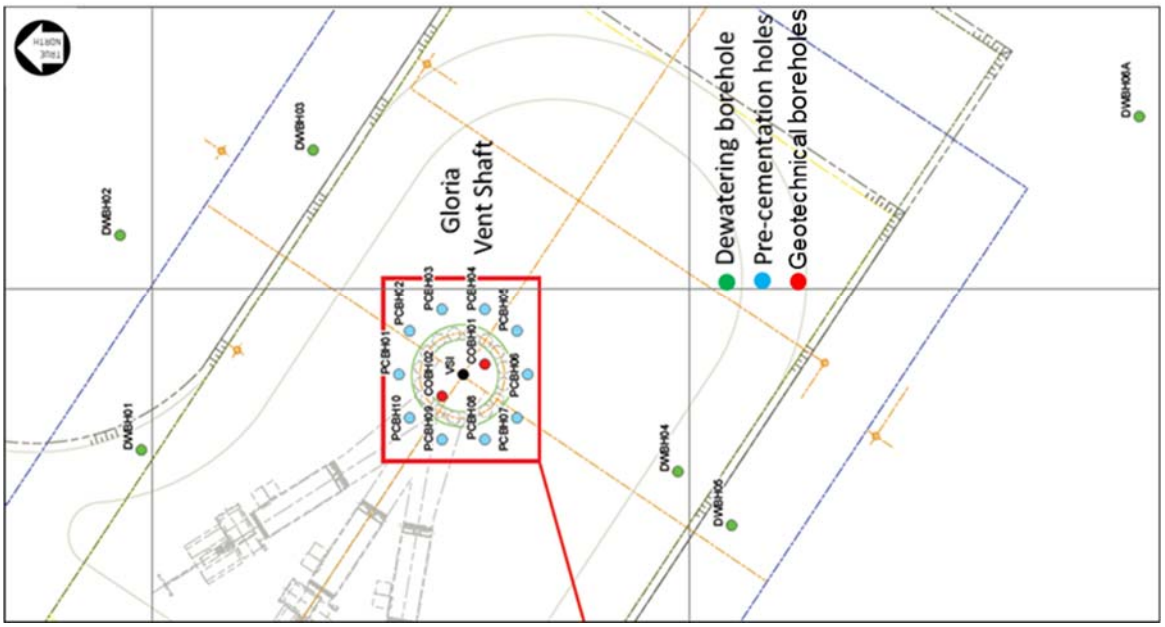



**Figure 24: Vent shaft pre-cementation and dewatering holes**

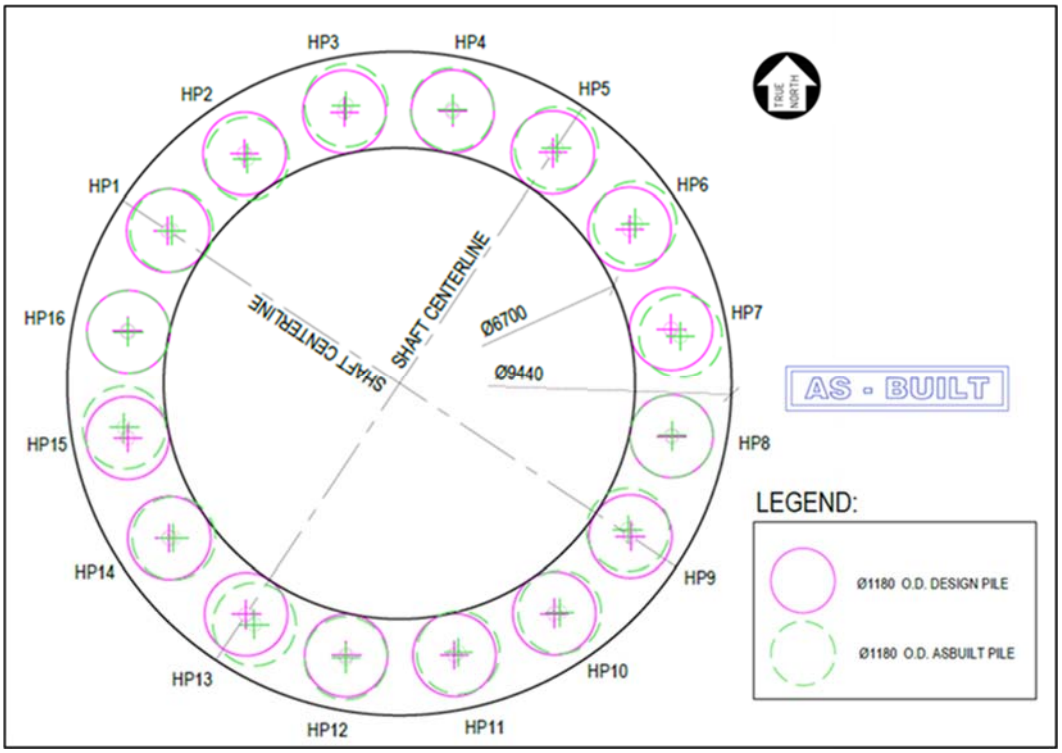



**Figure 25: As-built layout of Oscillator piles**



**Figure 26: Use of oscillator piles as temporary support in the sands**



**Figure 27: Use of ARMCO back shutters as temporary support in the red clay**

## 3.5 Delimitations

This study confined itself to the assessment of concrete lining using 2-dimensional, RS2 models. 3-dimensional, RS3 models were used to verify the maximum displacement around the excavation. Support capacity plots were used in the RS2 models to evaluate the concrete lining requirements. In this case, the researcher is aware of the differences between 2D vs 3D modelling assessments. The main aim was to establish a criterion for concrete lining design in the Kalahari formation.

# 4 RESULTS AND DISCUSSION

Chapter 3 outlined the methodology followed in the collection of information that was used to define the geotechnical setting of the project. It also outlined the numerical models analysed for the project. This Chapter presents the results of the geotechnical investigation and analyses conducted on the models described in Chapter 3. The results have been organised according to the following structure:

- Project Setting
- Geotechnical Characteristics
- Rock mass classification
- Inspection of Early Tunnelling Projects
- Numerical Modelling
- Tunnelling works: Ventilation Shaft

## 4.1 Project Setting

The area of the Kalahari in which the manganese field is situated is referred to as the Gordonia region. The average annual rainfall is in the range of 150 to 250 mm, of which some 60% occurs in the months of January to April (Thomas and Shaw, 1990). Monthly evaporation rates can exceed the precipitation by a factor of six or more (Meyer et al., 1985). Due to the low rainfall patterns, no permanent surface water is found in the Kalahari.

### 4.1.1 Geological Setting

The primary formations of interest in the Kalahari rock masses tunnelling are the uppermost sedimentary formations: the Kalahari, Dwkya, and Olifantshoek groups. Only the geological units encountered from the investigations carried out by the author for a small-scale shaft sinking project are described in detail in the sections that follow. The ventilation shaft at Gloria Mine is located near the eastern sub-outcrop margin of the deposit. The shaft is developed through the unconsolidated Aeolian sand of the Gordonia Formation and the clasto-chemical sediments of the Kalahari formation. It is also excavated through the highly oxidized horizon of the Dwyka Formation before it encounters fresh tillite.

***Gordonia Formation***: The top 5 m of the Gordonia Aeolian sand has a light orange-red colour and is very fine grained. The red colour is due to a very thin haematite coating of the sand grains. The typical colour of the Kalahari sand is illustrated in Figure 28. The bottom contact of the Gordonia Formation is usually gradational with the underlying hard calcrete layer. In the setting of the ventilation shaft, there is a sand lens in the upper part of the hard bank calcrete. The sand and calcrete are cemented, with calcrete becoming dominant over the sand with depth. Gravel beds are irregularly developed in this formation. The gravel beds represent paleo-river or stream beds. The gravels are local ironstone and quartzite and range in size from dominantly pebbles up to minor cobbles. Figure 28 also shows gravels recovered in the sand horizon.



**Figure 28: The range of Kalahari sand colours, orange in the top row and darker red-orange in the second and third row. A calcrete lens is visible in the fourth row and gravels in the bottom row on the right-hand side of the photo.**

***Kalahari Formation***: The top of the Kalahari formation is marked by hard calcrete. The lower portion of the hard calcrete unit contains pebbles and cobbles of ironstone and quartzite. The contact between the conglomerate layer and the underlying red clay unit is gradational (Figure 29). The top contact of the red clay unit has been calcified, but the original clay texture and structures, such as slickenside surfaces has been preserved.

The red clay unit is very dense and has a massive texture with a deep red colour. Slickenside surfaces are evident on core samples. The red clay is prone to expansion upon wetting but quickly dries up resulting in large desiccation cracks. The red clay unit has a very sharp contact with the bottom conglomerate layer. The conglomerate is a mixture of ironstone and quartzite pebbles and cobbles in a calcrete matrix (Figure 29). The lowermost calcrete layer is fine grained and has a light beige-yellow colour. It also contains small fragments of highly weathered tillite.

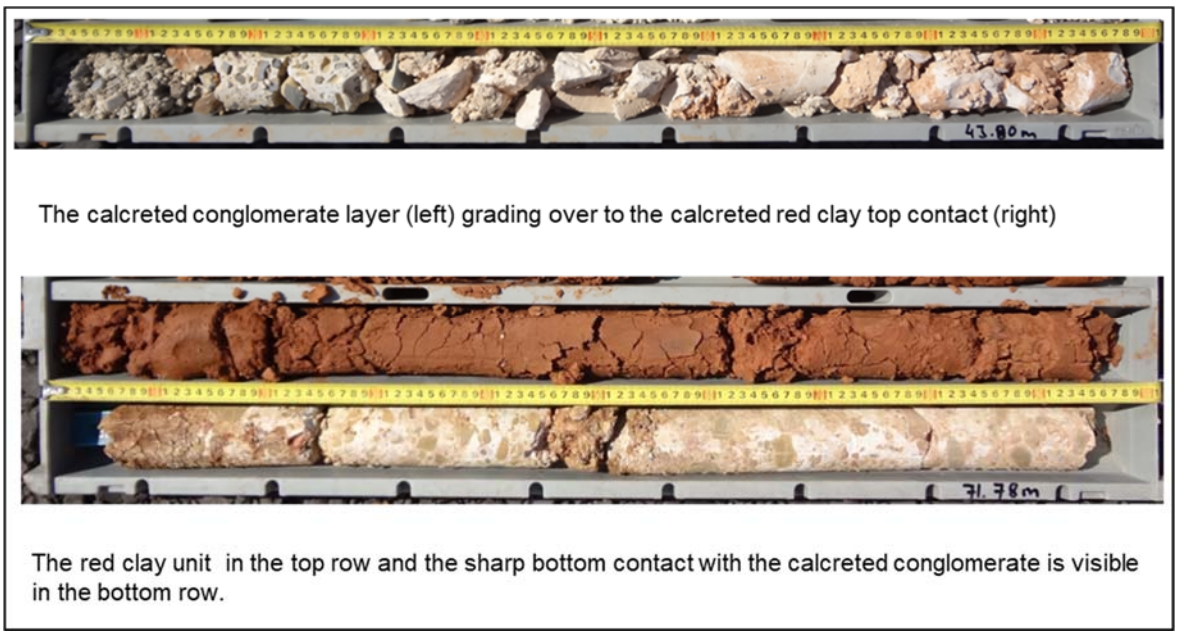


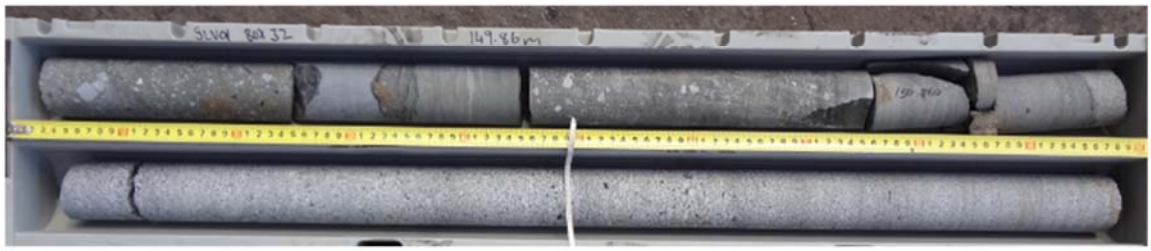

**Figure 29: The Calcreted Conglomerate and Calcreted red clay contacts.**

***Dwyka Formation:*** Forms part of the Karoo Supergroup and represents a glacial tillite deposit. The Dwyka Formation is preserved erratically around the ventilation shaft position. The top contact is highly broken with oxidised tillite gradually becoming dominant over hard calcrete. The oxidised tillite material has a very distinctive yellow colour, where the matrix clay material has been oxidised (Figure 30). The tillite contains ironstone and quartzite dropstones ranging in size from pebbles to cobbles. The oxidised horizon represents a paleo-land surface where the younger Karoo rocks were weathered and eroded away. With depth, the tillite has a light brown colour and becomes more competent.

The fresh tillite material has a dark blue-gray matrix with pebble to cobble-sized dropstones of quartzite and ironstone. No structure, such as joint sets or fault material was observed in the core examined. There are siltstone beds present in the main tillite succession, with very distinct lamination. The siltstone units are prone to disking along the bedding after exposure to the atmosphere. Near the bottom of the tillite interval, there is a distinct gritstone bed (Figure 30). The bottom of the Dwyka Formation is marked by a sharp contact.



Highly weathered tillite fragments (yellow) with calcrete lenses and stringers.



Typical fresh tillite is in the top row, the dropstones visible are quartzite and ironstone. The bottom row shows the gritstone.

**Figure 30: Highly weathered and fresh tillite**

***Hotazel Formation (Transvaal Supergroup):*** The sharp top contact of the Manganese Seam 1 (Mn1) unit is indicative of a glacial discontinuity (Figure 31). The overlying chemical (Banded Ironstone Formation) and clastic (shale and quartzite) sediments were eroded away. The Mn1 shows sub-vertical faulting with secondary calcite and iron-hydroxide staining of the smooth fault surface.

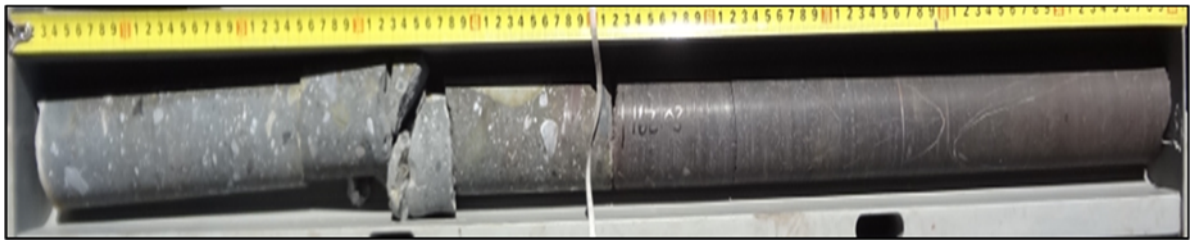


**Figure 31: The sharp discontinuity (centre of photo) between tillite (left) and manganese seam 1 (right).**

### 4.1.2 Hydrological Properties

The calcareous sands have a good porosity and permeability characteristics. Limited surface runoff occurs in the Kalahari area due to the high porosity and permeability of the Kalahari sands. The previous logging of core and aquifer testing undertaken in this area identified that the calcrete breccia zone forms the most significant aquifer in the area. The breccia zone overlies and underlies the red clay layer. The calculated average depth of the water table below surface in the boreholes found at Black Rock Mines is 69.6 metres below ground level, with a maximum depth of 110 m below surface. Figure 32 shows the hydrogeological log of the ventilation shaft indicating the zones where shaft inflows are expected during shaft sinking (Chironga, 2012).

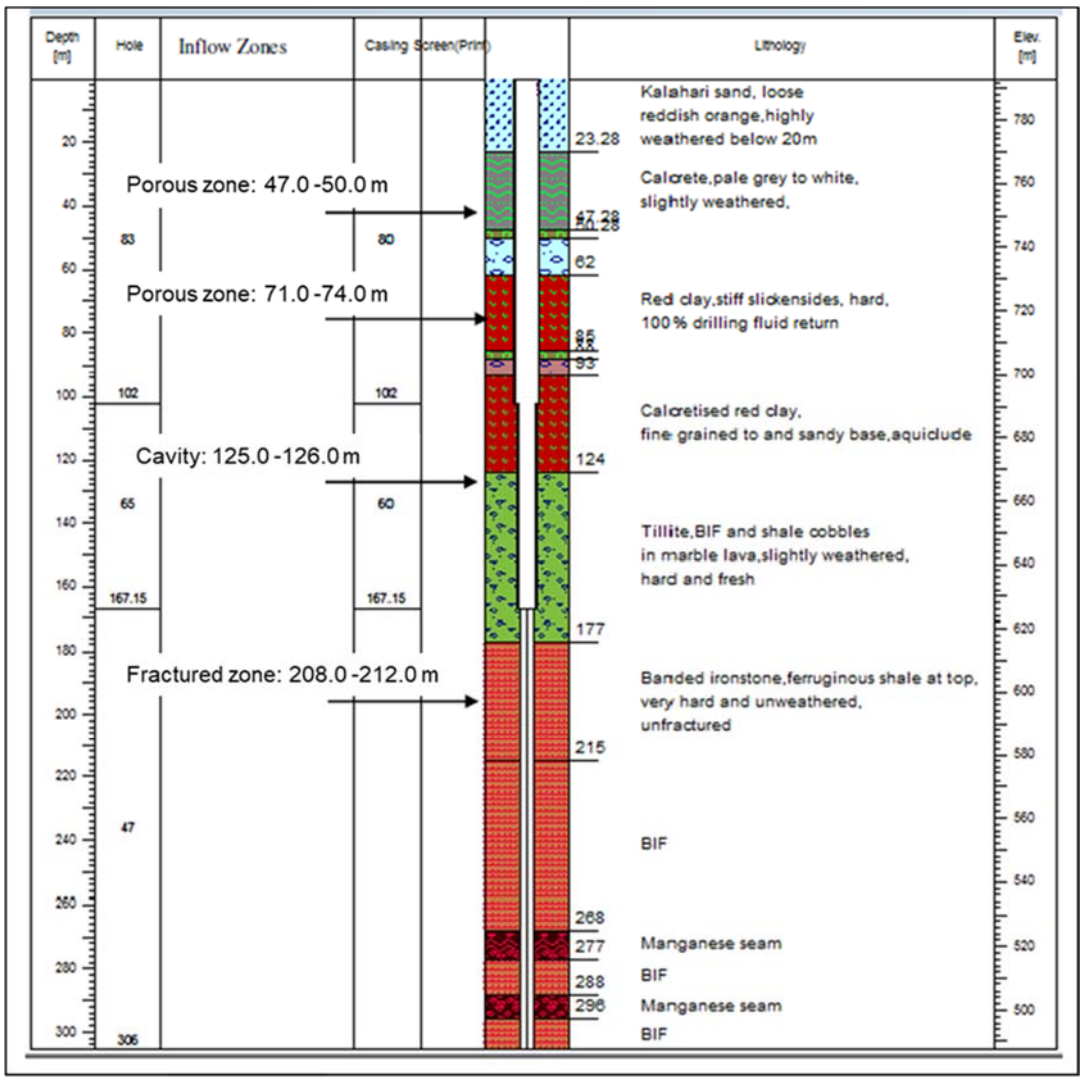



**Figure 32: Hydrogeological log of the ventilation shaft (Chironga, 2012).**

The conglomerate layer is the aquifer with the highest potential for inflow of water during the shaft sinking. A series of interconnected fractures are suspected to be the main conduits for groundwater movement and storage in the other lithologies (Chironga, 2012). The anticipated water inflow in the ventilation shaft is shown in Table 10.

**Table 10: Ventilation shaft water inflow**

| Unit | Drawdown (m) | Aquifer | Hydraulic conductivity, K (m/d) | Inflow rate Q, $m^3/d$ | Cumulative inflow ($m^3/d$) |
|---|---|---|---|---|---|
| 1 | 10 | Conglomerate | 0,42 | 48,9 | 48 |
| 2 | 30 | Red clay | 0,1 | 104,9 | 152 |
| 3 | 39 | Calcrete breccia | 0,42 | 744,6 | 897 |
| 4 | 77 | Tillite | 0,02 | 138,2 | 1035 |

## 4.2 Geotechnical Characteristics

Geotechnical data from the ventilation shaft borehole GLV 01 and data from numerous field investigations are used to characterize the rock mass properties. The data consists of geological core logging of GLV 01, as well as the results of laboratory testing for the individual rock units. For geotechnical classification, the Kalahari rock masses at the ventilation shaft are divided into two domains based on distinct geotechnical behaviours: sand, calcrete, red clay (weak formation); weathered tillite, fresh tillite, and manganese (competent formation).

The simplified lithology of borehole GLV 01 drilled on the shaft centre line is shown in Table 11. For the 'Kalahari' units, laboratory testing involved the grading analysis, Atterberg limits and van der Merwe's activity of the soil (Van der Merwe, 1964). The samples were also classified in terms of both the Highway Research Board (HRB) (AASHTO, 2012) and the Unified Classification System (USCS) (ASTM, 2006). A few samples of the Gordonia Formation sands and Kalahari red clay were obtained at incremental depths from geotechnical boreholes around the area of study. In the calcrete/conglomerate and Dwyka formation, samples were tested for the UCS and UCM. These samples were tested (at Civilab and Rocklab Laboratories, Johannesburg) and the results are summarised in the following section. All original test results are contained within Appendix B.

**Table 11: Simplified Stratigraphy of GLV 01**

| From (m) | To (m) | Rock Type | UCS (MPa) | Q | RMR | GSI |
|---|---|---|---|---|---|---|
| 0.00 | 4.22 | Red Kalahari Sand | 0 | N/A | N/A | N/A |
| 4.22 | 5.20 | Kalahari Sand | | | | |
| 5.20 | 26.00 | Red Kalahari Sand | | | | |
| 26.00 | 32.92 | Calcrete | 20.7 | 1.5 | 42 | 37 |
| 32.92 | 35.22 | Kalahari Sand | 0 | N/A | N/A | N/A |
| 35.22 | 40.00 | Calcrete | 20.7 | 0.7 | 30 | 25 |
| 40.00 | 43.00 | Calcreted Conglomerate | | | | |
| 43.00 | 50.75 | Calcreted Red Clay | 2.95 | N/A | N/A | N/A |
| 50.75 | 71.00 | Red Clay | | | | |
| 71.00 | 73.90 | Calcreted Conglomerate | 20.7 | 1.2 | 40 | 35 |
| 73.90 | 77.40 | Calcreted Conglomerate | | | | |
| 77.40 | 86.64 | Calcrete | | | | |
| 86.64 | 88.90 | Weahtered Tillite | 49.5 | 2.7 | 50 | 45 |
| 88.90 | 103.10 | Weahtered Tillite | | | | |
| 103.10 | 106.90 | Tillite | 74.7 | 7.2 | 59 | 54 |
| 106.90 | 150.60 | Tillite | | | | |
| 150.60 | 151.86 | Gritstone | | | | |
| 151.86 | 162.03 | Tillite | | | | |
| 162.03 | 166.90 | Manganese | 170.8 | 16.4 | 62 | 57 |

The summaries of the soil testing laboratory results for the 'Kalahari' units are shown in Table 13 and Table 14. The sample particle size distribution based on HRB material classification is shown in Figure 33. The Foundation indicator, moisture content and activity laboratory results show that the sand has a moisture content of between 11% and 15% and exhibits no swelling. The sand is however expected to exhibit dispersiveness when subjected to loads and groundwater changes. In terms of the van der Merwe's Activity analysis (Figure 34), the sand shows very low activity. Clays show moisture content of between 22% and 35%, and a swelling percentage of between 6% and 52% and show no dispersiveness. The clay is very active as shown by their very high activity in terms of the van der Merwe's activity analysis (Figure 34) (Van der Merwe, 1964).

In terms of shear strength test results, sand has no cohesion, and friction angle ranges from 31° to 35°. The clay has cohesion of between 0 and 25 kPa, with a friction angle of between 31° and 33°. Two clay samples were tested for free swelling and swelling pressures of 500 and 1200 kPa were recorded. A summary of the cohesion, frictional properties and swelling pressure for the clay is given in Table 12.

**Table 12: Summary of Geotechnical Properties of Sand and Clay**

| Property | | Sand | Clay |
|---|---|---|---|
| **Cohesion (C) (kPa)** | Minimum | 0,0 | 0,0 |
| | Average | 0,0 | 12,5 |
| | Maximum | 0,0 | 25,0 |
| **Frictional Angle (ϕ)** | Minimum | 31,0 | 31,0 |
| | Average | 33,0 | 32,0 |
| | Maximum | 35,0 | 33,0 |
| **Swelling Pressure (kPa)** | Minimum | - | 500,0 |
| | Average | - | 850,0 |
| | Maximum | - | 1200,0 |

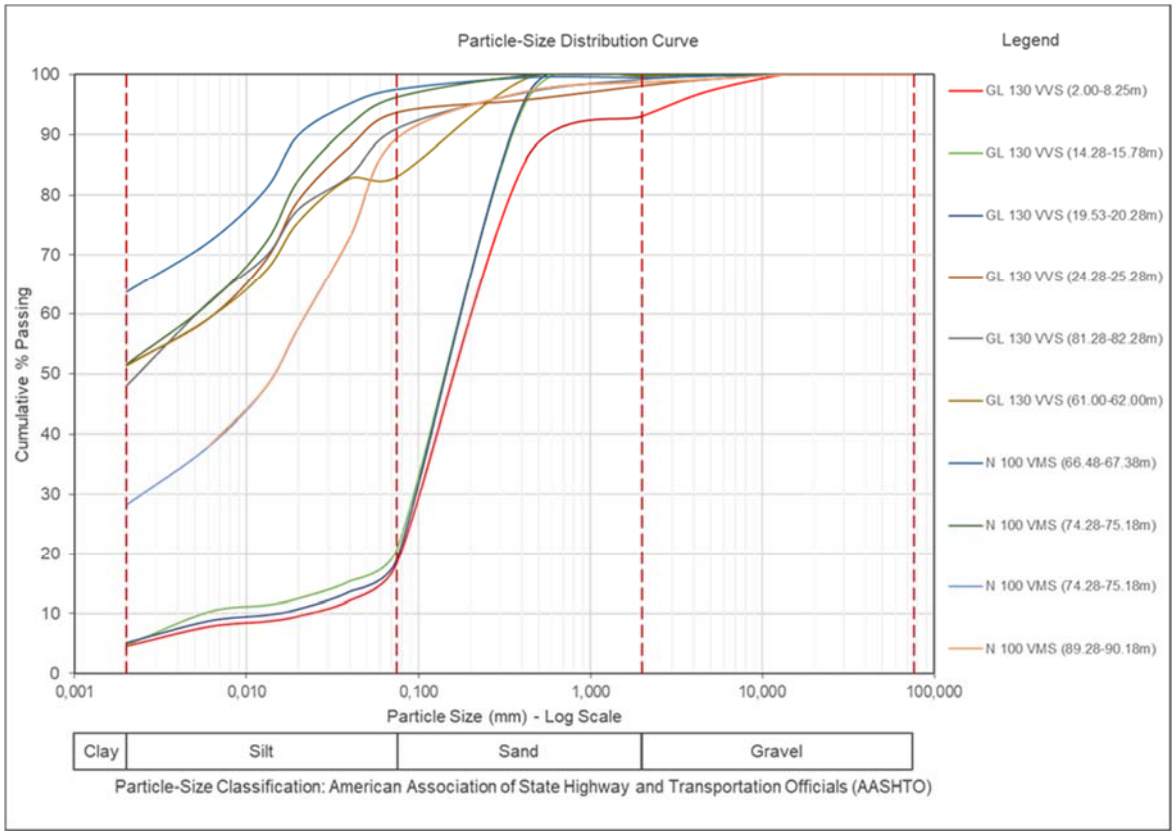



**Figure 33: Sample particle size distribution based on HRB material classification**

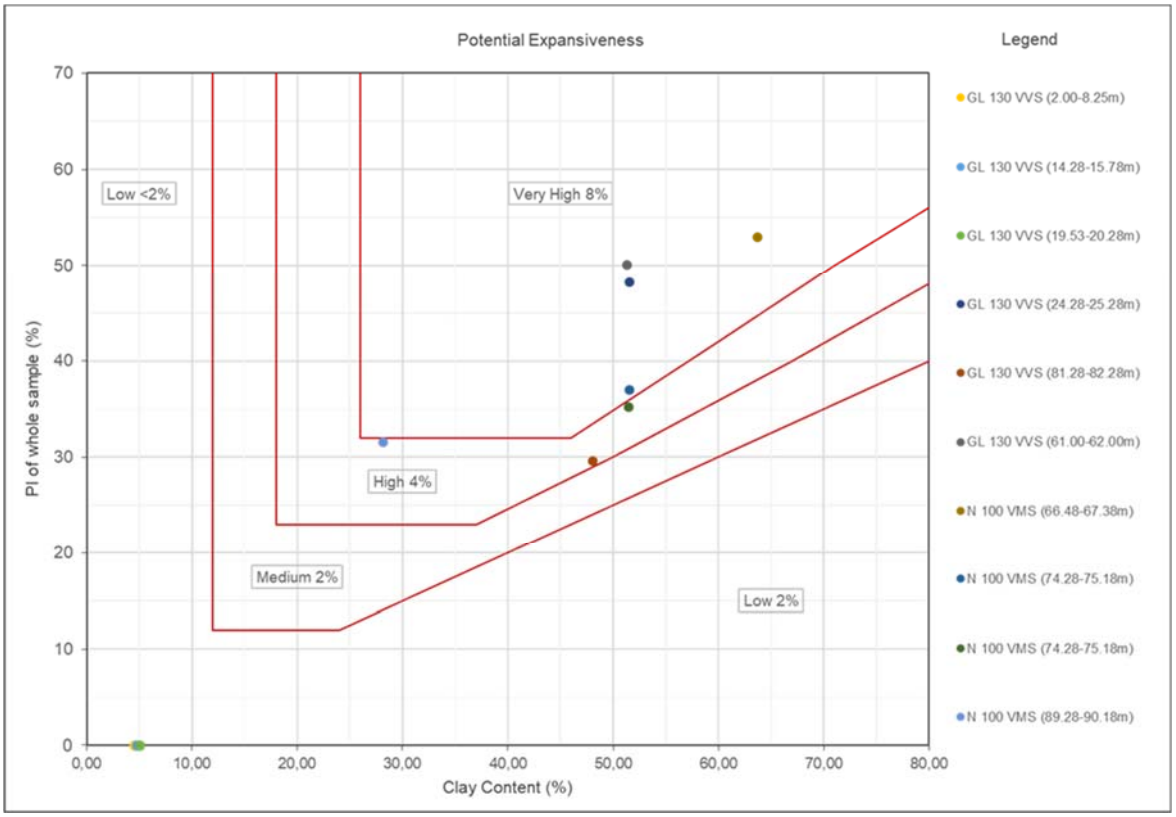



**Figure 34: Potential Expansiveness graph of Red clay (After van der Merwe, 1964)**

**Table 13: 'Kalahari' Laboratory results for the Grading Analysis, Atterberg Limits, Activity and material classification**

| BH ID | | Depth (m) | | Geotech Lith | Grading Analysis (%) | | | | Atterberg Limits | | | GM | NMC % | Swell (%) | Despersiveness | Activity | Material Classification | |
|---|---|---|---|---|---|---|---|---|---|---|---|---|---|---|---|---|---|---|
| | Sample No. | From | To | | Clay | Silt | Sand | Gravel | LL | PI | LS | | | | | van der Merwe | H.R.B. | Unified |
| GL130VVS | I203 | 2.00 | 8.25 | Sand | 5 | 11 | 78 | 7 | SP | SP | 1 | 1.0 | - | - | - | Low | A-2-4(0) | SM |
| GL130VVS | I204 | 14.28 | 15.78 | Sand | 5 | 14 | 82 | 0 | SP | SP | 1 | 0.8 | 15 | - | - | Low | A-2-4(0) | SM |
| GL130VVS | I205 | 19.53 | 20.28 | Sand | 5 | 12 | 83 | 0 | SP | SP | 1 | 0.9 | 11 | - | - | Low | A-2-4(0) | SM |
| GL130VVS | I206 | 24.28 | 25.28 | Red Clay | 52 | 40 | 6 | 2 | 85 | 50 | 21 | 0.1 | 31 | 13 | Non Dispersive | Very high | A-7-5(20) | CH |
| GL130VVS | I207 | 81.28 | 82.28 | Red Clay | 48 | 40 | 11 | 1 | 63 | 31 | 17 | 0.1 | 25 | 6 | Non Dispersive | High | A-7-5(20) | MH |
| GL130VVS | I208 | 61.00 | 62.00 | Red Clay | 51 | 32 | 17 | 0 | 83 | 50 | 18 | 0.2 | 35 | 10 | Non Dispersive | Very high | A-7-5(20) | CH |
| N100VMS | I209 | 66.48 | 67.38 | Red Clay | 64 | 33 | 3 | 0 | 94 | 53 | 18 | 0.0 | 22 | 52 | Intermediate | Very high | A-7-5(20) | MH |
| N100VMS | I210 | 74.28 | 75.18 | Red Clay | 52 | 43 | 5 | 0 | 64 | 37 | 17 | 0.0 | - | - | - | Very high | A-7-6(20) | CH |
| N100VMS | I210A | 74.28 | 75.18 | Red Clay | 51 | 43 | 6 | 0 | 61 | 35 | 18 | 0.1 | - | - | - | Very high | A-7-6(20) | CH |
| N100VMS | I211 | 89.28 | 90.18 | Red Clay | 28 | 55 | 15 | 1 | 59 | 32 | 14 | 0.2 | - | - | - | Very high | A-7-6(20) | CH |

**Table 14: 'Kalahari' Laboratory results for the Shear Box**

| BH ID | | Depth (m) | | Geotech Lith | Shear Box | |
|---|---|---|---|---|---|---|
| | Sample No. | From | To | | Cohesion (C) - kPa | Friction Angle (ϕ) - ° |
| GL130VVS | I204 | 14.28 | 15.78 | Sand | 0 | 31 |
| GL130VVS | I205 | 19.53 | 20.28 | Sand | 0 | 35 |
| GL130VVS | I206 | 68.28 | 69.28 | Red Clay | 0 | 33 |
| GL130VVS | I207 | 81.28 | 82.28 | Red Clay | 25 | 31 |

The rock strength testing was done by conducting Uniaxial Compressive Strength (UCS) and Uniaxial Compressive Strength with Young's Modulus and Poisson's Ratio (UCM), where both the 'Kalahari' and 'Pre-Kalahari' units were tested. Testing of the 'Kalahari' units was done on the calcretes and conglomerates. The Pre-Kalahari testing was done on weathered tillites, tillites, and manganese. The laboratory results are summarised in Table 15.

Calcretes/conglomerates show a UCS range of between 6.70 and 72.48 MPa. These lithological units also show Young's Modulus (E) of between 3.12 and 25.70 GPa and Poisson's Ratio (v) of between 0.14 and 0.38.

Tillites show a UCS range of between 6.07 and 245.4 MPa with weathered tillites having a low UCS range of between 6.07 and 17.3 MPa. The Young's Modulus (E) values are between 20.4 and 58.7 GPa and Poisson's Ratio (v) of between 0.10 and 0.30. Manganese shows a UCS range of between 129.75 and 392.68 MPa, a very strong to extremely strong rock; Young's Modulus (E) values of between 60 and 83 GPa and Poisson's Ratio (v) of between 0.20 and 0.33.

**Table 15: Summary of Geotechnical Properties of Calcrete, Tillite and Manganese**

| Property | | Calcrete | Tillite | Manganese |
|---|---|---|---|---|
| **Uniaxial Compressive Strength (MPa)** | Median | 20,7 | 74,7 | 170,8 |
| | Q1 | 10,6 | 49,5 | 153,5 |
| | Q3 | 32,0 | 96,3 | 194,5 |
| **Uniaxial Tensile Strength (MPa)** | Median | - | 8,3 | 11,7 |
| | Q1 | - | 7,4 | 11,4 |
| | Q3 | - | 12,3 | 12,5 |
| **Elastic Modulus (GPa)** | Median | 9,9 | 40,7 | 66,3 |
| | Q1 | 6,5 | 23,6 | 63,9 |
| | Q3 | 17,8 | 44,0 | 71,3 |
| **Poisson's Ratio** | Median | 0,17 | 0,19 | 0,25 |
| | Q1 | 0,16 | 0,15 | 0,23 |
| | Q3 | 0,27 | 0,24 | 0,28 |

### 4.2.1 Rock Mass Classification

The RMR classification system and Q-system, as described in the literature review, have been previously applied to Tunnelling projects in the Kalahari. There has been an attempt to apply rock classification systems to the red clay of the Kalahari. The clay layer is homogeneous and consists of very stiff heavily slickensided silty clay, with carbonate alteration along individual polished surfaces. This makes the clay vulnerable to the inappropriate application of rock mass classification systems such as RMR. The red clay must be appropriately classified as soil and tested to gather the relevant parameters for tunnel design.

The shaft borehole GLV-01 was geotechnically logged and the rock mass classification values are shown in Table 11. Values between 30 and 62 have been determined for RMR, and 0.7 and 16.4 using the Q-System. Using both the RMR system and Q system, the rock mass rates between 'Very Poor Rock' and 'Good Rock'. The large spread of classification values represents a significant challenge when applying the system for support or excavation design, even at preliminary stages of the design.

## 4.3 Inspection of Early Tunneling Projects

### 4.3.1 Decline

The decline was mapped from the entrance to the bottom and the findings of the mapping exercise are summarized in Table 16 and detailed in Appendix C.

**Table 16: Summary of findings of mapping exercise at the Decline**

| Depth along Decline (m) | % of Decline Length | Support Type | Observations |
|---|---|---|---|
| 0-50 | 9% | Concrete lining | Good condition |
| 50-270 | 37% | Shotcrete of variable thickness [5 cm-10 cm] | ▪ Fair to poor condition - peeling out, vehicle damaged, cracked and water damaged.<br>▪ Large water inflow into decline at 230 m-240 m. |
| 270-530 | 44% | Steel arches with concrete slabs | ▪ Fair to poor condition – voids mainly confined to this area.<br>▪ Voids (~0.3-1.2 m deep) visible through existing holes.<br>▪ Signs of previous rehabilitation – planks, cardboard and empty cement bags. |
| 530-587 | 10% | Spot bolting or none | ▪ High excavation (Height of 4.5 m to 5.5 m)<br>▪ No systematic support |

A square reinforced concrete lining was installed in the Kalahari sands and upper calcrete formation. The gravel, conglomerate and remaining calcrete formations were shotcreted. Water ingress point along the gravel-red clay intersection had a corrugated iron lining along which the water is channeled to flow along the sides of the decline to the bottom where it is pumped. Below the clay, the underlying rock types are not exposed but are indicated to consist of weathered to fresh tillite overlying shale and possibly quartzite and Banded Ironstone Formation (BIF). The tunnel support in these units is cast concrete and steel ribbing. Large portions appear to contain voids above the centreline of the decline, with limited cribbing observed. At the decline and manganese seam intersection, Thin Spray-on liner (TSL) and spot bolting was observed.

The major issues identified at the decline are the large water inflow into the excavation, from about 230 m to 240 m. Voids are clearly visible through small holes from about 220 m to 530 m. These voids (Figure 35) were mostly observed in areas supported using steel arches and concrete slabs. In some areas collapsed loose material was observed behind the slabs through the small holes. From 280 m-330 m in the clay section below the gravels which contain water, damage to the concrete lining was observed (Figure 36). In this area, cracks were observed in the concrete lining between the 1.0 m spaced steel sets (Figure 36). Blocks of concrete lining could dislodge between the sets. The fallout of concrete blocks would also result in the unraveling of the hanging wall.



**Figure 35: View inside a void showing cribbing support along the red clay section of the decline.**

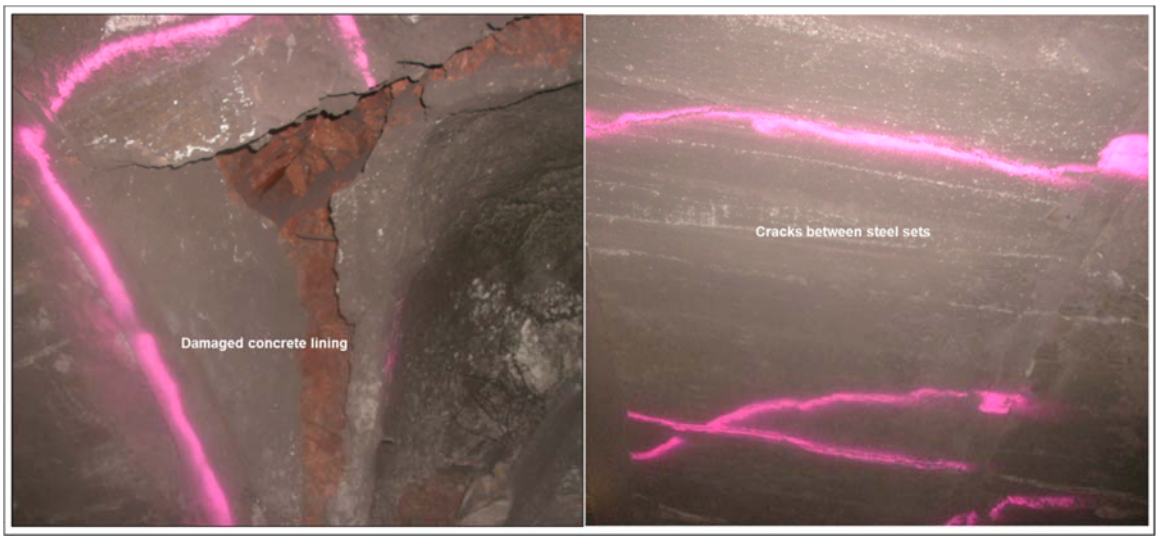



**Figure 36: Damaged concrete lining in the clay section.**

### 4.3.2 Old Ventilation Shaft

At the clay horizon, additional concrete lining was applied possibly to minimize the effects of squeezing conditions which are evident from the bent shaft guides in this area. The concrete restriction could also be a result of a massive concrete backfill to control cave-in failure during sinking. The additional concrete resulted in a smaller cross-sectional area than was originally designed. A 3D scan was carried out in the shaft to determine the restriction as shown in Figure 37. The 3D scan results are shown in Appendix C.




**Figure 37: Additional Lining Installed in Red Clay Horizon**

The shaft is concrete lined with the portion above the restriction being competent concrete which is approximately 350-400 mm thick. The thickness was confirmed by drilling into the shaft sidewalls. The area of the restriction is significantly thicker as the additional concrete that forms the restriction varies from 500 mm to about 1.1 m beyond the original lining.

The major issues identified in the shaft were the large water inflow from about 25 m to 75 m and voids that are clearly visible on shaft walls. At 65 m below the collar in the red clay, the shaft lining scaled off. The lining thickness where the sidewall scaled off (Figure 38 and Figure 39) is 50-100 mm, which is significantly less than 450 mm observed above the restriction.



**Figure 38: Shaft lining scaling off exposing the Red Clay**

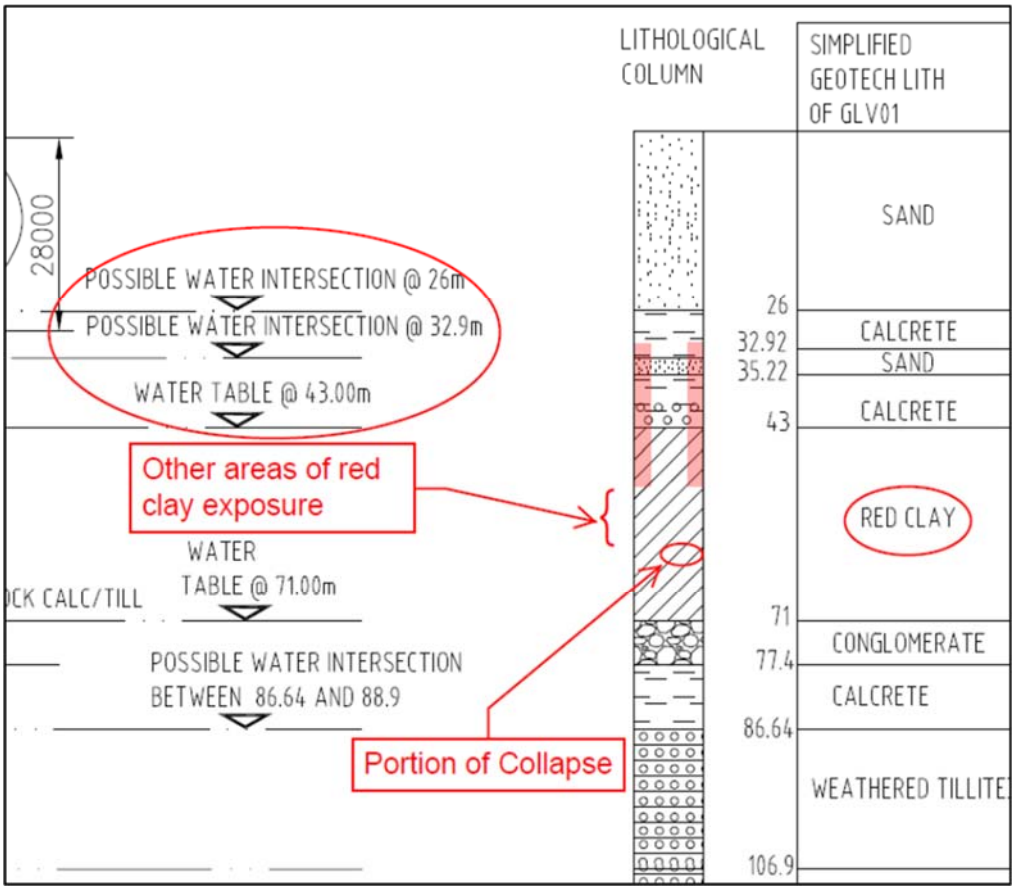



**Figure 39: Location where signs of instability were observed**

With the two inspections of the decline and the ventilation shaft, it can be inferred that in situ stresses and water infiltration are a long-term stability concern for inadequately lined tunnels through the red clay and weathered rock masses. The early tunnelling methods in these formations proved to be problematic and probably of high cost, associated with schedule overruns. The workmanship also proved to be poor as the lining thickness was not consistent in the same formation. There is also no record of the strength of materials used in tunnel lining, indicating that quality control was not done or was superficially conducted.

## 4.4 Numerical Analysis of a Small-Scale Shaft

The material properties of the units are shown in Table 17. The sand was not evaluated in this study as the design of piles is not included in this scope. The derivation of Drucker Prager, k and q constants from Mohr Coulomb parameters is attached in Appendix D. The Drucker Prager constitutive model was used for clay instead of Mohr-Coulomb since it is more suitable for the analysis of cohesive plastic materials. The Hoek and Brown constitutive model was used for calcrete, weathered and fresh tillite, and manganese.

The best constitutive model for clay is the Modified Cam Clay model (MCC). However, this model requires more input parameters, and these are not easy to get from simple tests. For estimating the MCC model parameters, a series of laboratory tests are to be performed. The tests which are required for this purpose are (Devi, 2014):

- Strain-controlled consolidated drained (CD) triaxial tests
- Or consolidated undrained triaxial tests (CU) with pore pressure measurements and
- Load-unload-reload consolidation tests

The abovementioned tests were not carried out due to time and budget constraints.

**Table 17: Rock mass properties of Kalahari units**

| Rockmass Properties | Calcrete | Red Clay | Weathered Tillite | Tillite | Manganese |
|---|---|---|---|---|---|
| Unit Weight (MN/m$^3$) | 0,0216 | 0,0194 | 0,0265 | 0,0265 | 0,0412 |
| Poisson's Ratio | 0,38 | 0,20 | 0,20 | 0,20 | 0,25 |
| Intact Young's Modulus (E) (MPa) | 9900 | 75 | 23600 | 40700 | 66300 |
| Intact Compressive Strength (MPa) | 20,7 | 2,95 | 49,5 | 74,7 | 170,8 |
| Geological Strength Index | 37 | - | 45 | 54 | 57 |
| Intact Rock Constant (mi) | 5 | - | 9 | 10 | 20 |
| k (MPa) (Drucker Prager) | - | 0,02 | - | - | - |
| q (Drucker Prager) | - | 0,5 | - | - | - |

For the weathered tillite, fresh tillite and manganese, large scale convergence or failure of the model is not expected. Failure is expected in the weak units of calcrete and clay. This section focuses on the results of the weak formations.

### 4.4.1 Rocscience RS2

#### *4.4.1.1 Displacement*

In the case of calcrete the model incurred a maximum deformation 0.0022 m and a plastic yield of 4.7 m as shown in Figure 40.

The clay experienced a greater extent and magnitude of deformation than calcrete, as expected. The model incurred a maximum deformation of 0.71 m and a plastic yield of 10.3 m as shown in Figure 41.

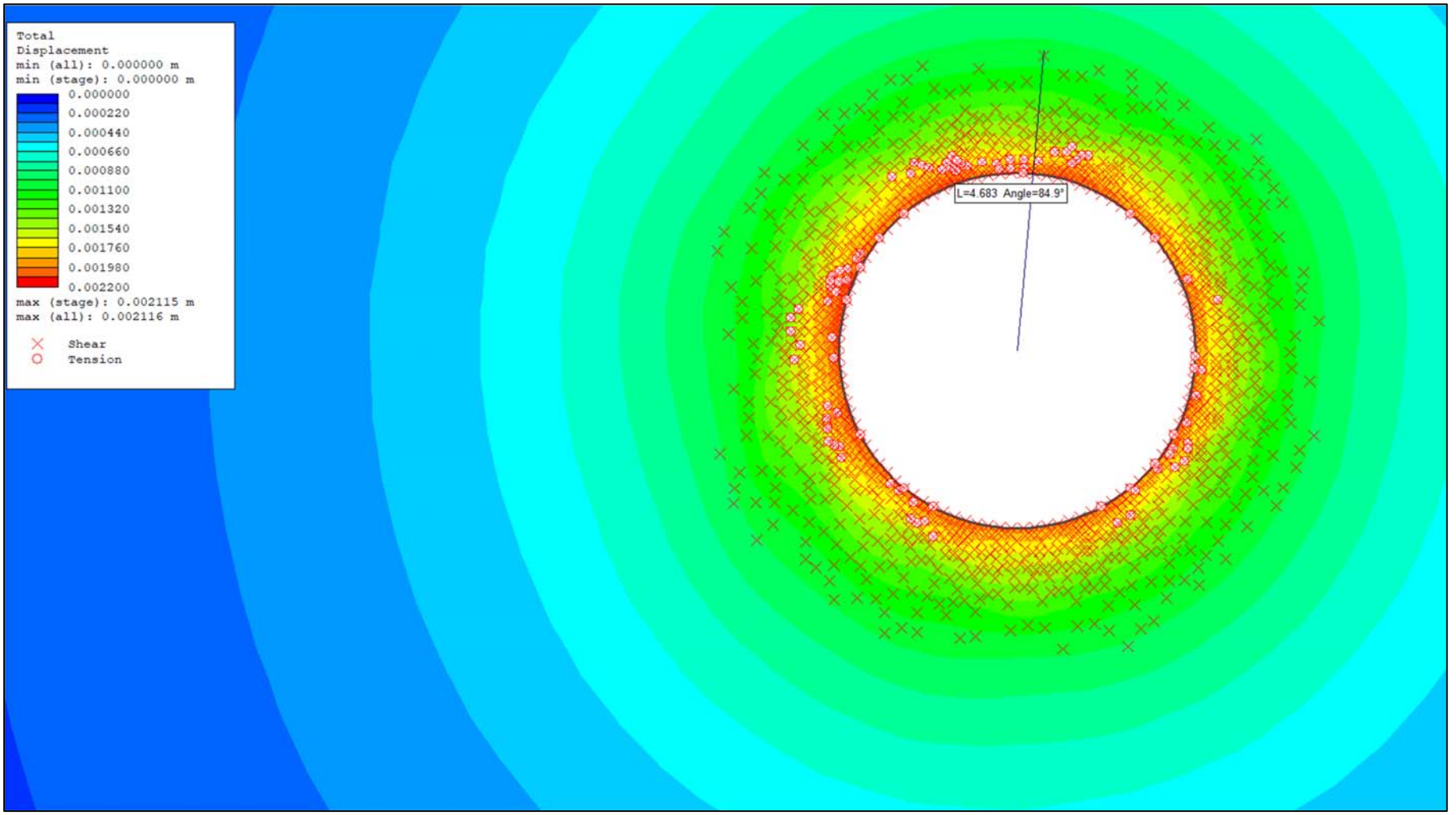



**Figure 40: Total displacement in Calcrete zone**

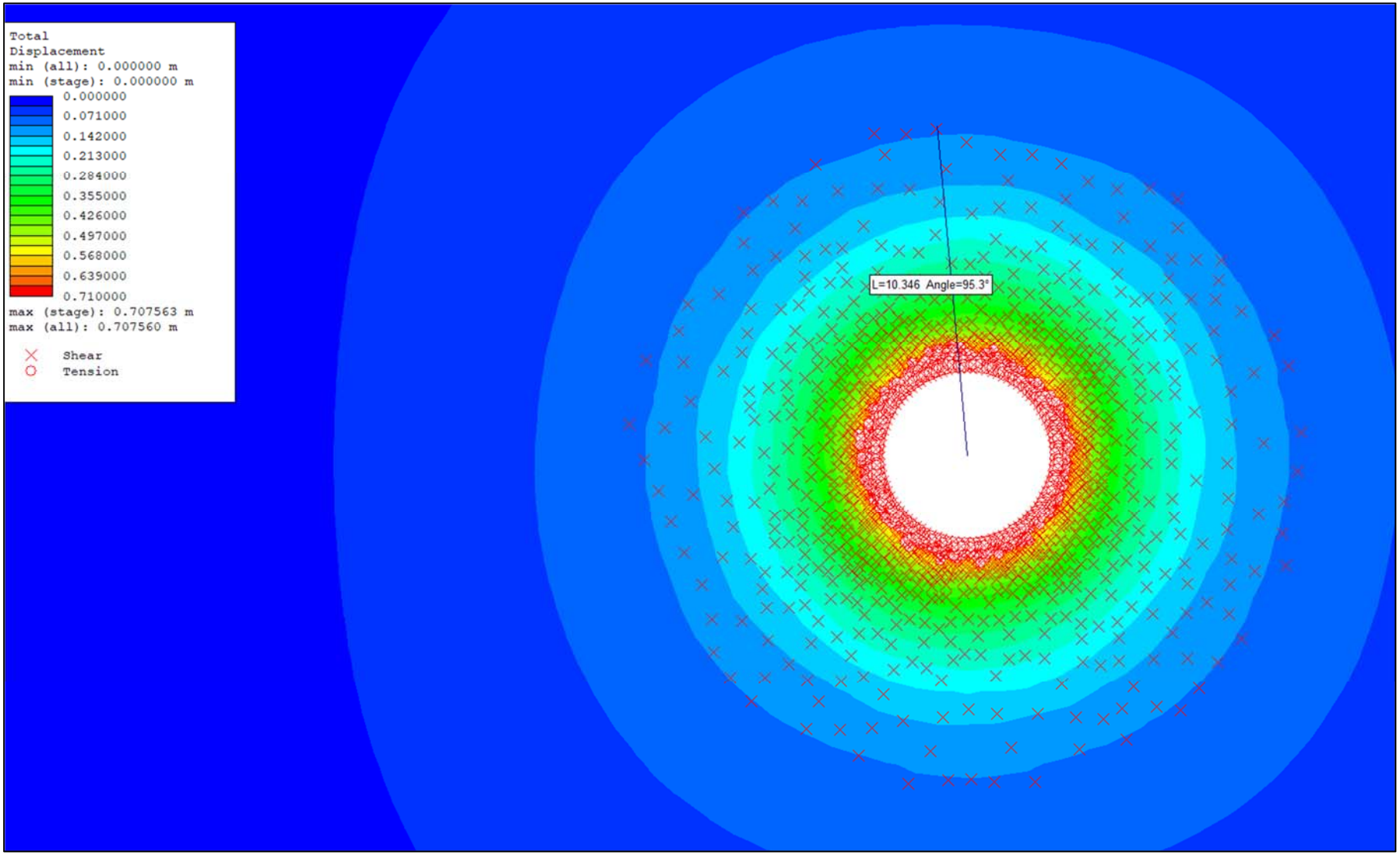



**Figure 41: Total displacement in Clay zone**

#### *4.4.1.2 Support Design*

RS2 has an inbuilt ability to test suggested support system designs for excavations. Support capacity plots were used to evaluate the liner thickness requirements. Design FOS values of 2.1 and 1.75 were used for unreinforced and reinforced concrete liner. The minimum permanent support requirements were a 300 mm thick, 30 MPa UCS concrete liner. The support capacity plot of a 300 mm thick, 30 MPa concrete liner in clay is shown in Figure 42. The plot shows that the liner meets the design FOS of 2.1 for unreinforced concrete.

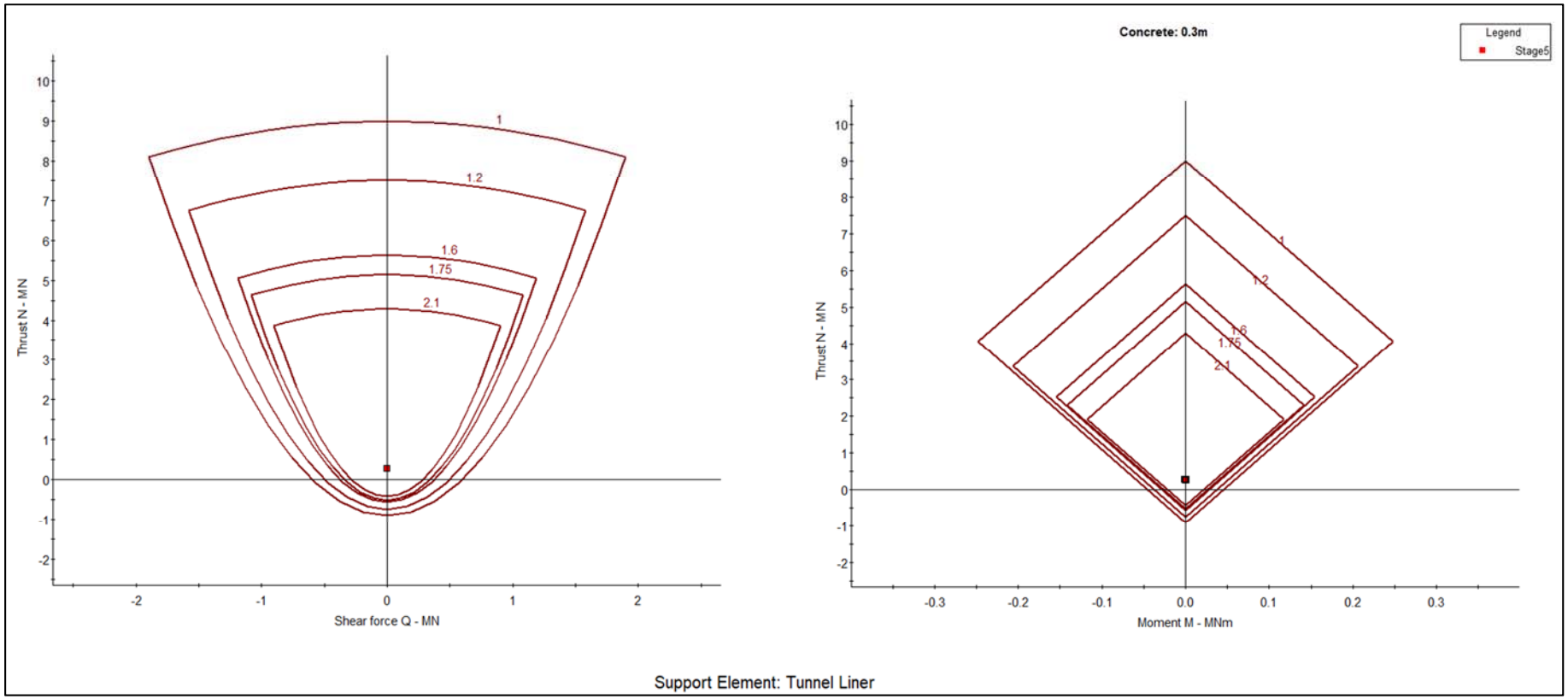



**Figure 42: Support Capacity plot for a 300 mm liner in Clay**

Swelling pressure is a potential risk in clay. The concrete liner support was assessed for different swelling pressures. The results of the assessment are shown in Figure 43.

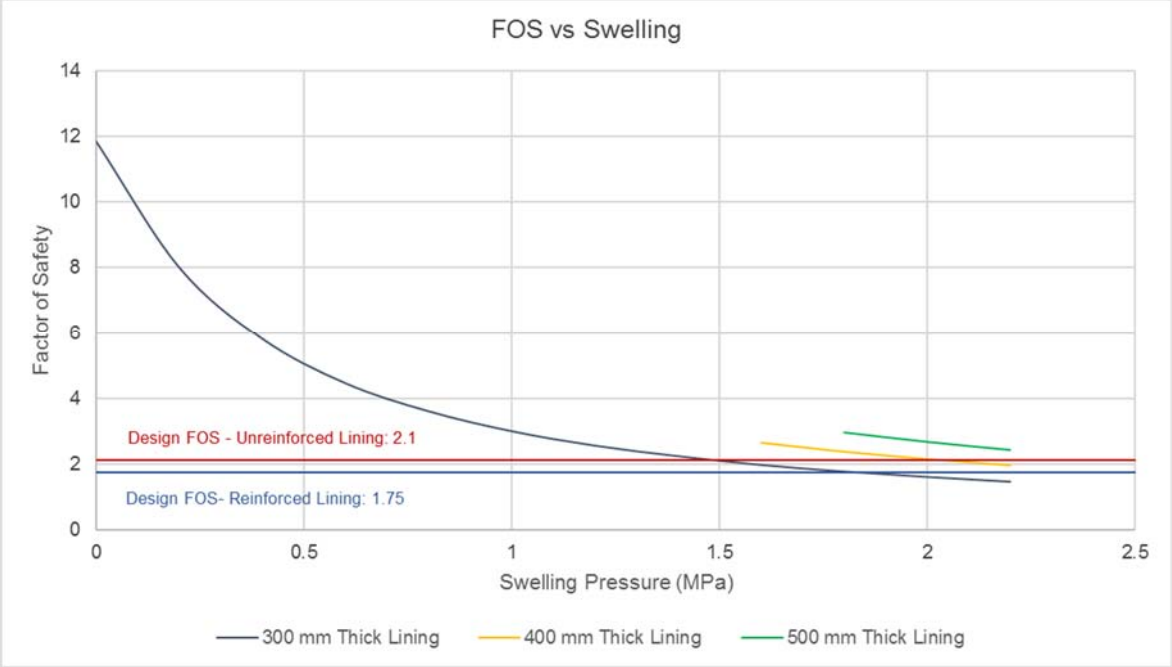



**Figure 43: FOS vs Swelling Pressure for the different liner thickness in Clay.**

From Figure 43, the 300 mm thick, 30 MPa UCS concrete liner fails to meet the unreinforced liner FOS of 2.1, at a swelling pressure of 1.6 MPa. For the 400 mm thick liner, it fails at a swelling pressure of more than 2.0 MPa. The 500 mm thick liner can withstand a swelling pressure in excess of 2.2 MPa. The support capacity plots for a 300 mm thick concrete liner in clay at 1.6 MPa swelling pressure is shown in Figure 44 and the plot for a 400 mm liner at 2.2 MPa is shown in Figure 45.

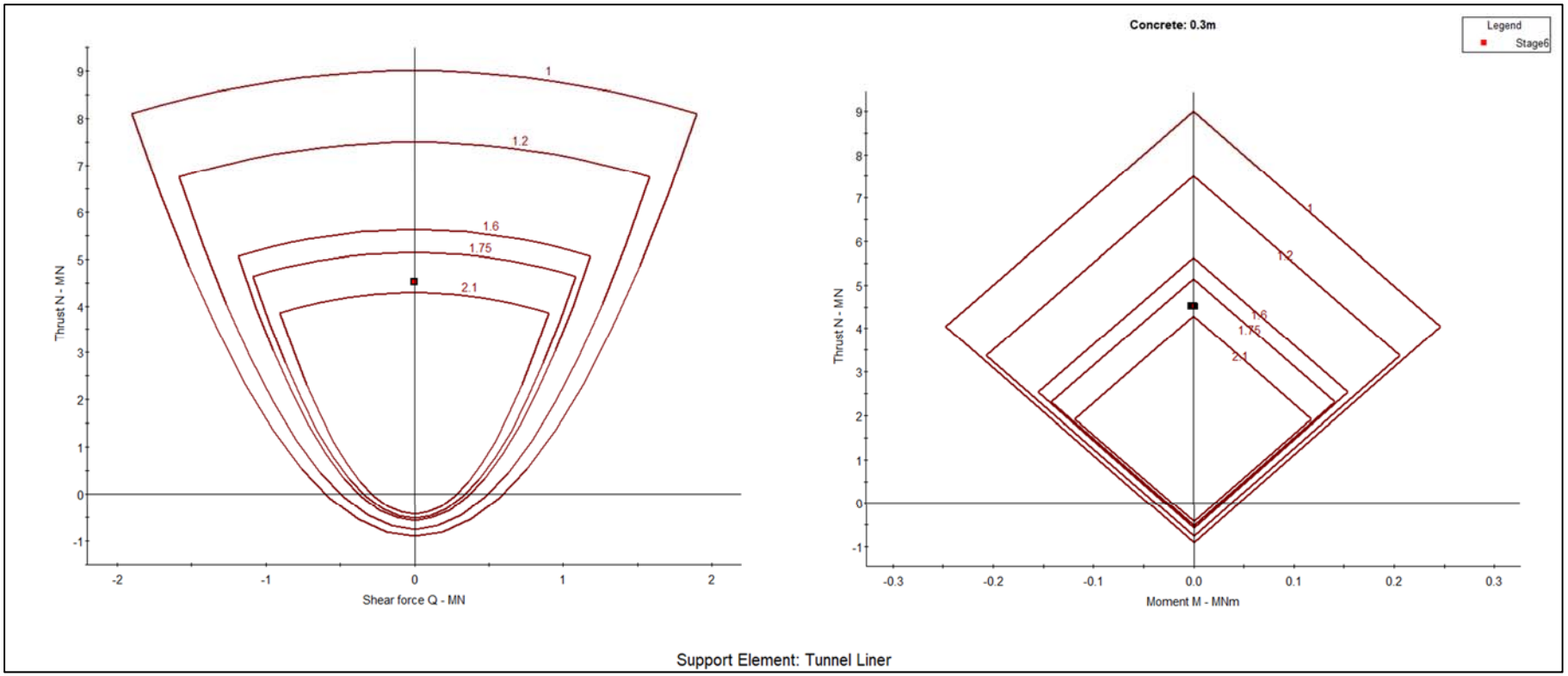



**Figure 44: Support Capacity plot for a 300 mm liner in Clay at a Swelling Pressure of 1.6.**

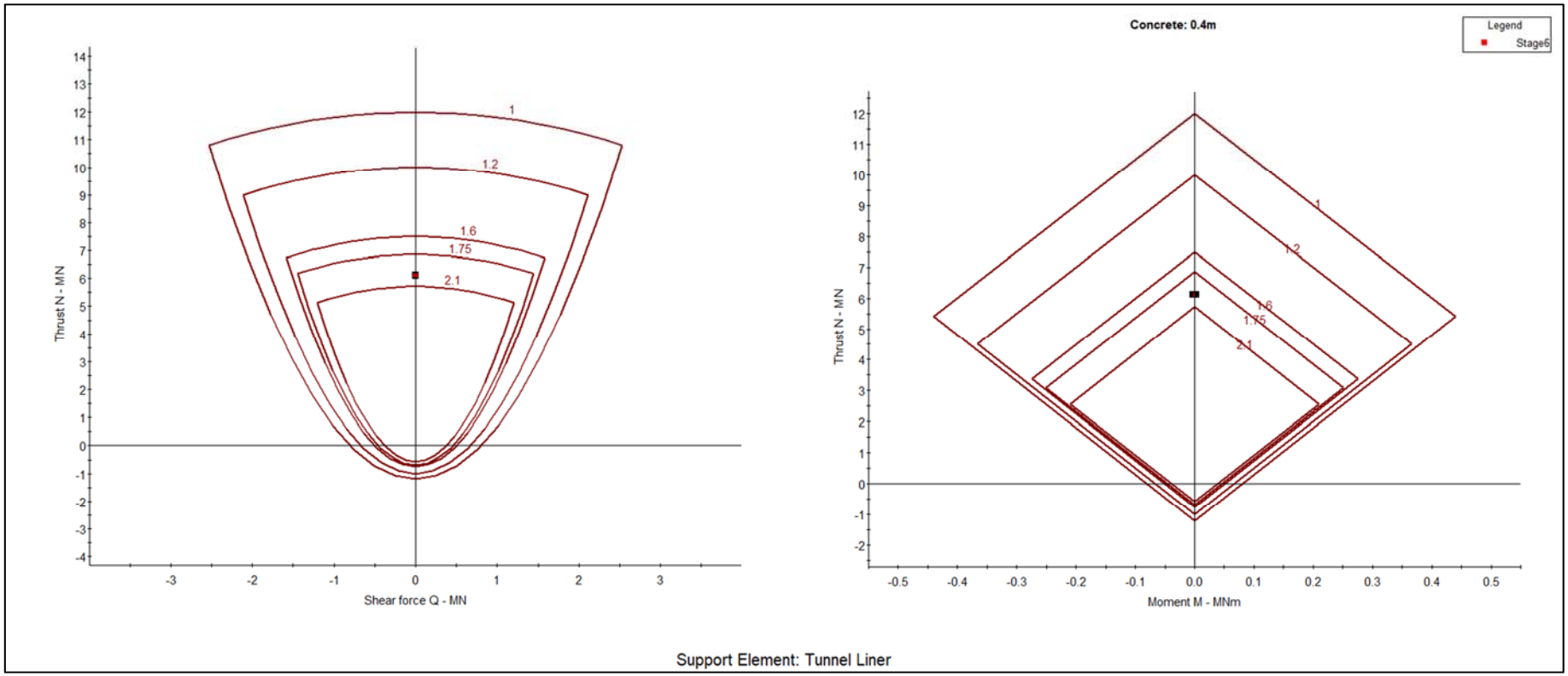



**Figure 45: Support Capacity plot for a 400 mm liner in Clay at a Swelling Pressure of 2.2.**

The benefit of using a reinforced concrete liner as compared to an unreinforced concrete liner was assessed by evaluating a 500 mm thick, 30 MPa UCS liner at a swelling pressure of 2.2 MPa. The results of the assessment are shown in Figure 46. From the figure, there is no benefit in using a reinforced liner as compared to an unreinforced liner. The project owner has the honor of deciding on the reinforcement requirements, reinforced or unreinforced liner.

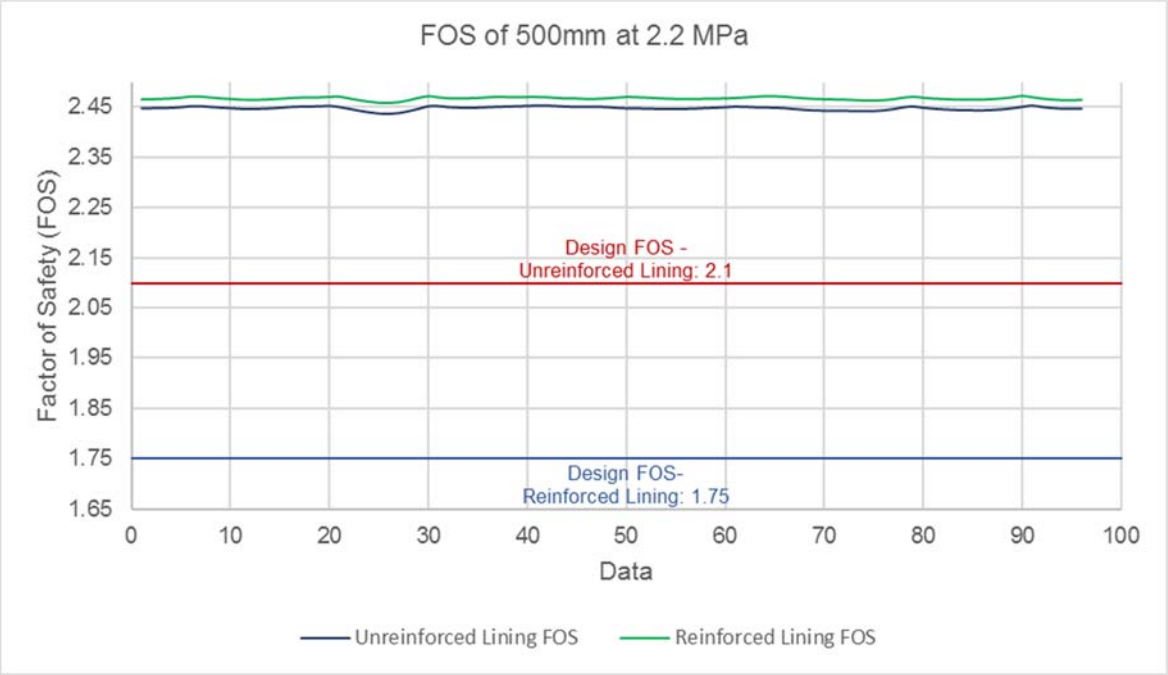



**Figure 46: Reinforced liner vs Unreinforced liner FOS**

### 4.4.2 Rocscience RS3

In the case of calcrete, it was found that the total displacement predicted by the RS2 model is 57% more than the displacement of the RS3 model. The total displacement predicted by RS3 model was 0.0014 m and the RS2 model predicted 0.0022 m.

The clay incurred a total displacement of 0.45 m in the RS3 model and 0.71 m in RS2. This is 58% more than the displacement of the RS3 model. Such a difference in simulation results may be mainly due to the different types of model elements. RS2 used 6 Noded Triangles and RS3 uses 10 Noded Tetrahedral elements. The total displacement of clay is shown in Figure 47.

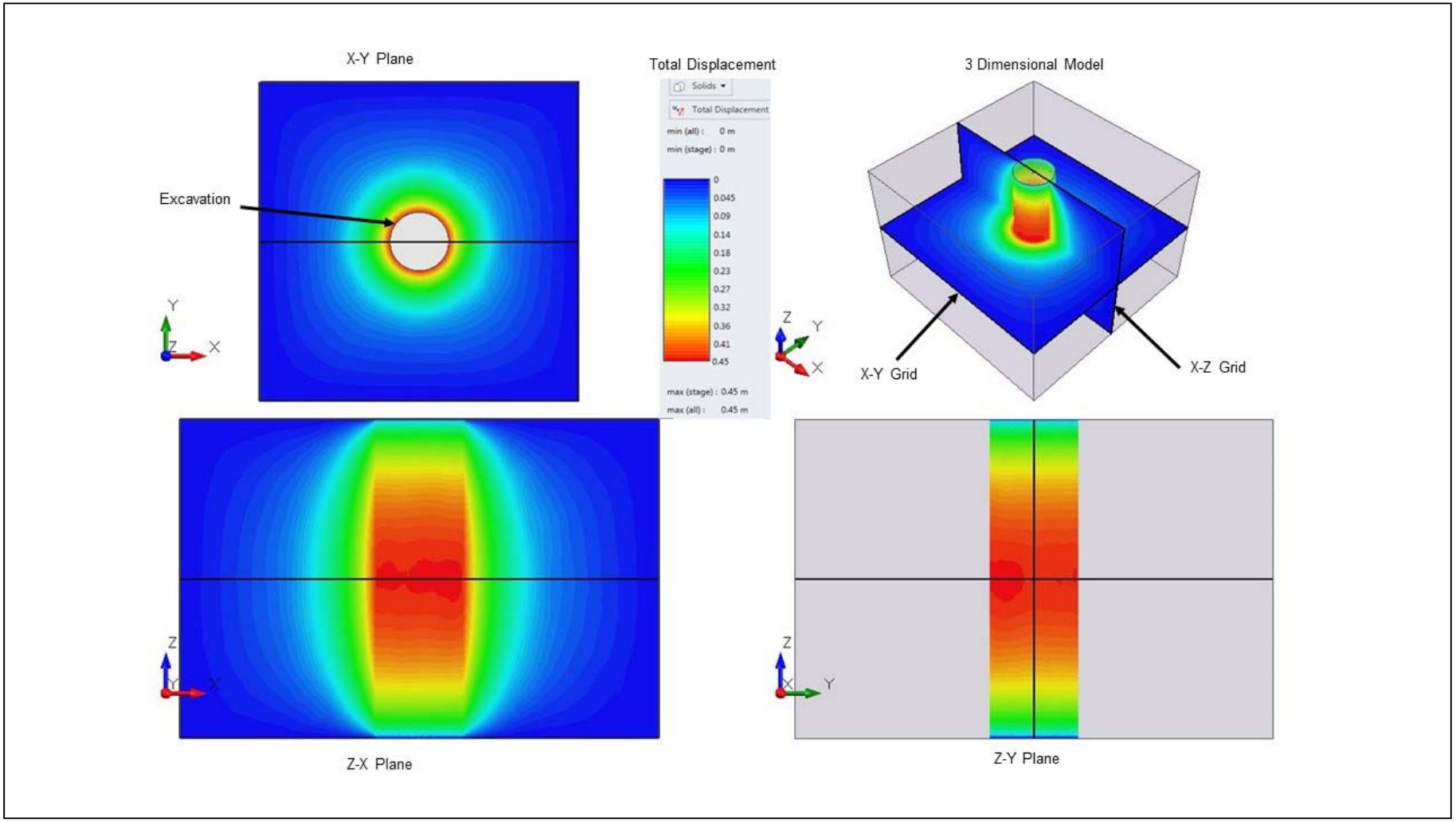



**Figure 47: Total displacement in Clay of the RS3 model**

## 4.5 Recent Tunnelling Works: Ventilation Shaft

The project used as a case study in this section is the development of a ventilation shaft whose geological and geotechnical environment has been already discussed. The groundwater control measures implemented prior to shaft sinking were evaluated during the excavation of the shaft. The shaft was logged daily, and the following was observed:

- The temporary support of oscillator piles installed in the Kalahari sands was effective in minimising the risk of the shaft walls caving in during sinking (Figure 26).
- The temporary support of ARMCO ring barriers used in the clay section was effective in providing areal coverage and maintaining the structural integrity of the shaft.
- Minimum water inflow was experienced in the shaft during sinking due to the ground control measures implemented.

The planned average advance rate of 1.2 m per day was achieved in the red clay, and excavation of the shaft was completed within the proposed schedule without any setback. No major water inflow was reported.

## 4.6 Implication on Future Projects

The detailed review of the geological and geotechnical settings and review of recent experience in tunnelling within the Kalahari formation allows for an evaluation of current excavation methods and the development of recommendations for future works. In similar projects in the Kalahari, cave in failure has been reported in the red clays due to hydration. The concrete lining has also failed in the red clay in a recent shaft sinking project not reviewed in this study. At Black Rock mines, no tunnelling project reported surface subsidence for the length of the decline, indicating that though the projects encountered several setbacks and recently stability issues, the ultimate goal of stability is still being met.

### 4.6.1 Key Lessons from Recent Project

The recent tunnelling project reviewed provides key lessons upon which future projects may build in order to improve tunnelling progress and limit setbacks.

- Detailed geotechnical investigations are of supreme importance in the development of a tunnel design. Geotechnical boreholes should be drilled to intercept the proposed excavation location as a minimum requirement. All the data obtained from the investigation must be incorporated into the design.
- A method to mitigate the adverse effect of groundwater inflow should be incorporated into the design. An impermeable curtain around the tunnel or shaft will not only prevent groundwater inflow but also strengthen the weak rock masses by improving cohesion.
- The medium through which a tunnel passes largely controls the water inflows and in transitioning from calcretes/ conglomerates to red clay, water inflow changes drastically. Most of the water is contained in the gravels and conglomerates and on the interception of these lithologies dewatering measures must be modified to improve removal of the increased water quantities.

- When passing through the different lithologies, variable temporary support measures are required, and ability to easily change and install the appropriate support would be beneficial, so as not to slow down the tunnel advance rate.
- Shaft sinking experience has a significant impact on advance rates in challenging ground, and experienced operators should at least be available for consultation when inexperienced operators are used.
- Dry months, though challenging for workers, were thought to have greatly reduced water inflows which was critical for shaft sinking. The projects must be planned in such a way that possible water intersections are excavated in the dry season.

# 5 CONCLUSIONS AND RECOMMENDATIONS

The impact of weak Kalahari formation on the design and tunnelling of structures is significant for both large scale and small-scale excavations. Currently, tunnel design and support is based on experience and empirical methods. The work carried out in this report focused on the impact of the Kalahari geotechnical environment on a small-scale project. The work also involved the use of a concrete lining design FOS in the assessment of support requirements. The effect of swelling pressure on the concrete lining in clay was assessed by applying a varying uniform load on the concrete liner and using support capacity plots to determine the FOS. Conclusions have been drawn from the use of unreinforced and reinforced concrete liner design FOS.

The major conclusion from the research is that the Kalahari rock masses present unique challenges to empirical designs and tunnelling methodologies with special considerations regarding swelling clay. Excavation sizes, geotechnical and geohydrological properties, and failure mechanisms all influence the initial stability of an excavation and the required support systems to maintain stability. Excavations through weak and challenging ground conditions are often evaluated with numerical models to better understand and predict expected conditions. The following is concluded on support design using numerical models:

- A design criterion for the unreinforced and reinforced long-term concrete liner is presented. Support capacity plots are easy to interpret, and they are a powerful tool for the designer.
- For the weak Kalahari rock masses, 2D modelling may result in a large deviation from the 3D results as shown by the total displacement of the RS2 models which is 1.6 times those obtained with RS3. The lower the strength of the weak formation the larger the deviation will be.
- For RS2 to be realistically used for analysing the effects of a weak formation which is perpendicular to the tunnel, the thickness of the zone has to be much wider than the excavation span.
- Using 2D models, it is a challenge to establish the stage for liner installation, using the core softening method. It is difficult to define the amount of deformation before the installation of the liner. Computing displacement prior to support installation using the Vlachopoulos and Diederichs (2009) method is not easy. If support is installed close to the face a higher support demand is required, therefore overestimating the liner thickness.
- There is no significant difference between the reinforced and unreinforced liner FOS.
- Swelling pressure may considerably increase the support demand on a liner and is simplified as a uniform load on the excavation in the model. The loading on the tunnel liner support is far less than its compressive strength, even for an unreinforced concrete liner. This suggests that the Kalahari weak formations may be excessively supported when the swelling clay is not very active.
- The laboratory results of swelling pressure and free swelling tests indicate the relative swelling potential, which is valuable for the evaluation of potential stability problems and tunnel support design. The swelling pressure measured in the laboratory is not representative of the in situ swelling pressure on tunnel support. This presents a challenge as to which maximum swelling pressure to use in the support evaluation.

- It is critical that the expected failure mode of the rock mass be adequately captured in the model. The appropriate constitutive failure model applicable to clay should be used for the correct evaluation of support.

The following is recommended for future projects:

- Due to the geological history of the Kalahari manganese field, the lithology is highly variable in nature, from cohesionless aeolian sands of the Gordonia Formation, red clay and relatively weak weathered formations to competent Cox formation (manganese). These rock units are significantly interfingered, laterally and vertically discontinuous. For each tunnelling project, it is important to complete a detailed site investigation, including geotechnical strength laboratory testing to determine the variation of in situ material properties. A significant number of samples should be collected and sent for the appropriate type of test to determine the correct parameter for assessment in the design process used to identify potential risks.
- Due to the presence of water-bearing rock mass formations, water inflow or discharge into the excavations can be catastrophic. A detailed hydrogeological investigation to gain an understanding of the pore water and groundwater conditions expected during shaft sinking must be done. To avoid setbacks related to water control, tunnelling in the red clays and water-bearing strata must be scheduled in the dry months of the year.
- Due to the discontinuous nature of the formations, it is important to always allow a fair amount of variability into the expected conditions during the excavation design process. It is important for contractors to use and incorporate the information provided by the geotechnical reports in the selection of the method of excavation and equipment for the project. The method of excavation must be tailor-made for each project and must not be a copy and paste exercise.
- Due to the fact that, the Red Clay deteriorates on exposure to the atmosphere and water, it is important that work stoppages in this horizon are avoided.

For tunnel support estimation in the weak Kalahari formation containing swelling clay, it is recommended to follow the flow chart shown in Figure 48 as a complement to empirical design. Empirical design is not sufficient since swelling effects are not fully accounted for in the Q-system or other commonly used rock mass classification systems.

Suggested areas for further research into the use of the 3D model include the comparison of 2D and 3D model support requirements in the weak formations. Additional studies evaluating the RS2 and RS3 models available in alternative numerical software, including but not limited to Itasca software (FLAC, FLAC3D, UDEC and 3DEC), are highly recommended.

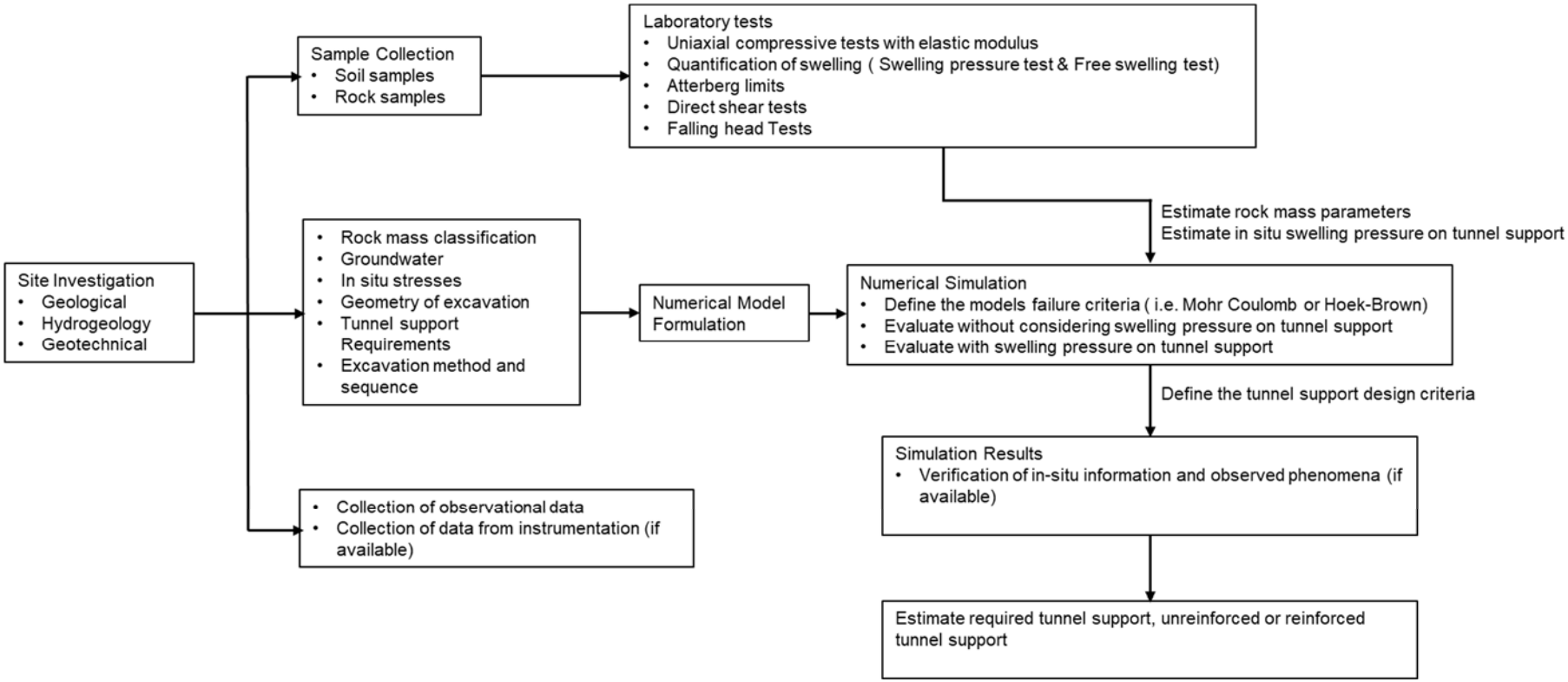



**Figure 48: Flow chart for tunnel support estimation in the Kalahari weak formations**

# 6 REFERENCES


AASHTO. (2012) Classification of soils and soil-aggregate mixtures for highway construction purposes. M145-91. American Association of State Highway and Transportation Officials. Washington, DC, USA.

Anagnostou, G. (1993) A model for swelling rock in tunnelling. Swiss Federal Institute of Technology, Zurich, Switzerland, Journal of Rock Mechanics and Rock Engineering, pp. 307-3.

Anagnostou, G. (2007) Design uncertainties in tunnelling through anhydrite swelling rocks. Journal of Rock and Soil Engineering, Vol. 25, No. 4, pp. 48-54.

Anagnostou, G., Pimentel, E. and Serafeimidis, K. (2010) Swelling of sulphatic claystones – some fundamental questions and their practical relevance. 59th Geomechanics Colloquy 2010, Session on “Tunnel construction in swelling ground”, Switzerland, pp. 12.

ASTM. (2006) Standard practice for classification of soils for engineering purposes. Unified Soil Classification System). D2487. West Conshohocken, PA, USA.

Barla, M. (1999) Tunnels in swelling ground - Simulation of 3D stress paths by triaxial laboratory testing. Politecnico di Torino, Italy, PhD Thesis, pp. 189.

Barton, N. and Abrahao, R. (2003) Employing the QTBM prognosis model. Tunnels & Tunnelling December 2003. 20-24.

Barton, N. (2002) Some new Q-value correlations to assist in site characterization and tunnel design. International Journal of Rock Mechanics and Mining Sciences 39(2): 185-216.

Barton, N., Lien, R. and Lunde, J. (1974) Engineering classification of rock masses for the design of tunnel support. Rock Mechanics. 6: 189-239.

Barton, N. (1998) Quantitative description of rock masses for the design of NMT reinforcement. Shimla, India.

Baynes, F.J. (2010) Sources of geotechnical risk. Quarterly Journal of Engineering Geology and Hydrogeology. 43: 321-331.

Berdugo, I.R. (2007) Lessons learned from tunnelling in sulphate-bearing rocks. Department of Geotechnical and Geosciences, Technical University of Catalonia, Barcelona, Spain, Presentation, pp. 77.

Beukes, N.J., and Dreyer, C.J.B. (1986) Crocidolite deposits of the Pomfret Area, Griqualand West, in: Mineral Deposits of Southern Africa, eds., C.R. Anhaeusser and S. Maske: Geol. Soc. S. Afr., v. I, pp. 911-921.

Bieniawski, Z.T. (1973a) Classification of rock masses for engineering: The RMR system for future trends. Comprehensive Rock Engineering, (ed. Hudson), Oxford, Pergamon. 3: 553-573.

Bieniawski, Z.T. (1973b) Engineering classification of jointed rock masses. Trans S. Afr.Inst. Civ. Engrs 15, 335-344.

Bieniawski, Z.T. (1974) Estimating the Strength of Rock Materials. Journal of South African Institute of Mining and Metallurgy, 8: p312~320.

Bieniawski, Z.T. (1984) The design process in rock engineering. Rock Mechanics and Rock Engineering. 17: 183-190.

Bieniawski, Z.T. (1989) Engineering rock mass classifications: A complete manual for engineers and geologists in mining, civil, and petroleum engineering. New York City: John Wiley & Sons, Inc.

Bobet, A. (2010) Numerical methods in geomechanics. The Arabian Journal for Science and Engineering. 35(1B): 27-48.

Brady, G.S. and Clauser, H.R. (1986) Material handbook. New York, USA: McGraw-Hill.

Brekke, T.L. and Selmer-Olsen, R. (1965) Stability problems in underground constructions caused by montmorillonite-carrying joints and faults. Norway Institute of Engineering Geology, 1: pg. 3-19.

British Tunnelling Society. (2004) Tunnel lining design guide. Thomas Telford, London.

Chamber of Mines South Africa. (2016) Mine SA Facts and Figures Pocket Book, pg 11-27.

Chamber of Mines South Africa. (2017) Mine SA Facts and Figures Pocket Book, pg 8.

Chironga, L. (2012) Black Rock Mine water study report, unpublished report.

Clayton, C.R.I., Matthews, M.C. and Simons, N.E. (1995) Site Investigation (2nd Edition). Hoboken: Wiley-Blackwell.

Cornell, D. H., Schutte, S. S. and Eglington, B. L. (1996) The Ongeluk basaltic andesite formation in Griqualand West, South Africa: Submarine Alteration in a 2222 Ma Proterozoic sea. Precambrian Research. 79; 101-123.

Council for Geoscience. (2012). Simplified geology of the Northern Cape Province [online]. <http://www.geoscience.org.za/index.php?option=com_content&view=article&id=341:simplified-geology-of-the-northern-cape-province&catid=68:more-onnorthern-cape-region&Itemid=449> [Accessed: 28 June 2012].

Crockford, A.M. (2012) Shallow Urban Tunnelling through Heterogeneous Rockmasses: Practical Experience from scale Tunnels in Calgary, Alberta and the Influence of Rockmass Layering on Excavation Stability and Support Design. 11-30

Deere, D.U. (1989) Rock quality designation (RDQ) after twenty years. U.S. Army Corps Engineers Contract Report GL-89-1. Vicksburg, MS: Waterways Experiment Station.

Deere, D.U., Hendron, A.J., Patton, F.D. and Cording, E.J. (1967) Design of surface and near surface construction in rock. Proceedings from the 8th U.S. Symposium on Rock Mechanics, Minneapolis, MN. 237-302.

Devi, D. (2014) On the determination of modified cam clay model parameters. International Journal of Innovative Research in Science, Engineering and Technology, India. Vol 3, 250-253.

DIN 1045. (1988) Structural Use of Concrete- Design and Construction, German Institute for Standardisation.

Duddeck, H. (1988) Guidelines for the Design of Tunnels. Prepared by the International Tunnelling Association Working Group on General Approaches to the Design of Tunnels. Tunneling and Underground Space Technology, 3(3). 237-249.

Einstein, H.H. and Bischoff, N. (1975) Design of Tunnels in Swelling Rocks, 16th Symposium on Rock Mechanics, University of Minnesota, Minneapolis, MN, pp. 185-195.

Fookes, P.G. (1997) The 1st Glossop Lecture: Geology for engineers: the geological model, prediction and performance. Quartely Journal of Engineering Geology. 30: 293-424.

Gioda, G. (1982) On the non-linear “squeezing” effects around circular tunnels. International Journal for Numerical and Analytical methods in Geomechanics, vol. 6, pp. 21-46.

Goel, R.K. (1994) Correlations for predicting support pressures and closures in tunnels. Ph.D. Thesis. Nagpur University, India.

Goel, R.K., Jethwa, J.L. and Dhar, B.B. (1996) Effect of tunnel size on support pressure. International Journal of Rock Mechanics and Mining Science & Geomechanics Abstracts 33(7): 749-755.

Grimstad, E. and Barton, N. (1993) Updating the Q-System for NMT. Proc. Int. Symp. on sprayed concrete - modern use of wet mix sprayed concrete for underground support, Fagernes. 46-66. Oslo: Norwegian Concrete Assn.

Grimstad, E., Kankes, K., Bhasin, R., Magnussen, A. and Kaynia, A. (2002) Rock mass quality Q used in designing reinforced ribs of sprayed concrete and energy absorption. In proceedings: International Symposium on Sprayed Concrete. Davos 2002, pp. 134-142.

Gustin E.J.G, Karim U.F.A. and Brouwers H.J.H. (2007) Bleeding characteristics for viscous cement and cement-bentonite grouts. Géotechnique; 57(4):391-395.

Gutzmer, J., Beukes, N.J. and Yeh, H.W. (1997) Fault-controlled metasomatic alteration of Early Proterozoic sedimentary manganese ore at Mamatwan Mine, Kalahari manganese field, South Africa. S. Afr. J. Geol. 100 (1), 53-71.

Guyer J.P. (2009) Introduction to Soil Grouting (2nd Edition). The Clubhouse Press, El Macero, California.

Haddon, I.G. and McCarthy, T.S. (2005) Mesozoic-Cenozoic interior sag basins of Central Africa: The Late-Cretaceous-Cenozoic Kalahari and Okavango basins. Journal of African Earth Science, 43, 316-333.

Hoek, E. and Brown, E.T. (1988) The Hoek-Brown Failure Criterion - A 1988 update. In Rock Engineering for Underground Excavations, Proceeding of 15th Canadian Rock Mechanics Symposium (ed. J.C. Curran), p31~38. Toronto: Department of Civil Engineering, University of Toronto.

Hoek, E and Brown, E.T. (1997) Practical estimates of rock mass strength. International Journal of Rock Mechanics and Mining Sciences. 34(8): 1165-1186.

Hoek, E. (1992) When is a design in rock engineering acceptable? - 1991 Müller lecture. Proc. 7th Congress Intnl. Soc. Rock Mech., Aachen. Rotterdam: A.A. Balkema.

Hoek, E. (1994) Strength of rock and rock masses. ISRM News Journal. 2(2): 4-16.

Hoek, E. (1998) Tunnel support in weak rock. Keynote address from The Symposium of Sedimentary Rock Engineering. Taipei, Taiwan.

Hoek, E. (1999) The 2nd Glossop Lecture: Putting numbers to geology - an engineer’s viewpoint. Quarterly Journal of Engineering Geology. 32(1): 1-19.

Hoek, E. (2003) Integration of geotechnical and structural design in weak rock tunnels. Discussion by Evert Hoek.

Hoek, E. (2007) Practical Rock Engineering. Retrieved from http://www.rocscience.com/education/hoeks_corner.

Hoek, E. and Palmeiri, A. (1998) Geotechnical risks on large civil engineering projects. Keynote address from International of Engineering Geologist Congress, Vancouver, Canada.

Hoek, E., Carranza-Torres, C., Diederichs, M and Corkum, B. (2008) Integration of geotechnical and structural design in tunneling. The 2008 Kersten Lecture.

Hoek, E., Kaiser, P.K. and Bawden, W.F. (1995) Support of Underground Excavations in Hard Rock (1st Edition). Rotterdam, A.A. Balkema.

Hoek, E., Marinos, P. and Benissi, M. (1998). Applicability of the Geological Strength Index (GSI) Classification for Very Weak and Sheared Rock Masses: The Case of the Athens Schist Formation. Bulletin of Engineering of Geology and the Environment, 1998, 57(2): p151~160.

Hoek, E., Marinos, P.G. and Marinos, V.P. (2005) Characterization and engineering properties of tectonically undisturbed but lithologically varied sedimentary rock masses. International Journal of Rock Mechanics and Mining Sciences. 42: 277-285.

Hoek, E., Wood, D. and Shah, S. (1992) A modified Hoek-Brown criterion for jointed rock masses. Proceeding from The Rock Mechanics Symposium, ISRM Eurock '92. London. 209-214.

Houlsby, C. (1990) Construction and design of cement grouting: a guide to grouting in rock. John Wiley and Sons.

Huder, J. and Amberg, G. (1970) "Soft swelling in mergel, opalinuston and anhydrite," Swiss Building Publication, 88 (43), 975-980. (Translated to English).

ISRM. (1979) Suggested methods for determining the Uniaxial Compressive Strength and Deformability of Rock Materials. ISRM Committee on Standardization of Laboratory Tests.

ISRM Commission on Swelling Rock. (1983) Characterisation of Swelling Rock. Pergamon, Oxford, U.K.

ISRM Commission on Swelling Rocks. (1999) Suggested methods for laboratory testing of swelling rocks. International Journal of Rock Mechanics and Mining Science & Geomechanics Abstracts 36 (3): 291-306.

Jennings, M. (1986) The Middleplaats manganese ore deposit, Griqualand West. In: Anhaeusser, C. R and Maske, S. (Eds). Mineral Deposits of Southern Africa. The Geological Society of South Africa. 979-983.

Jing, L. (2003) A review of techniques, advances and outstanding issues in numerical modelling for rock mechanics and rock engineering. International Journal of Rock Mechanics and Mining Sciences. 40: 283-353.

Jing, L. and Hudson, J.A. (2002) Numerical methods in rock mechanics. International Journal of Rock Mechanics and Mining Sciences. 39: 409-427.

Johnson, M.R., van Vuuren, C.J., Visser, J.N.J., Cole, D.I., Wickens, H.deV., Christie, A.D.M., Roberts, D.L. and Brandl, G. (2006) Sedimentary rocks of the Karoo Supergroup. In: Johnson, M.R., Anhaeusser, C.R. and Thomas, R.J., (Eds). The Geology of South Africa. Geological Society of South Africa, Johannesburg / Council for Geoscience, Pretoria. Pp 461 – 499.

Kaiser, P.K. (1985) Rational assessment of tunnel liner capacity. Proc. 5th Canadian Tunnelling Conference. Montreal.

Karol, R.H. (1990) Chemical grouting. 2nd ed. New York, USA: Marcel Dekker.

Key, R M., Tidi, J., McGeorge, I., Aitken, G., Cadman, A. and Anscombe, J. (1998) The lower Karoo Supergroup geology of the south-eastern part of the Gemsbok sub-basin of the Kalahari basin, Botswana. S. Afr. J Geol. 101,225-236.

Knill, J. (2003) Core values: The first Hans-Cloos lecture. Bulletin Engineering Geology and the Environment. 62: 1-34.

Kovári, K. (2007) Modular yielding support for tunnels in heavily swelling rock. STUVA Conference, Köln.

Kovári, K., Amstad, C. and Anagnostou, G. (1988) Design/Construction methods - Tunneling in swelling rocks, Key Questions in Rock Mechanics, Cundall et all (eds), proceedings of the 29th U.S. Symposium University of Minnesota/Minneapolis.

Marinos, P. and Hoek, E. (2000) GSI: Geologically friendly tool for rock mass strength estimation. Proceeding from GeoEng 2000 International Conference on Geotechnical and Geological Engineering, Melbourne. 1422-1446.

Marinos, P., and Hoek, E. (2001) Estimating the Geotechnical Properties of Heterogeneous Rock Masses Such as Flysch. Bulletin of Engineering of Geology and the Environment (IAEG), 2001, 60: p85~92.

Marinos, V., Marinos, P. and Hoek, E. (2005) The geological strength index: applications and limitations. Bulletin Engineering Geology and the Environment. 64: 55-65.

Meyer, R., Duvenhage, A.W.A., De Beer, J.H. and Huyssen, R.M.J. (1985) A geophysical-geohydrological study along the Kuruman River in the Kuruman and Gordonia districts. Trans. Geol. Soc. S. A.fr., 88, 501-515.

Minerals Council of South Africa. (2019) Safety in the Mining Industry: Performance at a glance booklet, pg 2.

Nel, C.J., Beukes, N.J. and De Villiers, J.P.R, (1986) The Mamatwan manganese mine of the Kalahari manganese field. In: Anhaeusser, C. R and Maske, S. (Eds). Mineral Deposits of Southern Africa. The Geological Society of South Africa. 963-978.

NGI. (2015) Using the Q-system Handbook, Norwegian Geotechnical Institute.

Nilsen, B. and Broch, E. (2009) Engineering Geology of Rocks, Basic Level Compendium. Department of Geology and Mineral Resources, NTNU. In Norwegian.

Palmstrom, A. and Broch, E. (2006) Use and misuse of rock mass classification systems with particular reference to the Q-system. Tunnelling and Underground Space Technology. 21: 575-593.

Pande, G.N., Beer, G., Williams, J.R. (1990) Numerical Methods in Rock Mechanics. John Wiley and Sons, Ltd., West Sussex, England.

Panthi, K. K. (2008) Analysis of Engineering Geological Uncertainties Related to Tunnelling in Himalayan Rock Mass Conditions. Doctoral theses, Norwegian University of Science and Technology (NTNU). Faculty of Engineering Science and Technology, Chapters 3 and 4.

Pusch, R. (2012) Environmental Soil Properties and Behaviour, Swelling Clays, Chapter 4. CRC Press, Taylor & Francis Group, LLC: pp.133-161.

Rocscience. (2018) 3D Tunnel Simulation Using Core Replacement Tutorial. Rocscience 2D and 3D software for civil, mining, and geotechnical engineers.

Sauer, G., Gall, V., Bauer, E and Dietmaier, P. (1994) Design of tunnel concrete linings using limit capacity curves. in Computer Methods and Advances in Geomechanics, Eds.: Siriwardane & Zaman, page 2621 - 2626 Rotterdam, NL.

Selmer-Olsen, R. and Palmstrom, A. (1989). Tunnel collapses in swelling clay zones. Tunnels & Tunnelling, Nov. 1989: pp. 49-51.

Sheorey, P. R. (1985) Support Pressure Estimate in Failed Rock Conditions. Engineering Geology 22: 127-140.

Simons, N., Menzies, B. and Matthews, M. (2002) A short course in geotechnical site investigation. London: Thomas Telford.

Singh, B., Goel, R.K., Jethwa, J.L., Dube, A.K. (1997) Support pressure assessment in arched underground openings through poor rock masses. Engineering Geology 48: 59-81.

Singh, B., Jethwa, J.L., Dube, A.K., Singh, B. (1992) Correlation between observed support pressure and rock mass quality. Tunnelling and Underground Space Technology 7(1): 59-74.

Steenkamp, N.C. (2013a) Nchwaning I Decline, Decline Inspection. Unpublished report.

Steenkamp, N.C. (2013b) Old Gloria Ventilation Shaft, Geological Summary. Unpublished report.

Steiner, W. (1993) Swelling rock in tunnels: rock characterisation, effect of horizontal stresses and construction procedures. Int. J. Rock Mech. Min. Sci. Vol. 30, No. 4, pp. 361-380.

Tankard, A.J., Jackson, M.P.A., Eriksson, K.A., Hobday, D.R., Hunter, D.R, Minter, W.E.L. (1982) Crustal evolution of southern Africa, 3.8 billion years of earth history. Springer-Verlag, Heidelberg, 523pp.

Thomas, D.S.G., and Shaw, P.A. (1991) The Kalahari Environment. Cambridge University Press. 284 pp.

Thomas, D.S.G. and Shaw, P.A. (1990) The deposition and development of the Kalahari Group sediments, central southern Africa. Journal of African Earth Sciences, 10, 187-97.

Van der Merwe, D. H. (1964) The prediction of heave from the plasticity index and percentage clay fraction of soils. SA Inst. Civ. Eng. 6 (6).103-107.

Van Schalkwyk, J.F. and Beukes, N.J. (1986) The Sishen Iron Ore deposit, Griqualand West. In: C.R. Anhaeusser and S. Maske (Eds). Mineral Deposits of Southern Africa, Geological Society of South Africa, Johannesburg, 931-956.

Visser, D.J.L. (1984) Geological map of the republics of South Africa, Transkei, Bophuthatswana, Venda, and Ciskei and the kingdoms of Lesotho and Swaziland (1:1 000 000). Department of Minerals and Energy Affairs, South Africa. Gravity edition.

Visser, J.N.J., von Brunn, V. and Johnson, M.R. (1990) Dwyka Group In: Johnson, M.R. Catalogue of South African Litho stratigraphic Units, South African Committee for Stratigraphy.

Vlachopoulos, N. and Diederichs M.S. (2009) Improved longitudinal displacement profiles for convergence confinement analysis of deep tunnels. Journal of Rock Mechanics and Rock Engineering, vol 42, Number 2, April 2009. pp 131–146.

Warner, J. (2004) Practical handbook of grouting: soil, rock, and structures. John Wiley and Sons.

Whittaker, B.N. and Frith, R.C. (1990) Tunnelling: Design, Stability and Construction. The Institution of Mining and Metallurgy, 1990, London.

Wittke-Gattermann, P. (1998) Methods for calculating tunnels in swellable mountains and calibration on a test structure. Geotechnical Engineering in Research and Practice, WBI PRINT, 1. Essen: Glückauf.

Wittke-Gattermann, P. and Wittke, M. (2004) Computation of strains and pressures for tunnels in swelling rocks. Foundation Engineering and Construction in Rock, Aachen / Stuttgart, Germany, pp. 8.

# Appendix A: Site Investigation

# GEOTECHNICAL LOGGING

| | | | | | |
|---|---|---|---|---|---|
| Client: | | Borehole ID.: | GLV01 | Page (s): | of |
| Site/Location: | Gloria Vent Hole | Borehole Orientation: | Dip: -90 Azmith: | Drilling Method: | DD |
| Project No: | 120266 | Borehole Length (m): | 166 m | Drilling Start Date: | |
| Logged by: | | Drilling Contractor: | Geomechanics | Logged Date: | |

| Borehole Depth | | Recovery | | RQD | | Rock Competence | | | | | | Macro Defects | | Discontinuity Orientation (°) | | | | | Discontinuity Condition | | | | | | | |
|---|---|---|---|---|---|---|---|---|---|---|---|---|---|---|---|---|---|---|---|---|---|---|---|---|---|---|
| From (m) | To (m) | TCR (m) | SCR (m) | RQD (m) | Rock Type | Solid (m) | Matrix (m) | Matrix Type (T5) | Hard (T1-T3) | Weathering (T4) | Alteration (T5) | Quantity (T13) | Strength (T14) | 1 0-30 | 2 30-60 | 3 60-90 | Total | Discontinuity Type | LSJR (T7) | SSJR (T8) | Wall (T9) Alteration | Fill Type (T10) | Fill Material | Fill (T12) Thickness | Comments |
| 0.00 | 4.22 | 1.4 | - | - | Red Kalahari Sand | - | - | M1 | S1 | W6 | A5 | - | - | - | - | - | 0 | - | - | - | - | - | - | - | Manganese stockpile float |
| 4.22 | 5.20 | 1.10 | - | - | Kalahari Sand | - | - | M1 | S1 | W6 | A5 | - | - | - | - | - | 0 | - | - | - | - | - | - | - | Calcrete nodules |
| 5.20 | 26.00 | 10.68 | - | - | Red Kalahari Sand | - | | M1 | S1 | W6 | A5 | - | - | - | - | - | 0 | - | - | - | - | - | - | - | |
| 26.00 | 32.92 | 4.25 | 2.00 | 1.57 | Calcrete | 2 | < 1 mm | M2 | R1 | W1 | A1 | - | - | - | - | - | 0 | Mechancial Breaks | - | - | - | - | - | - | Quarzite & Ironstone cobbles and pebbles on bottom contact |
| 32.92 | 35.22 | 0.51 | - | - | Kalahari Sand | - | - | M1 | S1 | W6 | A5 | - | - | - | - | - | 0 | - | - | - | - | - | - | - | Calcrete nodules |
| 35.22 | 40.00 | 1.72 | 0.93 | 0.87 | Calcrete | 0.93 | < 1 mm | M2 | R1 | W6 | A5 | - | - | - | - | - | 0 | Mechancial Breaks | - | - | - | - | - | - | Gravel on bottom contact |
| 40.00 | 43.00 | 1.31 | 0.56 | 0.35 | Calcreted Conglomerate | 0.56 | < 1 mm | M2 | R1 | W6 | A5 | - | - | - | - | - | 0 | Mechancial Breaks | - | - | - | - | - | - | Quarzite & Ironstone cobbles and pebbles in calcrete matix. Matrix material mostly lost |
| 43.00 | 50.75 | 6.99 | 5.31 | 2.82 | Calcreted Red Clay | 5.31 | <1 mm | M2 | R1 | W5 | A5 | - | - | 16 | 7 | 1 | 24 | Slicken-slides | 5 | 9 | 1 | 10 | - | 0 | |
| 50.75 | 71.00 | 13.62 | - | - | Red Clay | - | < 1mm | M1 | S1 | W6 | A5 | - | - | 37 | 7 | 0 | 44 | Slicken-slides | - | - | - | - | - | - | |
| 71.00 | 73.90 | 2.80 | 2.70 | 2.52 | Calcreted Conglomerate | 2.7 | < 1 mm | M2 | R1 | W1 | A1 | - | - | - | - | - | 0 | Mechancial Breaks | - | - | - | - | - | - | Quartzite and ironstone pebbles in calcrete matrix |
| 73.90 | 77.40 | 3.26 | 2.39 | 2.11 | Calcreted Conglomerate | 2.39 | < 1 mm | M2 | R1 | W1 | A1 | - | - | - | - | - | 0 | Mechancial Breaks | - | - | - | - | - | - | Quarztite and ironstone pebbles in sand matrix cemented by calcrete |
| 77.40 | 91.40 | | | | Calcrete | 0 | < 1 mm | M2 | R1 | W1 | A1 | - | - | - | - | - | 0 | Mechancial Breaks | - | - | - | - | - | - | Quartzite cobbles irregular |
| | | | | | | | | | | | | | | | | | | | | | | | | | RE-DRILL |
| 75.00 | 76.30 | 1.16 | 0.46 | 0.00 | Sandy Calcrete | 0.46 | < 1 mm | M1 | R1 | W6 | A5 | - | - | 0 | 0 | 0 | 0 | Mechancial Breaks | - | - | - | - | - | - | Sand and quartzite pebbles in calcrete matrix |
| 76.30 | 85.37 | 8.27 | 5.65 | 2.56 | Calcreted Tillite | 5.65 | < 1 mm | M1 | R1 | W1 | A1 | - | - | 0 | 0 | 0 | 0 | Mechancial Breaks | - | - | - | - | - | - | Yellow tillite fragments in calcrete matrix |
| 85.37 | 86.64 | 1.20 | 1.20 | 1.13 | Calcrete | 1.2 | < 1mm | M1 | R1 | W1 | A1 | - | - | 0 | 0 | 0 | 0 | Mechancial Breaks | - | - | - | - | - | - | Quartzite cobbles irregular |
| 86.64 | 88.90 | 2.23 | 2.23 | 1.33 | Weathered Tillite | 2.23 | < 1 mm | M1 | R3 | W3 | A4 | - | - | 23 | 0 | 0 | 23 | Mechancial Breaks | 5 | 8 | 1 | 6 | None | 1 | Quartzite cobbles and pebbles, calcrete veins |
| 88.90 | 103.10 | 10.19 | 9.05 | 6.94 | Weathered Tillite | 9.05 | < 1mm | M1 | R3 | W3 | A4 | - | - | 73 | 1 | 1 | 75 | Mechancial Breaks & | 5 | 8 | 3 | 3 | Calcite | 3 | Quartzite boulders, cobbles and pebble dropstones, calcite joint fills |
| 103.10 | 106.10 | 3.49 | 3.39 | 3.00 | Slightly Weathered Tillite | 3.39 | < 1 mm | M1 | R4 | W2 | A3 | - | - | 20 | 0 | 0 | 20 | Mechanical Breaks | 5 | 8 | 1 | 9 | None | 1 | Quartzite pebble dropstones |
| 106.10 | 150.60 | 43.46 | 43.14 | 37.61 | Tillite | 43.14 | < 1 mm | M1 | R5 | W1 | A1 | - | - | 179 | 3 | 0 | 182 | Mechanical Breaks | 5 | 8 | 1 | 10 | None | 0 | Breaks along quartzite boulder and cobble dropstone inclusions |
| 150.60 | 151.86 | 1.10 | 1.10 | 0.89 | Gritstone | 1.1 | < 1 mm | M1 | R6 | W1 | A1 | - | - | 3 | 0 | 0 | 3 | Mechanical Breaks | 5 | 8 | 1 | 10 | None | 0 | Quartz grit |
| 151.86 | 162.03 | 13.36 | 13.26 | 11.44 | Tillite | 13.26 | < 1 mm | M1 | R5 | W1 | A1 | - | - | 35 | 2 | 0 | 37 | Mechanical Breaks | 5 | 8 | 1 | 10 | None | 0 | Breaks along quartzite boulder and cobble dropstone inclusions |
| 162.03 | 166.90 | 4.94 | 4.94 | 4.56 | Manganese | 4.94 | < 1 mm | M1 | R6 | W1 | A1 | - | - | 25 | 1 | 0 | 26 | Joints | 5 | 8 | 1 | 9 | Calcite | 1 | Calcite on joint surfaces |

# SAMPLING

| | | | |
|---|---|---|---|
| **Client:** | | **Page (s):** | |
| **Site:** | **Black Rock** | **Sample type:** | **Rock/ Soil** |
| **Project No:** | **120266** | **Sample date:** | |
| **Logged by:** | | **Submission date:** | |

| Sample Interval | | | | | | | |
|---|---|---|---|---|---|---|---|
| From | To | Sample No | Borehole No | Lithology | Test | Rocklab | Civilab |
| 8.00 | 11.00 | 78 | GLV-01 | Kalahari Sand | ALT & Grading Analyses | | x |
| 16.00 | 17.00 | 79 | GLV-02 | Kalahari Sand | ALT & Grading Analyses | | x |
| 25.00 | 26.00 | 80 | GLV-03 | Kalahari Sand | ALT & Grading Analyses | | x |
| 29.82 | 30.12 | 81 | GLV-04 | Calcrete | UCS | x | |
| 32.00 | 35.00 | 82 | GLV-05 | Kalahari Sand | ALT & Grading Analyses | | x |
| 41.27 | 41.45 | 83 | GLV-06 | Conglomerate | UCS | x | |
| 59.10 | 60.02 | 84 | GLV-07 | Red Clay | ALT & Grading Analyses | | x |
| 73.45 | 73.72 | 85 | GLV-08 | Calcrete | UCS | x | |
| 85.70 | 85.90 | 86 | GLV-09 | Calcrete | UCS | x | |
| 97.15 | 97.50 | 87 | GLV-10 | Weathered Tillite | UCS | x | |
| 101.36 | 101.74 | 88 | GLV-11 | Slightly Weathered Tillite | UCS | x | |
| 104.12 | 104.40 | 89 | GLV-12 | Tillite | UCS | x | |
| 107.35 | 107.57 | 90 | GLV-13 | Tillite | UCS | x | |
| 164.68 | 165.00 | 91 | GLV-14 | Manganese | UCS | x | |
| | | | | | | | |
| | | | | | | | |
| | | | | | ALT = Atterburg Limits Test | | |

# Appendix B: Laboratory Test Results

TABLE 2 RESULTS OF UNIAXIAL COMPRESSIVE STRENGTH TESTS WITH MODULUS & POISSON'S RATIO MEASUREMENTS BY MEANS OF STRAIN GAUGES

ROCKLAB
DIVISION OF SOILLAB (PTY) LTD
Tel: 012 481 3894
Fax: 012 481 3812
E-mail: Chenj@rocklab.co.za

Client: TWP Projects (Pty) Ltd.

Sampling Location:

16-Jul-10

| SPECIMEN PARTICULARS | | | | | SPECIMEN DIMENSIONS | | | | | SPECIMEN TEST RESULTS | | | | | | | |
|---|---|---|---|---|---|---|---|---|---|---|---|---|---|---|---|---|---|
| Rocklab Specimen No 3992- | Borehole No | Sample No | Sample depth From... To... m | Rock Type | Diameter mm | Height mm | Ratio of Height to Diameter | Mass g | Density g/cm³ | Failure Load kN | Strength (UCS) MPa | Tangent Elastic Modulus @ 50% UCS GPa | Secant Elastic Modulus @ 50% UCS GPa | Poisson's Ratio Tangent @ 50% UCS | Poisson's Ratio Secant @ 50% UCS | Linear Axial Strain at Failure mm/mm | Failure Code | Note |
| UCM-02 | LEX 1A | LEH02 | 296.47 - 296.90 | BIF | 47.68 | 120.91 | 2.5 | 745.7 | 3.45 | 937.4 | 525.0 | 114.0 | 113.0 | 0.19 | 0.17 | 0.004605 | YB | |
| UCM-10 | LEX 1A | LEH10 | 311.99 - 312.37 | BIF | 47.66 | 124.95 | 2.6 | 1013.8 | 4.55 | 522.4 | 292.8 | 135.0 | 135.0 | 0.27 | 0.26 | 0.002194 | 2B | |
| UCM-39 | LEX6 | LEH39 | 240.46 - 240.85 | BIF | 47.57 | 121.96 | 2.6 | 875.6 | 4.04 | 948.1 | 533.5 | 162.0 | 159.0 | 0.24 | 0.24 | 0.003447 | YB | |
| UCM-17 | LEX3 | LEH17 | 259.09 - 259.70 | Manganese | 47.58 | 123.58 | 2.6 | 976.5 | 4.44 | 318.5 | 179.1 | 89.0 | 83.1 | 0.27 | 0.24 | 0.002096 | 1B | |
| UCM-22 | LEX3 | LEH22 | 264.53 - 264.82 | Manganese | 47.52 | 123.60 | 2.6 | 932.7 | 4.25 | 288.3 | 162.6 | 71.7 | 65.2 | 0.23 | 0.20 | 0.002620 | 1B | |
| UCM-44 | LEX5 | LEH44 | 316.69 - 316.93 | Manganese | 47.49 | 124.55 | 2.6 | 913.2 | 4.14 | 327.2 | 184.7 | 69.2 | 67.4 | 0.32 | 0.26 | 0.002870 | YA | |
| UCM-46 | LEX5 | LEH46 | 318.90 - 319.44 | Manganese | 47.85 | 125.97 | 2.6 | 931.9 | 4.11 | 278.3 | 154.8 | 60.5 | 59.9 | 0.48 | 0.33 | 0.002876 | 3B | |
| UCM-26 | LEX4A | LEH26 | 289.08 - 289.55 | Tillite | 47.26 | 126.90 | 2.7 | 592.2 | 2.66 | 102.6 | 58.5 | 23.9 | 24.2 | 0.17 | 0.14 | 0.002432 | XA | |
| UCM-27 | LEX4A | LEH27 | 292.71 - 293.06 | Tillite | 47.46 | 127.10 | 2.7 | 613.9 | 2.73 | 142.5 | 80.6 | 44.4 | 41.9 | 0.25 | 0.20 | 0.002045 | XA | |
| UCM-33 | LEX6 | LEH33 | 224.56 - 224.82 | Tillite | 47.44 | 124.16 | 2.6 | 596.7 | 2.72 | 407.0 | 230.3 | 53.5 | 58.7 | 0.34 | 0.30 | 0.004521 | XB | |
| UCM-34 | LEX6 | LEH34 | 229.70 - 230.00 | Tillite | 47.42 | 127.29 | 2.7 | 596.9 | 2.66 | 112.8 | 63.9 | 19.5 | 20.4 | 0.21 | 0.15 | 0.003402 | XA | |
| UCM-40 | LEX5 | LEH40 | 303.60 - 303.90 | Red Shale | 47.27 | 125.43 | 2.7 | 815.4 | 3.70 | 464.1 | 264.5 | 55.9 | 59.4 | 0.37 | 0.31 | 0.005047 | YA | |
| UCM-41 | LEX5 | LEH41 | 304.58 - 304.74 | Red Shale | 47.50 | 124.69 | 2.6 | 764.3 | 3.46 | 459.0 | 259.0 | 72.6 | 76.8 | 0.31 | 0.28 | 0.003625 | YA | |
| UCM-42 | LEX5 | LEH42 | 304.88 - 305.06 | Red Shale | 47.56 | 123.95 | 2.6 | 808.6 | 3.67 | 400.6 | 225.5 | 87.3 | 90.4 | 0.28 | 0.26 | 0.002593 | YA | |

Note: All tests were conducted according to the ISRM's specfications.

## TABLE 2 RESULTS OF UNIAXIAL COMPRESSION TESTS WITH ELASTIC MODULUS AND POISSON RATIO MEASUREMENTS BY MEANS OF STRAIN GAUGES

ROCKLAB
DIVISION OF SOILLAB (PTY) LTD
Tel: 012 481 3894
Fax: 012 481 3812
E-mail: Chenj@rocklab.co.za

Client: TWP Projects

Sampling site: Black Rock

27-06-2012

| SPECIMEN PARTICULARS | | | | | | SPECIMEN DIMENSIONS | | | | | SPECIMEN TEST RESULTS | | | | | | | | |
|---|---|---|---|---|---|---|---|---|---|---|---|---|---|---|---|---|---|---|---|
| Rocklab Specimen No 4878- | Borehole No | Sample No. | Depth From m | Depth To m | Rock Type | Diameter mm | Height mm | Ratio of Height to diameter | Mass g | Density g/cm³ | Failure Load kN | Strength (UCS) MPa | Tangent Elastic Modulus @ 50% UCS GPa | Secant Elastic Modulus @ 50% UCS GPa | Poisson's Ratio Tangent @ 50% UCS | Poisson's Ratio Secant @ 50% UCS | Linear Axial Strain at Failure mm/mm | Failure Code | Note |
| UCM-30 | GL129-VMS | 30 | 20.28 | 20.68 | Calcrete | 82.37 | 123.9 | 1.5 | 1384.4 | 2.10 | 302.7 | 56.8 | 7.8 | 9.9 | 0.20 | 0.14 | 0.007628 | YA | |
| UCM-31 | | 31 | 41.80 | 42.30 | Calcrete | 81.00 | 145.4 | 1.8 | 1586.7 | 2.12 | 44.0 | 8.5 | 2.1 | 3.1 | 0.31 | 0.17 | 0.003656 | 6B | |
| UCM-37 | | 37 | 98.50 | 99.00 | Calcrete | 61.37 | 129.2 | 2.1 | 971.8 | 2.54 | 97.2 | 32.9 | 22.3 | 25.7 | 0.62 | 0.37 | 0.001573 | XA | |
| UCM-38 | | 38 | 104.15 | 104.65 | Siltstone | 61.12 | 95.9 | 1.6 | 629.3 | 2.24 | 17.4 | 5.9 | 3.5 | 3.0 | 0.11 | 0.11 | 0.002365 | XB | |
| UCM-41 | | 41 | 146.15 | 146.65 | Tillite | 61.10 | 86.9 | 1.4 | 666.3 | 2.61 | 317.2 | 108.2 | 24.8 | 21.9 | 0.15 | 0.10 | 0.004664 | XB | |
| UCM-43 | | 43 | 203.00 | 203.40 | Tillite | 50.21 | 128.7 | 2.6 | 690.9 | 2.71 | 184.2 | 93.0 | 36.9 | 39.5 | 0.23 | 0.18 | 0.002721 | XA | |
| UCM-45 | | 45 | 227.00 | 227.57 | Ironstone | 50.50 | 93.9 | 1.9 | 685.3 | 3.64 | 1098.0 | 548.2 | 121.0 | 125.0 | 0.25 | 0.21 | 0.004493 | YB | |
| UCM-54 | | 54 | 310.71 | 311.11 | Ironstone | 50.39 | 131.3 | 2.6 | 998.4 | 3.81 | 1095.0 | 549.1 | 105.0 | 109.0 | 0.28 | 0.25 | 0.005181 | YB | |
| UCM-56 | | 56 | 356.82 | 357.37 | Andesite | 49.95 | 138.0 | 2.8 | 796.2 | 2.94 | 506.3 | 258.4 | 87.0 | 89.7 | 0.25 | 0.28 | 0.002919 | YA | |
| UCM-57 | | 57 | 397.78 | 398.35 | Andesite | 49.83 | 129.6 | 2.6 | 739.6 | 2.93 | 469.1 | 240.5 | 83.8 | 86.3 | 0.29 | 0.28 | 0.002938 | YA | |
| UCM-58 | GL130-VVS | 58 | 106.65 | 107.15 | Siltstone | 63.13 | 48.7 | 0.8 | 299.0 | 1.96 | 13.6 | 4.3 | 0.4 | 0.4 | 0.25 | 0.16 | 0.011036 | XB | |
| UCM-59 | | 59 | 115.40 | 115.90 | Siltstone | 57.98 | 58.4 | 1.0 | 314.4 | 2.04 | 31.7 | 12.0 | 1.3 | 1.4 | 0.29 | 0.34 | 0.007692 | XB | |
| UCM-62 | | 62 | 154.52 | 155.15 | Tillite | 60.87 | 157.8 | 2.6 | 1232.7 | 2.68 | 275.9 | 94.8 | 39.6 | 43.4 | 0.35 | 0.24 | 0.002332 | YA | |
| UCM-63 | | 63 | 172.44 | 172.98 | Tillite | 50.37 | 121.0 | 2.4 | 643.1 | 2.67 | 149.7 | 75.1 | 41.0 | 45.7 | 0.24 | 0.24 | 0.002106 | YA | |
| UCM-69 | | 69 | 252.34 | 252.85 | Banded Ironstone | 50.71 | 119.2 | 2.4 | 797.0 | 3.31 | 1045.0 | 517.4 | 106.0 | 84.9 | 0.19 | 0.13 | 0.005646 | YB | |
| UCM-75 | N100-VMS-UG | 75 | 14.35 | 14.77 | Andesite | 49.80 | 130.7 | 2.6 | 734.6 | 2.89 | 624.1 | 320.4 | 78.0 | 81.4 | 0.28 | 0.27 | 0.004143 | YB | |
| UCM-76 | | 76 | 41.56 | 42.08 | Andesite | 50.04 | 133.7 | 2.7 | 766.7 | 2.92 | 482.4 | 245.3 | 77.3 | 81.8 | 0.30 | 0.28 | 0.003161 | 2B | |

Note: All tests were conducted according to the ISRM's Specification.

# TABLE 1 RESULTS OF UNIAXIAL COMPRESSIVE STRENGTH TESTS

ROCKLAB
DIVISION OF SOILLAB (PTY) LTD
Tel: 012 481 3894
Fax: 012 481 3812
E-mail: Chenj@rocklab.co.za

Client: TWP

Sampling Site: Kalahari

30-04-2013

| SPECIMEN PARTICULARS | | | | | SPECIMEN DIMENSIONS | | | | | SPECIMEN TEST RESULTS | | | |
|---|---|---|---|---|---|---|---|---|---|---|---|---|---|
| Rocklab Specimen No. 5286- | Borehole ID | Depth From m | Depth to m | Rock Type | Diameter mm | Height mm | Ratio of Height to Diameter | Mass g | Density g/cm³ | Failure Load kN | Strength (UCS) MPa | Failure Code | Note |
| UCS-01 | GLV-04 | 29.82 | 30.12 | Calcrete | 83.59 | 156.4 | 1.9 | 2154.30 | 2.51 | 198.50 | 36.2 | XA | |
| UCS-02 | GLV-06 | 41.27 | 41.45 | Conglomerate | 60.83 | 122.2 | 2.0 | 845.67 | 2.38 | 19.46 | 6.7 | XA | |
| UCS-03 | GLV-08 | 73.45 | 73.72 | Calcrete | 61.10 | 98.2 | 1.6 | 609.75 | 2.12 | 31.82 | 10.9 | XB | |
| UCS-04 | GLV-09 | 85.70 | 85.90 | Calcrete | 50.32 | 134.0 | 2.7 | 658.00 | 2.47 | 59.68 | 30.0 | XA | |
| UCS-05 | GLV-10 | 97.15 | 97.50 | Weathered Tillite | 50.35 | 133.6 | 2.7 | 563.53 | 2.12 | 12.09 | 6.1 | XB | |
| UCS-06 | GLV-11 | 101.36 | 101.74 | Slightly Weathered Tillite | 50.10 | 132.4 | 2.6 | 607.69 | 2.33 | 34.18 | 17.3 | XB | |
| UCS-07 | GLV-12 | 104.12 | 104.40 | Tillite | 50.38 | 139.1 | 2.8 | 652.99 | 2.35 | 45.22 | 22.7 | XB | |
| UCS-08 | GLV-13 | 107.35 | 107.57 | Tillite | 50.36 | 118.1 | 2.3 | 558.84 | 2.38 | 39.17 | 19.7 | XA | |
| UCS-09 | GLV-14 | 164.68 | 165.00 | Manganese | 50.55 | 106.0 | 2.1 | 781.18 | 3.67 | 788.08 | 392.7 | YA | |

Note: All tests were conducted according to the ISRM's (International Society for Rock Mechanics) specification.

## TABLE 1 RESULTS OF UNIAXIAL COMPRESSION STRENGTH TESTS

ROCKLAB
DIVISION OF SOILLAB (PTY) LTD
Tel: 012 481 3894
Fax: 012 481 3812
E-mail: Chenj@rocklab.co.za

Client: TWP Projects (Pty) Ltd. Site: 21-07-10

| SPECIMEN PARTICULARS | | | | | SPECIMEN DIMENSIONS | | | | | SPECIMEN TEST RESULTS | | | |
|---|---|---|---|---|---|---|---|---|---|---|---|---|---|
| Rocklab Specimen No 3992- | Borehole No | Sample No | Depth From.. To.. m | Rock Type | Diameter mm | Height mm | Ratio of Height to diameter | Mass g | Density g/cm³ | Failure Load kN | Strength (UCS) MPa | Failure Code | Note |
| UCS-01 | LEX 1A | LEH01 | 291.91 - 292.18 | Tillite | 47.68 | 117.06 | 2.5 | 562.3 | 2.69 | 179.9 | 100.8 | XA | |
| UCS-15 | LEX 3 | LEH15 | 250.70 - 251.00 | Tillite | 47.40 | 124.35 | 2.6 | 606.9 | 2.77 | 433.0 | 245.4 | YA | |
| UCS-26 | LEX 4A | LEH26 | 289.08 - 289.55 | Tillite | 47.32 | 123.12 | 2.6 | 574.2 | 2.65 | 130.5 | 74.2 | 1B | |
| UCM-34 | LEX6 | LEH34 | 229.70 - 230.00 | Tillite | 47.42 | 127.30 | 2.7 | 596.9 | 2.65 | 112.8 | 63.9 | XA | |
| UCS-05 | LEX 1A | LEH05 | 301.45 - 301.82 | BIF | 47.66 | 122.57 | 2.6 | 1040.2 | 4.76 | 410.1 | 229.9 | XB | |
| UCS-06 | LEX 1A | LEH06 | 302.18 - 302.46 | BIF | 47.64 | 124.54 | 2.6 | 1049.5 | 4.73 | 782.8 | 439.1 | YB | |
| UCS-24 | LEX 3 | LEH24 | 267.82 - 267.98 | BIF | 47.52 | 124.65 | 2.6 | 1057.0 | 4.78 | 440.3 | 248.2 | 2B | |
| UCS-48 | LEX5 | LEH48 | 321.30 - 321.46 | BIF | 48.11 | 121.95 | 2.5 | 1038.0 | 4.68 | 256.0 | 140.8 | 2B | |
| UCS-32 | LEX4A | LEH32 | 305.88 - 306.149 | Manganese | 47.48 | 125.27 | 2.6 | 940.6 | 4.24 | 229.7 | 129.7 | 2B | |
| UCS-43 | LEX5 | LEH43 | 313.35 - 313.58 | Manganese | 47.62 | 123.80 | 2.6 | 992.5 | 4.50 | 398.7 | 223.9 | XB | |
| UCS-47 | LEX5 | LEH47 | 319.44 - 319.70 | Manganese | 47.79 | 125.01 | 2.6 | 917.8 | 4.09 | 268.6 | 149.8 | XA | |
| UCM-46 | LEX5 | LEH46 | 318.90 - 319.44 | Manganese | 47.85 | 126.00 | 2.6 | 931.9 | 4.11 | 278.3 | 154.8 | 3B | |

Note: All tests were conducted according to the ISRM's Specification.

## TABLE 3 RESULTS OF BRAZILIAN TENSILE STRENGTH TESTS

ROCKLAB
DIVISION OF SOILAB (PTY) LTD
Tel: 012 481 3894
Fax: 012 481 3812
E-mail: Cheryj@rocklab.co.za

Client: TWP Projects (Pty) Ltd.

Sampling Site:

15-Jul-10

| SPECIMEN PARTICULARS | | | | | | SPECIMEN DIMENSIONS | | | | SPECIMEN TEST RESULT | | |
|---|---|---|---|---|---|---|---|---|---|---|---|---|
| ROCKLAB Specimen No 3992- | Borehole No | Sample No | Depth of Core From .. (m) | Depth of Core To.. (m) | Rock Type | Diameter mm | Height mm | Mass gram | Density g/cm³ | Failure Load kN | Brazilian Tensile Strength MPa | Note |
| UTB-02 | LEX 1A | LEH02 | 296.47 | 296.90 | BIF | 47.7 | 22.5 | 140.5 | 3.50 | 43.1 | 25.6 | |
| UTB-10 | | LEH10 | 311.99 | 312.37 | BIF | 47.7 | 23.1 | 183.4 | 4.46 | 37.8 | 21.9 | |
| UTB-17 | LEX 3 | LEH17 | 259.09 | 259.70 | MANGANESE | 47.5 | 23.4 | 184.1 | 4.44 | 20.4 | 11.7 | |
| UTB-22 | | LEH22 | 264.53 | 264.82 | MANGANESE | 47.5 | 23.1 | 173.4 | 4.24 | 27.2 | 15.8 | |
| UTB-26 | LEX 4A | LEH26 | 289.08 | 289.55 | TILLITE | 47.3 | 22.7 | 105.1 | 2.63 | 14.0 | 8.3 | |
| UTB-32 | | LEH32 | 305.88 | 306.19 | MANGANESE | 47.4 | 23.1 | 165.9 | 4.08 | 21.4 | 12.5 | |
| UTB-33 | LEX 6 | LEH33 | 224.56 | 224.82 | TILLITE | 47.4 | 22.7 | 109.4 | 2.72 | 27.6 | 16.3 | |
| UTB-34 | | LEH34 | 229.70 | 230.00 | TILLITE | 47.4 | 23.1 | 107.3 | 2.64 | 11.0 | 6.4 | |
| UTB-39 | | LEH39 | 240.46 | 240.85 | BIF | 47.5 | 22.9 | 158.4 | 3.89 | 52.3 | 30.6 | |
| UTB-41 | LEX 5 | LEH41 | 304.58 | 304.74 | RED SHALE | 47.5 | 23.0 | 142.3 | 3.50 | 40.2 | 23.5 | |
| UTB-42 | | LEH42 | 304.88 | 305.06 | RED SHALE | 47.2 | 22.7 | 140.1 | 3.53 | 43.4 | 25.8 | |
| UTB-44 | | LEH44 | 316.69 | 316.93 | MANGANESE | 47.5 | 23.2 | 169.9 | 4.14 | 19.4 | 11.2 | |
| UTB-46 | | LEH46 | 318.90 | 319.44 | MANGANESE | 47.8 | 22.7 | 172.3 | 4.23 | 19.5 | 11.4 | |

Note: All tests were conducted according to the ISRM's suggested method.

A SANAS accredited testing laboratory No T0062
36/38 Fourth Street, Booysens Reserve, Johannesburg 2091
P O Box 82223, Southdale 2135
Tel: +27 (0)11 835-3117 • Fax: +27 (0)11 835-2503
Email: jhb@civilab.co.za • Website: www.civilab.co.za

Civilab
Civil Engineering Testing Laboratories

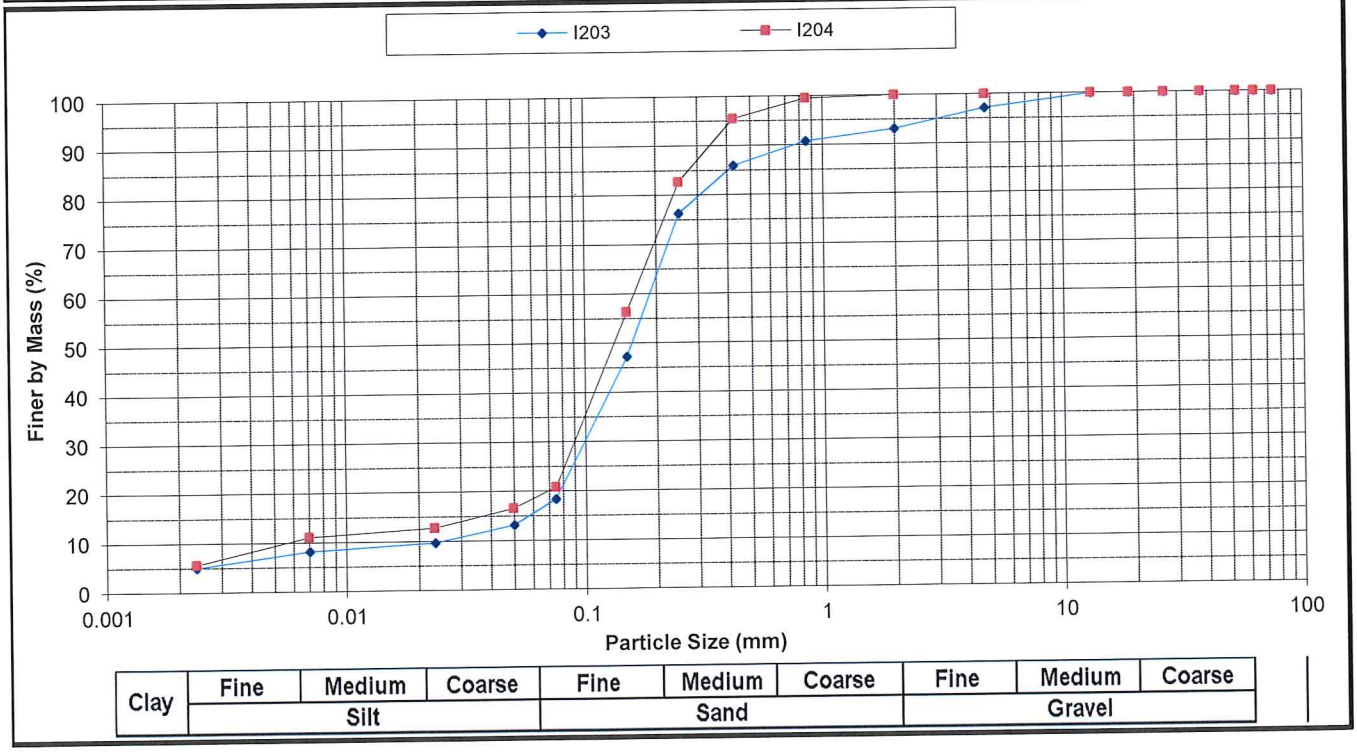
# Foundation Indicator Test Data

| | | | |
|---|---|---|---|
| Project | BLACK ROCK | | |
| Project No. | 1039/F42/04/2012 | Date | 4 May 2012 |

| Sample No. | I203 | I204 | |
|---|---|---|---|
| Field Ref. No. | GL 130 VVS | GL 130 VVS | |
| Depth | 2.0 - 8.25 | 14.28 - 15.78 | |
| Sieve size | %Passing | % Passing | % Passing |
| 75 | 100 | 100 | |
| 63 | 100 | 100 | |
| 53 | 100 | 100 | |
| 37.5 | 100 | 100 | |
| 26.5 | 100 | 100 | |
| 19.0 | 100 | 100 | |
| 13.2 | 100 | 100 | |
| 4.75 | 97 | 100 | |
| 2.00 | 93 | 100 | |
| 0.85 | 91 | 100 | |
| 0.425 | 86 | 95 | |
| 0.250 | 76 | 83 | |
| 0.150 | 47 | 56 | |
| 0.075 | 18 | 21 | |
| 0.04 | 12 | 15 | |
| 0.02 | 10 | 13 | |
| 0.006 | 8 | 10 | |
| 0.002 | 5 | 5 | |

| Sample No. | I203 | I204 | |
|---|---|---|---|
| %Gravel | 7 | 0 | |
| %Sand | 78 | 82 | |
| %Silt | 11 | 14 | |
| %Clay | 5 | 5 | |
| NMC % | Not Tested | 14.6 | |
| Liquid Limit | SP | SP | |
| Plasticity Index | SP | SP | |
| Linear Shrink. | 1. | 1. | |
| Overall P.I. | SP | SP | |
| Grading Modulus | 1.03 | 0.84 | |
| H.R.B. | A-2-4 (0) | A-2-4 (0) | |
| Unified | SM | SM | |
| Weston swell (%) at 1 kPa | | | |

Analysis as per method D422 of ASTM of 1985
The results reported relate only to the samples tested.
Documents may only be reproduced or published in their full context.




Remarks:

A SANAS accredited testing laboratory No T0062
36/38 Fourth Street, Booysens Reserve, Johannesburg 2091
P O Box 82223, Southdale 2135
Tel: +27 (0)11 835-3117 • Fax: +27 (0)11 835-2503
Email: jhb@civilab.co.za • Website: www.civilab.co.za

**Civilab**
**Civil Engineering Testing Laboratories**

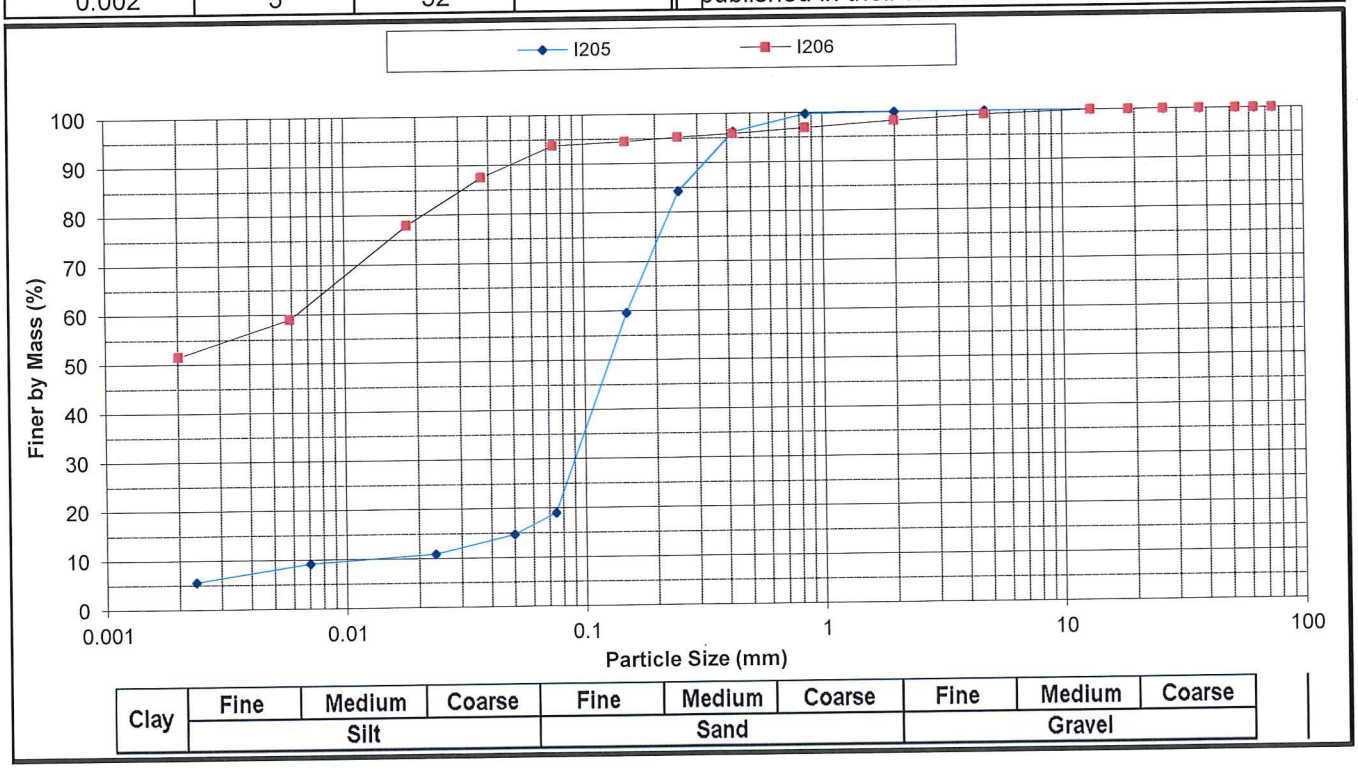
# Foundation Indicator Test Data

| | | | |
|---|---|---|---|
| Project | BLACK ROCK | | |
| Project No. | 1039/F42/04/2012 | Date | 11 May 2012 |

| Sample No. | I205 | I206 | |
|---|---|---|---|
| Field Ref. No. | GL 130 VVS | GL 130 VVS | |
| Depth | 19.53 - 20.28 | 24.28 - 25.28 | |
| Sieve size | %Passing | % Passing | % Passing |
| 75 | 100 | 100 | |
| 63 | 100 | 100 | |
| 53 | 100 | 100 | |
| 37.5 | 100 | 100 | |
| 26.5 | 100 | 100 | |
| 19.0 | 100 | 100 | |
| 13.2 | 100 | 100 | |
| 4.75 | 100 | 99 | |
| 2.00 | 100 | 98 | |
| 0.85 | 100 | 97 | |
| 0.425 | 96 | 96 | |
| 0.250 | 84 | 95 | |
| 0.150 | 60 | 95 | |
| 0.075 | 19 | 94 | |
| 0.04 | 14 | 88 | |
| 0.02 | 11 | 79 | |
| 0.006 | 9 | 59 | |
| 0.002 | 5 | 52 | |

| Sample No. | I205 | I206 | |
|---|---|---|---|
| %Gravel | 0 | 2 | |
| %Sand | 83 | 6 | |
| %Silt | 12 | 40 | |
| %Clay | 5 | 52 | |
| NMC % | 11.4 | 31.2 | |
| Liquid Limit | SP | 85 | |
| Plasticity Index | SP | 50 | |
| Linear Shrink. | 1. | 20.5 | |
| Overall P.I. | SP | 48 | |
| Grading Modulus | 0.85 | 0.12 | |
| H.R.B. | A-2-4 (0) | A-7-5 (20) | |
| Unified | SM | CH | |
| Weston swell (%) at 1 kPa | | 12.5 | |

Analysis as per method D422 of ASTM of 1985
The results reported relate only to the samples tested.
Documents may only be reproduced or published in their full context.




Remarks:

A SANAS accredited testing laboratory No T0062
36/38 Fourth Street, Booysens Reserve, Johannesburg 2091
P O Box 82223, Southdale 2135
Tel: +27 (0)11 835-3117 • Fax: +27 (0)11 835-2503
Email: jhb@civilab.co.za • Website: www.civilab.co.za

Civilab
Civil Engineering Testing Laboratories

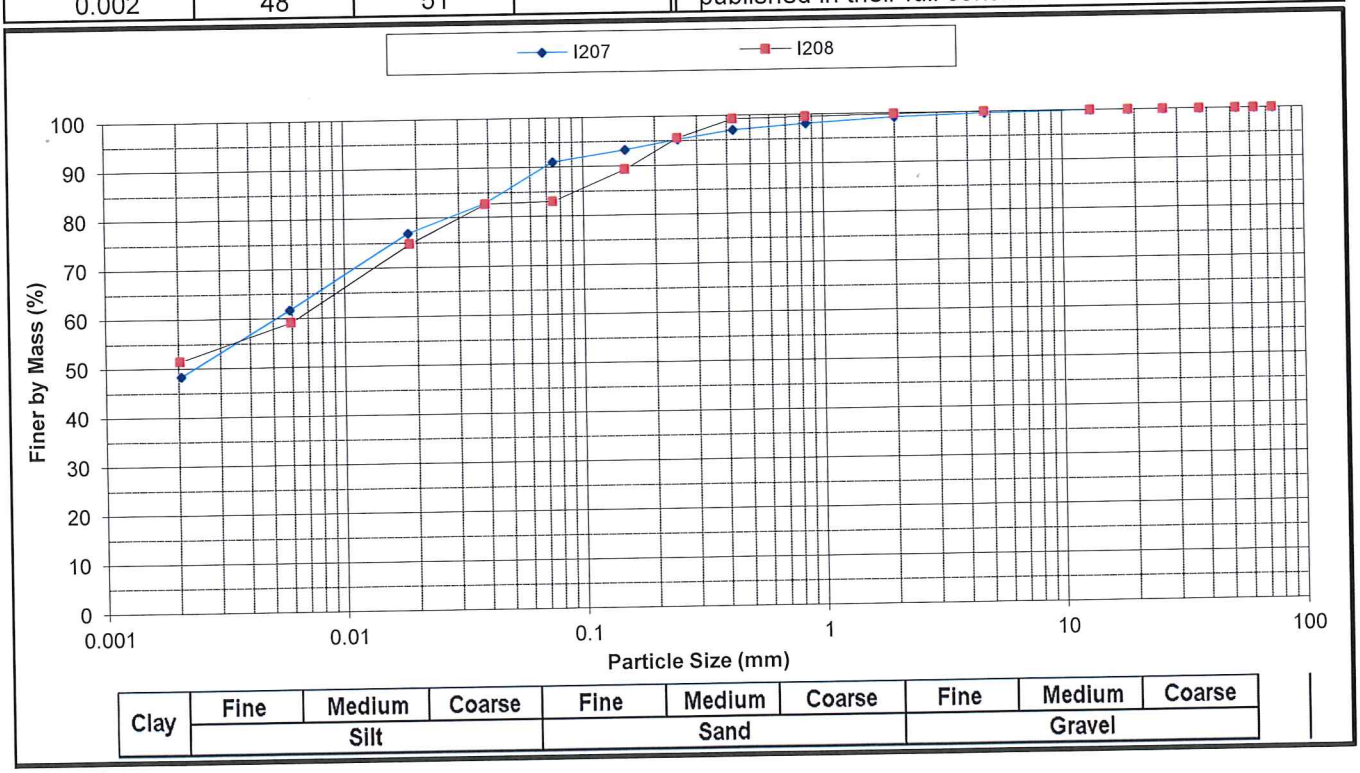
# Foundation Indicator Test Data

| | | | |
|---|---|---|---|
| Project | BLACK ROCK | | |
| Project No. | 1039/F42/04/2012 | Date | 11 May 2012 |

| Sample No. | I207 | I208 | |
|---|---|---|---|
| Field Ref. No. | GL 130 VVS | GL 130 VVS | |
| Depth | 81.28 - 82.28 | 61.0 - 62.0 | |
| Sieve size | %Passing | % Passing | % Passing |
| 75 | 100 | 100 | |
| 63 | 100 | 100 | |
| 53 | 100 | 100 | |
| 37.5 | 100 | 100 | |
| 26.5 | 100 | 100 | |
| 19.0 | 100 | 100 | |
| 13.2 | 100 | 100 | |
| 4.75 | 100 | 100 | |
| 2.00 | 99 | 100 | |
| 0.85 | 98 | 100 | |
| 0.425 | 97 | 99 | |
| 0.250 | 95 | 96 | |
| 0.150 | 93 | 89 | |
| 0.075 | 91 | 83 | |
| 0.04 | 83 | 83 | |
| 0.02 | 78 | 75 | |
| 0.006 | 62 | 59 | |
| 0.002 | 48 | 51 | |

| Sample No. | I207 | I208 | |
|---|---|---|---|
| %Gravel | 1 | 0 | |
| %Sand | 11 | 17 | |
| %Silt | 40 | 32 | |
| %Clay | 48 | 51 | |
| NMC % | 25.0 | 34.8 | |
| Liquid Limit | 63 | 83 | |
| Plasticity Index | 31 | 50 | |
| Linear Shrink. | 17. | 18. | |
| Overall P.I. | 30 | 50 | |
| Grading Modulus | 0.13 | 0.18 | |
| H.R.B. | A-7-5 (20) | A-7-5 (20) | |
| Unified | MH | CH | |
| Weston swell (%) at 1 kPa | 6.3 | 10.0 | |

Analysis as per method D422 of ASTM of 1985
The results reported relate only to the samples tested.
Documents may only be reproduced or published in their full context.




Remarks:

A SANAS accredited testing laboratory No T0062
36/38 Fourth Street, Booysens Reserve, Johannesburg 2091
P O Box 82223, Southdale 2135
Tel: +27 (0)11 835-3117 • Fax: +27 (0)11 835-2503
Email: jhb@civilab.co.za • Website: www.civilab.co.za

**Civilab**
**Civil Engineering Testing Laboratories**

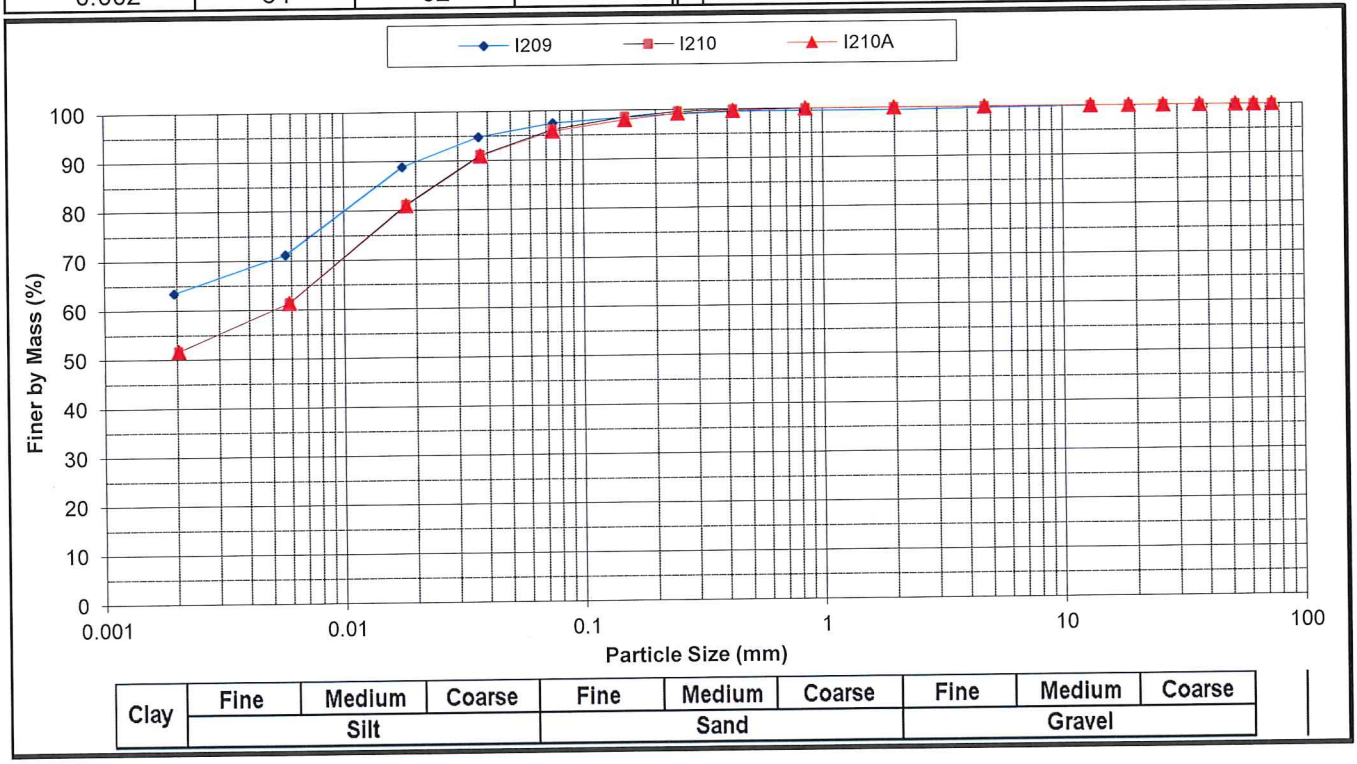
# Foundation Indicator Test Data

| | | | |
|---|---|---|---|
| Project | BLACK ROCK | | |
| Project No. | 1039/F42/04/2012 | Date | 11 May 2012 |

| Sample No. | I209 | I210 | I210A |
|---|---|---|---|
| Field Ref. No. | N 100 VMS | N 100 VMS | N 100 VMS |
| Depth | 66.48 - 67.38 | 74.28 - 75.18 | 74.28 - 75.18 |
| Sieve size | %Passing | % Passing | % Passing |
| 75 | 100 | 100 | 100 |
| 63 | 100 | 100 | 100 |
| 53 | 100 | 100 | 100 |
| 37.5 | 100 | 100 | 100 |
| 26.5 | 100 | 100 | 100 |
| 19.0 | 100 | 100 | 100 |
| 13.2 | 100 | 100 | 100 |
| 4.75 | 100 | 100 | 100 |
| 2.00 | 100 | 100 | 100 |
| 0.85 | 100 | 100 | 100 |
| 0.425 | 100 | 100 | 100 |
| 0.250 | 99 | 100 | 99 |
| 0.150 | 99 | 99 | 98 |
| 0.075 | 98 | 96 | 96 |
| 0.04 | 95 | 92 | 91 |
| 0.02 | 90 | 82 | 82 |
| 0.006 | 72 | 62 | 62 |
| 0.002 | 64 | 52 | 51 |

| Sample No. | I209 | I210 | I210A |
|---|---|---|---|
| %Gravel | 0 | 0 | 0 |
| %Sand | 3 | 5 | 6 |
| %Silt | 33 | 43 | 43 |
| %Clay | 64 | 52 | 51 |
| NMC % | 21.7 | Not Tested | Not Tested |
| Liquid Limit | 94 | 64 | 61 |
| Plasticity Index | 53 | 37 | 35 |
| Linear Shrink. | 18. | 17. | 18. |
| Overall P.I. | 53 | 37 | 35 |
| Grading Modulus | 0.03 | 0.04 | 0.05 |
| H.R.B. | A-7-5 (20) | A-7-6 (20) | A-7-6 (20) |
| Unified | MH | CH | CH |
| Weston swell (%) at 1 kPa | 52.3 | | |

Analysis as per method D422 of ASTM of 1985
The results reported relate only to the samples tested.
Documents may only be reproduced or published in their full context.




Remarks:

A SANAS accredited testing laboratory No T0062
36/38 Fourth Street, Booysens Reserve, Johannesburg 2091
P O Box 82223, Southdale 2135
Tel: +27 (0)11 835-3117 • Fax: +27 (0)11 835-2503
Email: jhb@civilab.co.za • Website: www.civilab.co.za

**Civilab**
**Civil Engineering Testing Laboratories**

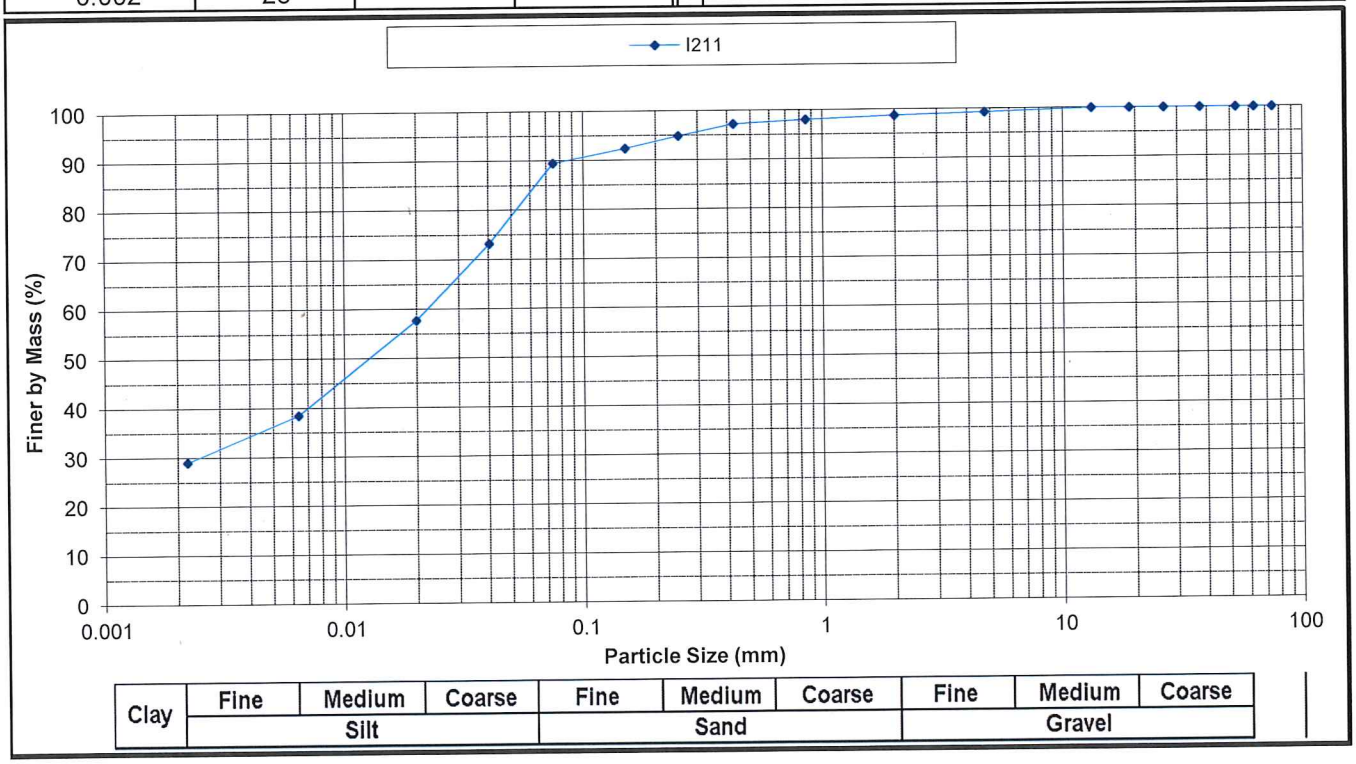
# Foundation Indicator Test Data

| | | | |
|---|---|---|---|
| Project | BLACK ROCK | | |
| Project No. | 1039/F42/04/2012 | Date | 11 May 2012 |

| Sample No. | I211 | | |
|---|---|---|---|
| Field Ref. No. | N 100 VMS | | |
| Depth | 89.28 - 90.18 | | |
| Sieve size | %Passing | % Passing | % Passing |
| 75 | 100 | | |
| 63 | 100 | | |
| 53 | 100 | | |
| 37.5 | 100 | | |
| 26.5 | 100 | | |
| 19.0 | 100 | | |
| 13.2 | 100 | | |
| 4.75 | 99 | | |
| 2.00 | 99 | | |
| 0.85 | 98 | | |
| 0.425 | 97 | | |
| 0.250 | 95 | | |
| 0.150 | 92 | | |
| 0.075 | 89 | | |
| 0.04 | 73 | | |
| 0.02 | 58 | | |
| 0.006 | 38 | | |
| 0.002 | 28 | | |

| Sample No. | I211 | | |
|---|---|---|---|
| %Gravel | 1 | | |
| %Sand | 15 | | |
| %Silt | 55 | | |
| %Clay | 28 | | |
| NMC % | Not Tested | | |
| Liquid Limit | 59 | | |
| Plasticity Index | 32 | | |
| Linear Shrink. | 14. | | |
| Overall P.I. | 32 | | |
| Grading Modulus | 0.15 | | |
| H.R.B. | A-7-6 (20) | | |
| Unified | CH | | |
| Weston swell (%) at 1 kPa | | | |

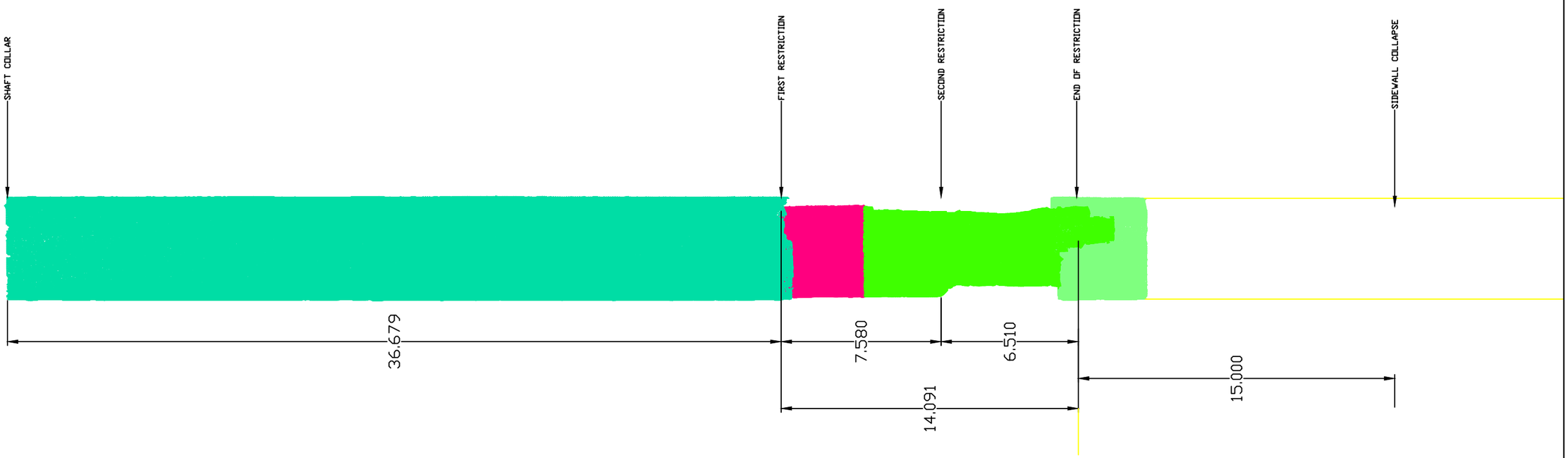
Analysis as per method D422 of ASTM of 1985
The results reported relate only to the samples tested.
Documents may only be reproduced or published in their full context.




Remarks:

# Appendix C: Early Tunnelling Projects Inspection

ASSMANG LIMITED




| | | | | | | | | |
|---|---|---|---|---|---|---|---|---|
| SURVEYOR | J.H.ERASMUS | 24 FEB'16 | | | | | | |
| | | | | | | | | |
| | | | | | | | | |
| TITLE | SIGNATURE | DATE | TITLE | SIGNATURE | DATE | TITLE | SIGNATURE | DATE |

CLIENT: ASSMANG LIMITED

TITLE: ASSMANG LIMITED
GLORIA SHAFT
RESTRICTION
3D SCAN

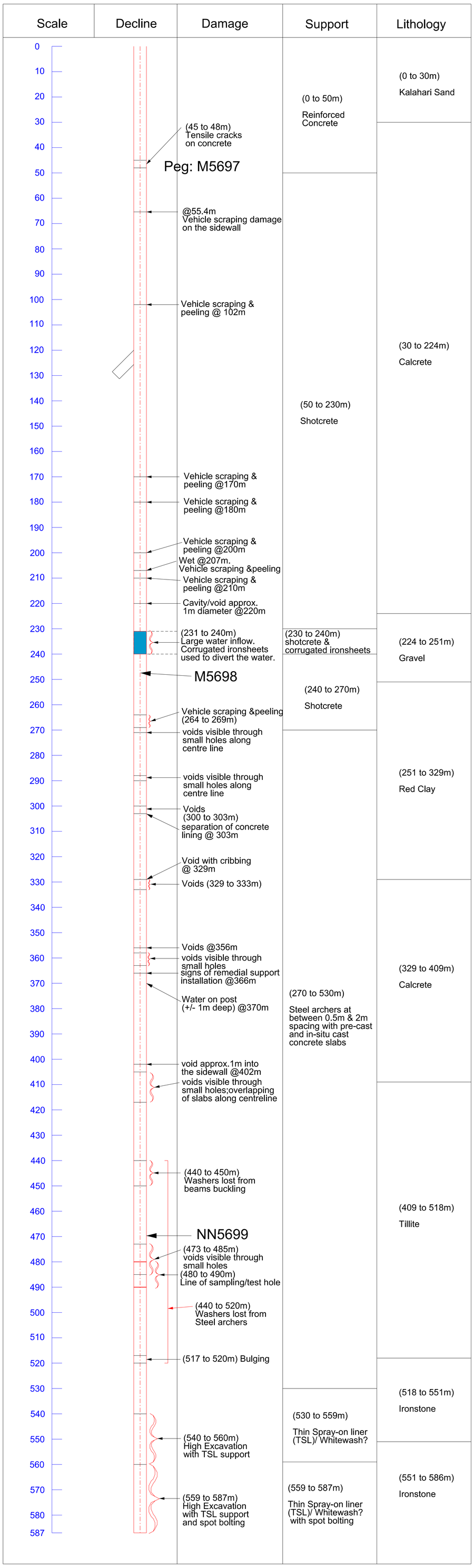
SCALE: N.T.S

DRAWN DATE: 24 FEBRUARY 2016

REV: △

# Nchwaning I - Decline

Scale 1:1000



# Appendix D: Derivation of Drucker Prager Constants

Calculating Drucker-Prager strength parameters from Mohr-Coulomb strength parameters for use in Phase2:

For associated flow:

$$q = \frac{\sin\phi}{\sqrt{1+\frac{1}{3}\sin^2\phi}} \qquad k = \frac{c\cos\phi}{\sqrt{1+\frac{1}{3}\sin^2\phi}}$$

For non-associated flow (0 dilatancy):

$$q = \sin\phi \qquad k = c\cos\phi$$